King Abdulaziz University
Engineering Sciences

Volume 32 Issue 1 2022 ISSN: 1319-1047


بسم الله الرحمن الرحيم

Journal of
King Abdulaziz University
Engineering Sciences

Volume 32 Issue1

2022

Contents

King Abdulaziz Journal: Engineering Sciences, 2022 Volume 32 No 1 pp.:1-24, O DOI:xx.xxx/

Dimensional Analysis via an Electromagnetically-Oriented Set of Fundamental Dimensions

Mostafa Ali Rushdi[1,2], Ali Muhammad Rushdi[3,*]

[1]Faculty of Engineering and Technology, Future University in Egypt, New Cairo, 11835, Egypt

[2]Research Institute for Applied Mechanics, Kyushu University, Fukuoka, 816-8580, Japan)

E-mail: Mostafa.Roshdi@fue.edu.eg; rushdimostafa@riam.kyushu-u.ac.jp

[3]Electrical and Computer Engineering, King Abdulaziz University, Jeddah 21589, Saudi Arabia

Abstract. This paper describes the electromagnetically-oriented $LTI\emptyset$ dimensional basis that is based on the reference dimensions of Length (L), Time (T), Electric Current (I), and Electric Potential ($\emptyset$). We utilize this basis in the matrix solution of dimensional-analysis (DA) problems involving mainly electromagnetic quantities. Representations of electromagnetic quantities in the $LTI\emptyset$ basis (compared with the standard $MLTI$ basis that uses Mass (M) instead of Potential ($\emptyset$)) are more informative, much simpler, and have salient duality features. Moreover, DA computations of electromagnetic problems via the Gauss-Jordan algorithm in the $LTI\emptyset$ basis are more efficient, much less error prone, and quicker to detect linear dependencies in the dimensional equations. Both details and advantages of the proposed method are explored via demonstrative examples, which are of obvious significance in the learning and teaching of electromagnetism.

Key words. Dimensional analysis**,** dimensionless products, basis and regime variables, Gauss-Jordan elimination, electromagnetically-oriented dimensional basis, learning and teaching electromagnetism.

1. Introduction

Dimensional analysis (DA), fundamentally related to the principle of similitude, is an effective way to analyze a physical phenomenon without explicit knowledge of its governing physical laws, provided we are confident that such laws exist. In fact, DA can be used along with experimental data to develop an empirical mathematical model of the physical phenomenon concerned. The use of DA is justified by the single premise that the phenomenon can be described by a dimensionally correct equation among the pertinent variables. We do not need or assume pre-knowledge of this equation or model, for, otherwise, DA application would not be warranted. The prominent advantage of DA is that it dispenses with any knowledge of the inner mechanisms of the physical phenomenon. Dimensional analysis reduces the number of variables used, thereby facilitating fitting of equations to data. Another major advantage of DA is that it can partition the original variables in a general way into appropriate sets of basis (independent) variables and regime (dependent) ones, with each of the regime variables appearing (possibly with basis variables) in a dimensionless grouping that enjoys a concrete physical interpretation.

* Corresponding author: arushdi@kau.edu.sa

Successful DA application necessitates that we understand the underlying phenomenon well enough just to identify all the pertinent variables, which must be all quantifiable. While DA does not need to know the inner mechanisms of the underlying phenomenon, it does not offer to explain these mechanisms, either. A complete model of the phenomenon is not supplied by DA alone, since DA must be supplemented with further information, usually in the form of experimental data. Direct utility of DA is limited to product formulas, in which variables are raised to certain exponents.

Dimensional analysis has a long history extending for several centuries, but it was almost one century ago that Buckingham laid the mathematical foundation for classical DA [1, 2]. During those centuries electricity and magnetism were developing as independent phenomena, and it was only in the nineteenth century that they were realized to be different manifestations of a single underlying theory, collectively called Maxwell's equations of electromagnetism (EM). One might observe the existence of an intimate relation between dimensional analysis and electromagnetism, even from the times of their infancies. In fact, dimensional analysis aided Maxwell, the undisputed father of modern electromagnetism, in the formulation of his celebrated equations [3]. The utility of dimensional analysis in solving problems of electromagnetics is exemplified by an example in the seminal paper of Buckingham [1]. Casting Maxwell's equations in a dimensionless form facilitates utilizing them in mathematical proofs [4], and allows their solution without dealing with very large numbers [5]. A modern prominent technique in electromagnetics (and other branches of physics), viz., that of differential forms, relies heavily on DA concepts to classify various quantities as volume, area, line, or none densities or quotients [6-9]. There are many publications linking DA and EM units and dimensions [10-29], and many others applying the most fundamental DA theorem (Buckingham Pi Theorem) to EM problems [30-49].

This paper offers a detailed exposition on using the electromagnetically-oriented $LTI\emptyset$ dimensional basis (instead of the mechanically-oriented $MLTI$ dimensional basis associated with the SI system of units) for solving DA problems mainly involving electromagnetic quantities. We describe transformations between the two bases, and report novel observations on characteristic features of EM and non-EM quantities, which are revealed by their dimensional exponents in the $LTI\emptyset$ basis. We supplement the use of this basis by the utilization of a modern matrix approach for Dimensional Analysis [49-59] in the derivation of dimensionless products via the celebrated Gauss-Jordan algorithm [60], which possesses many obvious advantages for handling linear dependencies, and for partitioning variables into basis and regime ones. The task of this algorithm is to reduce the augmented dimensional matrix into a reduced row echelon form (RREF). This task is considerably facilitated when the submatrix associated with the basis variables is shaped as closely as possible to a unit matrix, a goal that can be achieved with the use of the $LTI\emptyset$ basis, provided electromagnetic quantities dominate the basis variables of the DA problem, and, not necessarily its regime variables.

Rushdi and Rushdi [54] list many salient features of the Gauss-Jordan algorithm that makes it our unrivaled choice for handling DA problems (whether in a manual or an automated fashion). This algorithm acts as a mechanism of switching from an initial basic set of agreed-upon fundamental dimensions to a final set of desirable base dimensions. That role resembles this algorithm's role as a part of the Simplex Method of linear programming. The Gauss-Jordan algorithm does not make any presupposition of the rank r of the dimensional matrix. Neither does it need any preparatory work to determine the matrix rank (for example, by evaluating determinants via Cramer's rule as suggested by Middendorf [33]). This algorithm integrates the step of rank determination with its own work. If it encounters a row whose entries are all 0 (an all-0 row) it avoids this row by interchanging it with a latter row that is not all-0. The procedure terminates if there is no

remaining row that is not all-0. The matrix rank is simply the number of rows successfully processed by the procedure (for which, there exist non-zero pivoting elements). For our manual solutions here, if the algorithm creates an all-0 row, then we will simply omit it in the next stage to avoid notorious swapping operations.

The remainder of this paper is structured as follows. Section 2 discusses the issue of selecting fundamental dimensions for electromagnetics. The problem of transformations between the $LTI\emptyset$ basis and the $MLTI$ basis is subsequently explored, first by scalar techniques (Section 3), and later by a novel application of the Gauss-Jordan algorithm (Section 4). Section 5 lists the dimensional exponents for EM and non-EM quantities in both the $LTI\emptyset$ and $MLTI$ bases, and points out the superior features possessed by the $LTI\emptyset$ basis for handling electromagnetic quantities. Several illustrative examples are then presented in Section 6 to demonstrate the effectiveness of the proposed approach which makes the most of the Gauss-Jordan algorithm through the use of the electromagnetically-oriented basis for the dimensional analysis of EM problems. Section 7 concludes the paper.

2. Selection of Fundamental Dimensions for Electromagnetics

The fundamental dimensions *may* be chosen rather *arbitrarily*, but, for practical reasons, *should* be chosen *appropriately*, and should be scientifically justifiable. The first step in the selection of a dimensional system is to choose the number N of fundamental dimensions. There are two extreme values for N as it can be as small as *one* in a mono-dimensional system, and it might be large enough to allow *all* dimensions to be fundamental ones in an omni-dimensional system. Szirtes [43] demonstrates the *possibility* and (at the same time) the *impracticality* of these two extreme systems:

- In a mono-dimensional system, all dimensions, except a single fundamental one, are derived and expressed as positive, zero, or negative powers of that single fundamental dimension. Such a system is totally impractical, suffers from excessive ambiguities, and it forces its users to use dimensions which are terribly inappropriate. It is particularly inferior to a (moderately) multidimensional one, since it drastically undermines the utilization of the requirement of dimensional homogeneity in deriving and verifying formulas and in constructing dimensionless products.
- In an omni-dimensional system, no ambiguity is encountered, since every dimension is fundamental and none is derived. Therefore, variables of different dimensions must be measured entirely independently, and every physical relation would be a separate scientific discovery requiring at least one mandatory dimensional 'constant of nature,' that would have to be determined separately so as to make the formula dimensionally homogeneous.

Since many drawbacks result from the selection of too few or too many fundamental or reference dimensions, the best choice seems to be a traditional (moderately) multidimensional system [43]. A considerable convenience can stem from using three to five reference dimensions as rendered feasible by the problem at hand. Bridgman [61] emphasizes the fact that there is nothing sacrosanct about the number of reference dimensions and that dimensional analysis is merely a man-made tool that may be manipulated at will. This principle of free choice of the reference dimensions has been widely accepted, preached and practiced [62]. In fact, the International System of Units (SI System) uses seven fundamental dimensions ($N = 7$), namely mass, length, time, electric current, temperature, amount of substance, and luminous intensity. It also employs two supplementary fundamental units for two particular dimensionless quantities, namely: the plane angle (length/length) and the solid angle (area/length squared). Treatment of these dimensionless quantities as fundamental dimensions leads to a convenient and systematic way of conversion between different systems [11, 51]. The SI

system suffers from few ambiguities such as its assignment of non-distinct designations for torque and energy or for pressure, normal stress and shear stress [43].

The SI system is an outgrowth of the MLT system covering the *kinetic* quantities of Mass (M), Length (L), and Time (T). This mass-based system was competitive with (and more popular, albeit less efficient than) another three-dimensional system, *viz.*, the FLT system, in which force (F) replaces Mass as a fundamental dimension. The MLT system can express all mechanical quantities in a unique way, but it experiences ambiguities with many electromagnetic quantities [29]. To extend the MLT system to cover *electromagnetic* quantities appropriately, it suffices to add only one additional quantity [11], which originally was the electric charge (Q) [63], but was later superseded with the electric current (I). Dimensional analysis involving electromagnetic/electromechanical quantities, therefore, is typically based on the use of the $MLTI$ multidimensional system. An alternative system using the same number of fundamental dimensions is the $LTI\emptyset$ system [43, 57, 64, 65], where $\emptyset$ stands for electric potential or voltage. Though this system has been known for more than a century, it has never been fully developed or adequately utilized. It starts as a system covering the *kinematic* quantities of Length (L) and Time (T), and augments it with the *two* electric (or electromagnetic) quantities of current and potential. Likewise, in the $LTQ\Phi$ system that was proposed by Kalantaroff in 1929 [12, 27, 29], electric charge (Q) and magnetic flux (Φ) are taken as fundamental dimensions, again in addition to Length and Time. All these modern multidimensional systems use four fundamental dimensions, but the split of these four dimensions to purely mechanical and purely electromagnetic ones is $3+1$ for mechanically-oriented systems ($MLTQ, MLTI, FLTQ,$ and $FLTI$) and $2+2$ for the electromagnetically-oriented ones ($LTI\emptyset$ and $LTQ\Phi$). The two electromagnetic quantities employed in these two latter systems are *dual* quantities, where dual electromagnetic quantities are obtained by interchanging the dimensions of current and voltage (or, equivalently, by interchanging the dimensions of electric charge and magnetic flux) [64]. A more elaborate understanding of the concept of 'duality' might be secured by referring to any standard text on electromagnetics [66-68].

Thomas [64] offers a lucid justification for the introduction of the $LTI\emptyset$ system that essentially goes as follows. In a mechanical system, dimensional simplification is usually achieved by employing 'force' as a fundamental or basis quantity. By direct electromechanical analogy, the electrical analogous quantity for 'force', namely 'voltage', is suggested to be a fundamental quantity. Since 'voltage' acts as the '*forcing function'* in a series electric circuit, the '*response*' in such a circuit, namely 'current' is proposed as a second fundamental quantity. Alternatively, one might view a parallel electric circuit, in which 'current' is the 'forcing function' and 'voltage' is the 'response', thereby coming to the same conclusion. 'Time' is an indispensable choice for a third fundamental quantity, since many electric phenomena are *dynamic*, in which many prominent quantities stand for the time rate of change of other quantities. It is remarkable to note that the product $TI\emptyset$ of the three fundamental quantities chosen so far stands for 'energy', and that many other important physical quantities of electric circuits rely solely on the three-element basis of $TI\emptyset$. However, to extend our coverage from that of lumped electric-circuit phenomena to that of *distributed* electromagnetic phenomena, we need to add 'length' as a fourth fundamental quantity.

3. Transformation between Two Fundamental Dimensional Systems for Electromagnetics

The basic liaison between mechanical and electromagnetic quantities arises from the fact that mechanical energy and electromagnetic energy share the same nature and dimension. Now, the dimension of mechanical energy is given by

$$[Mechanical\ energy] = [Mechanical\ work] = [Force][displacement] = [Mass][Acceleration]L = M\,L^2\mathrm{T}^{-2}, \quad (1)$$

while the dimension of electromagnetic energy is given by

$$[Electromagnetic\ energy] = [Poynting\ vector][Area][Time] = [Electric\ field\ intensity][Magnetic\ field\ intensity]\ L^2T = \emptyset L^{-1} I L^{-1} L^2 T = \emptyset I T\ , \quad (2)$$

The result in (2) could be obtained by employing a lumped electric circuit rather than a distributed electromagnetic phenomenon, for then (2) could be replaced by the dimension of electric energy, which is [Electric voltage] [Electric current] [Time], which is again $\emptyset IT$. Equating (1) to (2) results in

$$M\ L^2\mathrm{T}^{-2} = \emptyset IT. \quad (3)$$

Hence, we express the dimension of Mass (M) in the $LTI\emptyset$ basis, and the dimension of electric potential ($\emptyset$) in the $MLTI$ basis as

$$M\ = L^{-2}\, T^3\, I\, \emptyset. \quad (4)$$

$$\emptyset = M\, L^2\, T^{-3}\, I^{-1}. \quad (5)$$

Now, we consider an arbitrary physical quantity Q expressed in the $MLTI$ and $LTI\emptyset$ bases by the vectors of exponents $\boldsymbol{r} = [r_1\ \ r_2\ \ r_3\ \ r_4]^T$ and $\boldsymbol{R} = [R_1\ \ R_2\ \ R_3\ \ R_4]^T$. Our aim is to find the transformation matrix $\boldsymbol{T}$ that transforms the vector of exponents $\boldsymbol{R}$ in the $LTI\emptyset$ basis to the vector of exponents $\boldsymbol{r}$ in the $MLTI$ basis. The dimension $[Q]$ of Q is given by

$$[Q] = M^{r_1}\, L^{r_2}\, T^{r_3}\, I^{r_4} = L^{R_1}\, T^{R_2}\, I^{R_3}\, \emptyset^{R_4} = (L^{-2}\, T^3\, I\, \emptyset)^{r_1}\, L^{r_2}\, T^{r_3}\, I^{r_4} = L^{R_1}\, T^{R_2}\, I^{R_3}\, (M\, L^2\, T^{-3}\, I^{-1})^{R_4},$$

and hence, the various exponents are related by

$$R_1 = -2r_1 + r_2,\ R_2 = 3r_1 + r_3,\ R_3 = r_1 + r_4,\ R_4 = r_1. \quad (6)$$

$$r_1 = R_4,\ r_2 = R_1 + 2\,R_4,\ r_3 = R_2 - 3\,R_4,\ r_4 = R_3 - R_4\ . \quad (7)$$

These scalar relations can be written as a pair of matrix equations

$$\boldsymbol{r} = \boldsymbol{TR},\ \boldsymbol{R} = \boldsymbol{T^{-1}}\,\boldsymbol{r}. \quad (8)$$

The two matrix equations (8) are conveniently displayed in scalar form in Fig. 1, in which the column vector at the right of the square transformation matrix $\boldsymbol{T}$ or its inverse $\boldsymbol{T^{-1}}$ is written as a row vector on top of the matrix [49, 53-59, 69], and the equality sign is omitted and implicitly understood. The four vectors comprising the transformation matrix $\boldsymbol{T}$ are the vectors of exponents for the variables L, T, I, and $\emptyset$ in the $MLTI$ basis, while the four vectors comprising the inverse transformation matrix $\boldsymbol{T^{-1}}$ are the vectors of exponents for the variables M, L, T, and I in the $LTI\emptyset$ basis. In Fig. 1, $\boldsymbol{T}\,\boldsymbol{T^{-1}} = \boldsymbol{T^{-1}}\,\boldsymbol{T} = \boldsymbol{I}$, as required.

	R_1	R_2	R_3	R_4
r_1	**0**	**0**	**0**	**1**
r_2	**1**	**0**	**0**	**2**
r_3	**0**	**1**	**0**	**−3**
r_4	**0**	**0**	**1**	**−1**

	r_1	r_2	r_3	r_4
R_1	**−2**	**1**	**0**	**0**
R_2	**3**	**0**	**1**	**0**
R_3	**1**	**0**	**0**	**1**
R_4	**1**	**0**	**0**	**0**

Figure 1. Convenient display for the transformations $\boldsymbol{r} = \boldsymbol{TR}$ and $\boldsymbol{R} = \boldsymbol{T^{-1}}\,\boldsymbol{r}$ from the $LTI\emptyset$ dimensional basis to the $MLTI$ dimensional basis and back.

The two matrix equations (8) can be used to construct a table of dimensional exponents for all electromechanical quantities of interest in both the mechanically-oriented $MLTI$ dimensional basis and the electromagnetically-oriented $LTI\emptyset$ dimensional basis. Such a table has appeared earlier in Thomas [64], and is split here into two tables (Table 2 and Table 3) in order to give further explanations (in forthcoming sections) of the concept of duality in electromagnetism.

4. Transformation Derivation via the Gauss-Jordan Algorithm

Throughout this paper, we consider that a sought product π_j of a set of physical variables is dimensionless if, and only if, the exponents of these variables are a solution of the set of p homogeneous linear equations (not necessarily linearly independent) in n unknowns,

expressed in matrix form as [33, 43, 49, 53-59, 62]:

$$\boldsymbol{D}\boldsymbol{z} = \boldsymbol{0}, \tag{9}$$

where $\boldsymbol{D}$ is the $p \times n$ dimensional matrix. This matrix has p rows ($p \leq N$), which represent the adopted fundamental reference dimensions or elements of the dimensional basis, and n columns, which denote the variable exponents in the sought dimensionless product, or, with a gross (albeit common and appealing) abuse of notation, designate the variables themselves. We will designate a column twice: (a) by the correct exponent notation, and (b) by the common variable notation. A typical entry of this matrix is the exponent to which a reference dimension (row) is raised in the dimensional product formula representing the particular variable (column).

The vector $\boldsymbol{z}$ comprises the n variable exponents in the sought dimensionless product, which are unknown constants, yet to be interrelated (partially determined). The Gauss-Jordan algorithm [60] achieves this purpose of inter-relating the exponents by applying elementary row operations that transform the matrix $\boldsymbol{D}$ into a reduced row echelon form (RREF). The vector of exponents $\boldsymbol{z}$ is not written as a column vector to the right of the dimensional matrix as suggested by Eq. (9), but is written (in a non-conventional way) as a row vector on top of it [53-59, 69]. In addition, the equality sign in Eq. (9) is omitted and implicitly understood, while the zero vector in the R.H.S. of Eq. (9) is added as an extra vector for $\boldsymbol{D}$ resulting in an *augmented matrix*, to whose entire rows we apply the same elementary row operations in the tableaus of the Gauss-Jordan (GJ) algorithm. Such operations are explained by assignment operations written in the leftmost column of the algorithm tableaus, wherein ${E_i}^{(k)}$ denotes the equation of augmented row i at stage k of the algorithm. The structure so obtained constitute standard Gauss-Jordan tableaus and is exemplified by the tableaus in Tables 1 and 4-11.

As a prelude to employing the Gauss-Jordan procedure in solving DA problems, we report herein an unusual application for it as an alternative instructive means for deriving the transformations in Eqs. (6-8). Table 1 uses the Gauss-Jordan procedure for moving from the mechanically-oriented $MLTI$ dimensional basis to the electromagnetically-oriented $LTI\emptyset$ dimensional basis and back. The table involves six exponents (m, l, t, i, f and q), which correspond to the variables $M, L, T, I, \emptyset$ and Q, and hence it covers all variables of the $MLTI$ and $LTI\emptyset$ bases as well as the quantity of interest Q (not to be confused with the electric charge). The table consists of five stages, of which each of stages 0, 2, and 4 has a specified dimensional basis (while each of the remaining stages lacks such a basis). Stage 0 (and also its identical stage 4) is characterized by the $MLTI$ dimensional basis, since the submatrix of $\boldsymbol{D}$ under the $M, L, T,$ and I variables is a unit matrix, while stage 2 is characterized by the $LTI\emptyset$ dimensional basis, since the submatrix of $\boldsymbol{D}$ under the L, T, I and $\emptyset$ variables is a unit matrix. Therefore, the column under the variable of interest Q is its vector of dimensional exponents, which is $\boldsymbol{r}$ in stages 0 and 4 (of the $MLTI$ basis) and $\boldsymbol{R}$ in stage 2 (of the $LTI\emptyset$ basis).

Table 1 elegantly recovers the transformations in Eqs. (6-8) that are displayed in Fig. 1. In fact, it does so *twice*, consistently giving the same result. On one hand, the scalar values expressed in the Q column recover Eq. (6) at stage 2 and recover Eq. (7) at stage 4. On the other hand, going in column Q from $\boldsymbol{r}$ at stage 0 to $\boldsymbol{R}$ at stage 2 amounts to a left multiplication of the entire matrix by the inverse transformation matrix $\boldsymbol{T^{-1}}$, and going in the same column from $\boldsymbol{R}$ at stage 2 to $\boldsymbol{r}$ at stage 4 amounts to a left multiplication, again of the entire matrix, by the transformation matrix $\boldsymbol{T}$ itself**.** Therefore, the submatrix of $\boldsymbol{D}$ under the $M, L, T,$ and I variables (which is a unit matrix in stage 2) is the transformation matrix $\boldsymbol{T}$ in each of stages 0 and 4 (highlighted in pale bluish-green). Likewise, the submatrix of $\boldsymbol{D}$ under the L, T, I and $\emptyset$ variables (which is a unit matrix in stages 0 and 4) is the inverse matrix $\boldsymbol{T^{-1}}$ in stage 2 (highlighted in pale orange).

This present situation is reminiscent of the initial and final tableaus in *the Simplex Method*

used for solving linear-programming problems [54]. In the Simplex Method, the $MLTI$ variables depart their list of basic variables in stage 0, so that the $LTI\emptyset$ variables can enter this list (replacing them one by one) in stage 2. The only difference between the two situations is that: in the present case these entering and departing variables are known *a priori*, while in the linear-programming case, each entering or departing variable is selected at a specific step, according to rules dictated by some objective function [54].

We stress that though Table 1 outlines a specific procedure that is apparently of a limited value (one for moving from the $MLTI$ dimensional basis to the $LTI\emptyset$ one, and *vice versa*), that table can be modified to handle the matrix transformation and inverse transformation (if any) between any two dimensional bases.

5. Dimensional Exponents for EM and non-EM Quantities

The electromagnetically-oriented $LTI\emptyset$ dimensional basis is a four-dimensional basis that devotes two of its four reference dimensions to two electromagnetic (EM) quantities, electric current and electric potential (or voltage), which happen to be dual. As a result, this basis relates the $LTI\emptyset$ vectors of indices

$\boldsymbol{R}^a = [{R_1}^a \ {R_2}^a \ {R_3}^a \ {R_4}^a]^T$ and $\boldsymbol{R}^b = [{R_1}^b \ {R_2}^b \ {R_3}^b \ {R_4}^b]^T$ of two dual EM quantities a and b as follows

$$ {R_1}^a = {R_1}^b , \tag{10a} $$

$$ {R_2}^a = {R_2}^b , \tag{10b} $$

$$ {R_3}^a = {R_4}^b , \tag{10c} $$

$$ {R_4}^a = {R_3}^b . \tag{10d} $$

Equations (10) indicate that any two dual EM quantities have identical L and T exponents, and swapped I and $\emptyset$ exponents in the $LTI\emptyset$ basis. Table 2 displays dimensional exponents of pairs of dual electromagnetic quantities in the mechanically-oriented $MLTI$ dimensional basis and the electromagnetically-oriented $LTI\emptyset$ dimensional basis.

A physical quantity such that

$r_4 = 0$, or equivalently,

$$ R_3 = R_4 , \tag{11} $$

is a self-dual quantity (in the electromagnetic (EM) sense), i.e., a quantity that lacks an EM dimension genuinely or through cancellation. A self-dual quantity might be

a) A genuine non-EM quantity, such as any of the six fundamental quantities of mass, length, time, temperature, amount of substance, luminous intensity, as well as many quantities composed solely of these six quantities. Note that the aforementioned six fundamental quantities are precisely the seven fundamental SI dimensions with the electromagnetic dimension excluded.
b) A product of two dual EM quantities, such as $\epsilon\mu, LC, VI, \boldsymbol{E} \times \boldsymbol{H}$ and QΦ (see Table 2), where each of the original EM quantities violates each of the two equivalent conditions (11). Note that two dual quantities of exponents $\boldsymbol{R}^a$ and $\boldsymbol{R}^b$ satisfying (10) have a product of indices $2{R_1}^a, 2{R_2}^a, {R_3}^a + {R_4}^a$ and ${R_4}^a + {R_3}^a$, and hence it satisfies each of the two equivalent conditions of self-duality (11).

In Table 2, the exponent R_1 for the length dimension in the $LTI\emptyset$ dimensional basis is such that:

- $R_1 = 0$ for the lumped quantities I, V, L, C, Z, R, Y and G, in addition to the quantities Q and Φ which are the time integrals of the fundamental quantities I and $\emptyset$.

Table 1. The Gauss-Jordan procedure for moving from the mechanically-oriented $MLTI$ dimensional basis to the electromagnetically-oriented $LTI\emptyset$ dimensional basis and back.

	Stage Number	M	L	T	I	$\emptyset$	Q	
		m	l	t	i	f	q	
$E_1{}^{(0)}$	0	1	0	0	0	1	r_1	0
$E_2{}^{(0)}$		0	1	0	0	2	r_2	0
$E_3{}^{(0)}$		0	0	1	0	-3	r_3	0
$E_4{}^{(0)}$		0	0	0	1	-1	r_4	0
$E_1{}^{(1)} \leftarrow E_2{}^{(0)}$	1	0	1	0	0	2	r_2	0
$E_2{}^{(1)} \leftarrow E_3{}^{(0)}$		0	0	1	0	-3	r_3	0
$E_3{}^{(1)} \leftarrow E_4{}^{(0)}$		0	0	0	1	-1	r_4	0
$E_4{}^{(1)} \leftarrow E_1{}^{(0)}$		1	0	0	0	1	r_1	0
$E_1{}^{(2)} \leftarrow E_1{}^{(1)} - 2E_4{}^{(1)}$	2	-2	1	0	0	0	$R_1 = -2r_1 + r_2$	0
$E_2{}^{(2)} \leftarrow E_2{}^{(1)} + 3E_4{}^{(1)}$		3	0	1	0	0	$R_2 = 3r_1 + r_3$	0
$E_3{}^{(2)} \leftarrow E_3{}^{(1)} + E_4{}^{(1)}$		1	0	0	1	0	$R_3 = r_1 + r_4$	0
$E_4{}^{(2)} \leftarrow E_4{}^{(1)}$		1	0	0	0	1	$R_4 = r_1$	0
$E_1{}^{(3)} \leftarrow E_4{}^{(2)}$	3	1	0	0	0	1	R_4	0
$E_2{}^{(3)} \leftarrow E_1{}^{(2)}$		-2	1	0	0	0	R_1	0
$E_3{}^{(3)} \leftarrow E_2{}^{(2)}$		3	0	1	0	0	R_2	0
$E_4{}^{(3)} \leftarrow E_3{}^{(2)}$		1	0	0	1	0	R_3	0
$E_1{}^{(4)} \leftarrow E_1{}^{(3)}$	4	1	0	0	0	1	$r_1 = R_4$	0
$E_2{}^{(4)} \leftarrow E_2{}^{(3)} + 2\,E_1{}^{(3)}$		0	1	0	0	2	$r_2 = R_1 + 2\,R_4$	0
$E_3{}^{(4)} \leftarrow E_3{}^{(3)} - 3\,E_1{}^{(3)}$		0	0	1	0	-3	$r_3 = R_2 - 3\,R_4$	0
$E_4{}^{(4)} \leftarrow E_4{}^{(3)} - E_1{}^{(3)}$		0	0	0	1	-1	$r_4 = R_3 - R_4$	0

- $R_1 = -1$ for the per-line quantities H, E, μ and $\in$. Among these, the vector quantities $\boldsymbol{H}$ and $\boldsymbol{E}$ frequently appear in the form $\boldsymbol{H}.\boldsymbol{dl}$ and $\boldsymbol{E}.\boldsymbol{dl}$ **(**with $\boldsymbol{dl}$ depicting infinitesimal length**)**, which are conveniently represented as 1-(differential) forms Hdl and Edl, or as integrands over curves (quantities

that can be integrated along a one-dimensional curve) [6-9].

- $R_1 = -2$ for the per-surface quantities $\boldsymbol{B}$ and $\boldsymbol{D}$. These frequently appear in the form $\boldsymbol{B}.\boldsymbol{ds}$ and $\boldsymbol{D}.\boldsymbol{ds}$ **(**with $\boldsymbol{ds}$ depicting infinitesimal area**)**, which are conveniently represented as 2-(differential) forms Bds and Dds, or as integrands over surfaces (quantities that can be integrated over a two-dimensional surface) [6-9].
- $R_1 = -3$ for the per-volume quantities $\boldsymbol{B}.\boldsymbol{H}$ and $\boldsymbol{D}.\boldsymbol{E}$. These frequently appear in the form $\boldsymbol{B}.\boldsymbol{H}\,dV$ and $\boldsymbol{D}.\boldsymbol{E}\,dV$ **(**with dV depicting infinitesimal volume**)**, which are conveniently represented as 3-(differential) forms $BHdl$ and $DEdl$, or integrands over volumes (quantities that can be integrated over a three-dimensional space) [6-9].

Table 2. Dimensions of pairs of dual EM quantities in the mechanically-oriented $\boldsymbol{MLTI}$ dimensional basis and the electromagnetically-oriented $\boldsymbol{LTI\emptyset}$ dimensional basis.

Physical Quantity	Symbol	The $MLTI$ Dimensional Basis				The $LTI\emptyset$ Dimensional Basis			
		r_1	r_2	r_3	r_4	R_1	R_2	R_3	R_4
Electric current	I	0	0	0	1	0	0	1	0
Electric voltage	V	1	2	−3	−1	0	0	0	1
Magnetic field intensity	H	0	−1	0	1	−1	0	1	0
Electric field intensity	E	1	1	−3	−1	−1	0	0	1
Permeability	μ	1	1	−2	−2	−1	1	−1	1
Permittivity	$\in$	−1	−3	4	2	−1	1	1	−1
Magnetic flux density	B	1	0	−2	−1	−2	1	0	1
Electric flux density	D	0	−2	1	1	−2	1	1	0
Magnetic flux	Φ	1	2	−2	−1	0	1	0	1
Electric Charge	Q	0	0	1	1	0	1	1	0
Inductance	L	1	2	−2	−2	0	1	−1	1
Capacitance	C	−1	−2	4	2	0	1	1	−1
Impedance, resistance or	Z, R or	1	2	−3	−2	0	0	−1	1
Admittance, conductance	Y, G or	−1	−2	3	2	0	0	1	−1
Magnetic dot product	B.H	1	−1	−2	0	−3	1	1	1
Electric dot product	D.E	1	−1	−2	0	−3	1	1	1

In line with the observations above, Thomas [64] point out that the $LTI\emptyset$ dimensional basis justifies the unit names of farad/m and henry/m assigned to permittivity $\in$ and permeability μ when compared with the unit names of farad and henry given to capacitance C and inductance L. Likewise, this basis justifies the unit names of field intensities: H (ampere/m) and E (volt/m), as well as those of flux densities: B (weber/m^2) and D (coulomb/m^2).

Table 3 displays dimensional exponents of self-dual physical quantities in the $MLTI$ dimensional basis and the $LTI\emptyset$ dimensional basis. The quantities in this table are partitioned as mass-independent quantities with rather simple $LTI\emptyset$ exponents (highlighted in pale blue) and mass-dependent ones with rather non-simple $LTI\emptyset$ exponents (highlighted in pale orange). According to Eq. (11), these quantities do not need an electromagnetic dimension ($r_4 = 0$), and can be described in the MLT basis (which was sufficient before the era of electricity and magnetism). For all quantities in Tables 2 and 3, the absolute value of each of the two electromagnetic exponents is bounded and does not exceed one ($R_3, R_4 \in \{-1,0,1\}$).

Tables 2 and 3 clearly indicate that representations of electromagnetic quantities in the $LTI\emptyset$

basis (compared with the standard $MLTI$ basis) are more informative, much simpler, and partially self-checking (thanks to the boundedness of the two electromagnetic exponents and the inter-relations (10) among exponents of dual quantities). Our thesis herein is that the $LTI\emptyset$ basis should be the one of choice in the matrix solution of dimensional-analysis problems involving predominantly electromagnetic quantities.

The following section demonstrates, by way of examples, that DA computations of electromagnetic problems via the Gauss-Jordan algorithm in the $LTI\emptyset$ basis are more efficient, much less error prone, and quicker to detect linear dependencies (if any) in the dimensional equations.

6. Various Examples Comparing the $LTI\emptyset$ and $MLTI$ Dimensional Bases

6.1. Transient analysis of an RL parallel circuit

This subsection deals with a problem of electric-circuit theory, which models the lumped special case of the (generally distributed) electromagnetic phenomena.

Let us consider the situation in which a DC current source of constant value I is imposed for time $t \geq 0$ on a parallel combination of a resistance R and an inductance L (Figure 2).

The transient voltage $v(t)$ on this parallel combination is required for time $t \geq 0$, and hence the variable v must be a regime variable [53, 54, 70], and it is placed last in a proposed dimensionless product

$$\pi = k\ L^l\ R^r\ I^i\ t^\tau\ v^V, \qquad (12)$$

where k is a dimensionless constant. The most important variable among the remaining variables is t, and it is placed immediately before v. Table 4 demonstrates the Gauss-Jordan procedure for solving this problem in the $LTI\emptyset$ dimensional basis, while Table 5 demonstrates the same procedure for solving this problem in the $MLTI$ dimensional basis. Here, $p = 4,\ n = 5$, and $r = 3$. The same final solution is obtained in both tables. However, the $LTI\emptyset$-based solution is obviously more efficient, entails simpler numbers (all of which are integers belonging to $\{-1, 0, 1\}$), and hence it is less error prone, and it also detects linear dependency (manifested by an all-0 row) from the outset. The operations involved in the two tables include the following operations (arranged in decreasing complexity): floating-point row computation (f), row summation or differencing (s), row negation (n), and row assignment (a). The $LTI\emptyset$-based solution requires 2 stages beyond the initial stage involving $(3s + 3a)$ operations. The $MLTI$-based solution requires also 2 stages beyond the initial stage involving $(3f + s + n + 2a)$ operations.

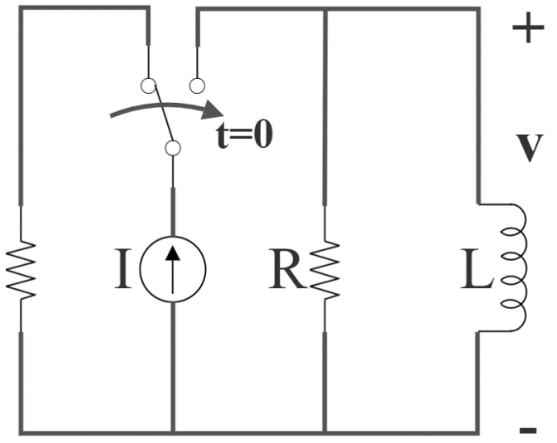

Figure 2. An electric circuit with a constant current source imposed at time 0 on a parallel combination of a resistor and inductor.

At the last stage of each solution, the $p \times n$ dimensional matrix $\boldsymbol{D}$ would be changed to an $r \times n$ matrix that is partitioned into two parts. The left part is an $r \times r$ unit matrix (shaded in light blue) and the right part is an $r \times (n - r)$ matrix $\boldsymbol{C}$ (shaded in dark blue). We now construct a full-rank $(n - r) \times n$ matrix $\boldsymbol{K}$ of exponents depicting the dimensionless products as shown at the bottom of Table 4 and Table 5. This product matrix is comprised of two juxtapositioned matrices: (a) the negative transpose $-\boldsymbol{C}^{\boldsymbol{T}}$, an $(n - r) \times r$ matrix (shaded in dark green), which is obtained by negating and transposing $\boldsymbol{C}$ (the right part of the last stage of the dimensional matrix after implementing the Gauss-Jordan algorithm, of course, after removing the all-zero row), and (b) an $(n - r) \times (n - r)$ unit matrix (shaded in light green) [54]. The matrix $\boldsymbol{K}$ is called the nullspace or kernel of $\boldsymbol{D}$, and is such that $rank(\boldsymbol{K}) = (n - r)$ is the nullity or defect of $\boldsymbol{D}$, the $(n - r)$ by p matrix $\boldsymbol{K}\boldsymbol{D}^{\mathbf{T}}$ is a zero matrix, and the $(n - r)$ rows of $\boldsymbol{K}$ form a basis for the nullspace of $\boldsymbol{D}$ [54, 62]

Table 3. Dimensions of individual self-dual ($r_4 = 0$ or $R_3 = R_4 \epsilon \{-1, 0, 1\}$) physical quantities in the $MLTI$ mechanically-oriented dimensional basis and the electromagnetically-oriented $LTI\emptyset$ dimensional basis.

Physical Quantity	Symbol	The $MLTI$ Dimensional Basis				The $LTI\emptyset$ Dimensional Basis			
		r_1	r_2	r_3	r_4	R_1	R_2	R_3	R_4
Mass	M	1	0	0	0	−2	3	1	1
Length	L	0	1	0	0	1	0	0	0
Time	t	0	0	1	0	0	1	0	0
Wavenumber	k	0	−1	0	0	−1	0	0	0
Frequency	ν	0	0	−1	0	0	1	0	0
Area	A	0	2	0	0	2	0	0	0
Volume	V	0	3	0	0	3	0	0	0
Moment of inertia	I	1	2	0	0	0	3	1	1
(Volumetric) density (of	ρ	1	−3	0	0	−5	3	1	1
Area density of mass	ρ_s	1	−2	0	0	−4	3	1	1
Linear density of mass	ρ_l	1	−1	0	0	−3	3	1	1
Specific volume	v	−1	3	0	0	5	−3	−1	−1
Humidity	η	1	−3	0	0	−5	3	1	1
Mass flow rate	q_m	1	0	−1	0	−2	2	1	1
Volumetric flow rate	q	0	3	−1	0	3	−1	0	0
Velocity	$\boldsymbol{v}$	0	1	−1	0	1	−1	0	0
Angular velocity	$\boldsymbol{\omega}$	0	0	−1	0	0	−1	0	0
Acceleration	$\boldsymbol{a}$	0	1	−2	0	1	−2	0	0
Angular acceleration	ω_a	0	0	−2	0	0	−2	0	0
Momentum	$\boldsymbol{p}$	1	1	−1	0	−1	2	1	1
Angular momentum	$\boldsymbol{L}$	1	2	−1	0	0	2	1	1
Force	$\boldsymbol{F}$	1	1	−2	0	−1	1	1	1
Pressure or stress	$\boldsymbol{P}$ or $\boldsymbol{\sigma}$	1	−1	−2	0	−3	1	1	1
Dynamic viscosity	μ	1	−1	−1	0	−3	2	1	1
Kinematic viscosity	μ	0	2	−1	0	2	−1	0	0
Work or energy	E	1	2	−2	0	0	1	1	1
Torque	T	1	2	−2	0	0	1	1	1
Power	P	1	2	−3	0	0	0	1	1
Volumetric density of en-	U	1	−1	−2	0	−3	1	1	1
Planck's constant	h	1	2	−1	0	0	2	1	1
Gravitational constant	h	−1	3	−2	0	5	−5	−1	−1
Hubble's constant	H	0	0	−1	0	0	−1	0	0

Each of the two identical versions of the matrix $\boldsymbol{K}$ at the bottom of Tables 4 and 5 indicates that there are two products:

$\pi_1 = tR/L = t/(L/R)$ and $\pi_2 = v/RI$, which constitute a (non-unique) complete set of dimensionless products. These two products are called regimes for the regime variables v and t [53, 70]. According to Buckingham Pi Theorem, these two dimensionless products are related by an arbitrary function Φ equated to zero, namely:

$$\Phi\,(\pi_1\,, \pi_2) = 0. \tag{13}$$

Finally the mathematical model of the transient voltage v can be stated by expressing its regime π_2 as an arbitrary function Ψ (to be determined experimentally) of the other regime, namely

$$\pi_2 = \Psi\,(\pi_1). \tag{14}$$

It is known (outside the scope of dimensional analysis, through the theory of first-order linear ordinary differential equations) that the function Ψ is a decaying exponential, namely.

$$v/RI = exp\,(-t/(L/R)\,). \qquad (14a)$$

This result is usually referred to as the exponential relaxation of a first-order (single-time-constant) linear circuit or a first-order linear ordinary differential equation. The transients in the circuit in Fig. 1 are described by a single time constant $(\tau = L/R)$, where $[\tau] = [L]/[R] = (T\emptyset/I)/(\emptyset/I) = T$, i.e., by a parameter τ, which has the dimensions of time, indeed.

In retrospect, we might have not insisted on taking voltage and time as regime variables. Table 6 shows an alternative ordering of variables for the $LTI\emptyset$-based solution in Table 4, in which the regime variables are taken (arbitrarily, and ignoring the problem requirements) as the inductance and resistance. Here, the Gauss-Jordan algorithm does absolutely nothing beyond constructing its initial tableau. Now, we obtain two products: $\pi_3 = IL/vt$ and $\pi_4 = RI/v$ which constitute another complete set of dimensionless products. This new complete set is related to the old one via

$$\pi_3 = 1/(\pi_1\,\pi_2),\ \ \pi_4 = 1/\pi_2, \qquad (15a)$$

$$\pi_1 = \pi_4/\pi_3,\ \ \pi_2 = 1/\pi_4. \qquad (15b)$$

Table 7 shows yet another ordering of variables for the $LTI\emptyset$-based solution in Table 4. Since the rank of the dimensional matrix is now known to be 3, this ordering suggests that the variables are partitioned into a set $\{t, L, R\}$ of basis variables and a set $\{v, I\}$ of regime variables. An advantage of the Gauss-Jordan algorithm is that it detects the impossibility of this partitioning and corrects it *en route.* Contrary to widespread belief, the Gauss-Jordan algorithm does not necessarily partition $\boldsymbol{D}$ into two matrices such that the first of which is a unit matrix. Generally, the Gauss-Jordan algorithm replaces $\boldsymbol{D}$ by its reduced row echelon form (RREF) [54], an example of which is shown in the second stage of Table 7. In this more general (albeit less appealing situation), the algorithm employs two correct sets of basis and regime variables as $\{t, L, v\}$ and $\{R, I\}$ by swapping the roles of the variables R and v as basis or regime variables.

Table 4. The Gauss-Jordan procedure for solving the circuit problem of Sec. 6.1 in the $LTI\emptyset$ dimensional basis. The final stage of matrix $\boldsymbol{D}$ is shaded in blue (partitioned into a unit matrix in light blue, followed by $\boldsymbol{C}$ in dark blue), while the matrix $\boldsymbol{K}$ is shaded in green (partitioned into the negative transpose of matrix $\boldsymbol{C}$ in dark green, followed by a unit matrix in light green).

	l	i	r	τ	V	
	L	I	R	t	v	
$E_1^{(0)}$	0	0	0	0	0	0
$E_2^{(0)}$	1	0	0	1	0	0
$E_3^{(0)}$	−1	1	−1	0	0	0
$E_4^{(0)}$	1	0	1	0	1	0
$E_2^{(1)} \leftarrow E_2^{(0)}$	1	0	0	1	0	0
$E_3^{(1)} \leftarrow E_3^{(0)} + E_2^{(0)}$	0	1	−1	1	0	0
$E_4^{(1)} \leftarrow E_4^{(0)} - E_2^{(0)}$	0	0	1	−1	1	0
$E_2^{(2)} \leftarrow E_2^{(1)}$	1	0	0	1	0	0
$E_3^{(2)} \leftarrow E_3^{(1)}+E_4^{(1)}$	0	1	0	0	1	0
$E_4^{(2)} \leftarrow E_4^{(1)}$	0	0	1	−1	1	0
π_1	−1	0	1	1	0	
π_2	0	−1	−1	0	1	

Table 5. The Gauss-Jordan procedure for solving the circuit problem of Sec. 6.1 in the *MLTI* dimensional basis.

	l	r	i	τ	V	
	L	R	I	t	v	
${E_1}^{(0)}$	1	1	0	0	1	0
${E_2}^{(0)}$	2	2	0	0	2	0
${E_3}^{(0)}$	−2	−3	0	1	−3	0
${E_4}^{(0)}$	−2	−2	1	0	−1	0
${E_1}^{(1)} \leftarrow {E_1}^{(0)}$	1	1	0	0	1	0
${E_2}^{(1)} \leftarrow {E_2}^{(0)} - 2\,{E_1}^{(0)}$	0	0	0	0	0	0
${E_3}^{(1)} \leftarrow {E_3}^{(0)} + 2\,{E_1}^{(0)}$	0	−1	0	1	−1	0
${E_4}^{(1)} \leftarrow {E_4}^{(0)} + 2\,{E_1}^{(0)}$	0	0	1	0	1	0
${E_1}^{(2)} \leftarrow {E_1}^{(1)} + {E_3}^{(1)}$	1	0	0	1	0	0
${E_3}^{(2)} \leftarrow -{E_3}^{(1)}$	0	1	0	−1	1	0
${E_4}^{(2)} \leftarrow {E_4}^{(1)}$	0	0	1	0	1	0
π_1	−1	1	0	1	0	0
π_2	0	−1	−1	0	1	0

Table 6. The Gauss-Jordan procedure for solving the circuit problem of Sec. 6.1 in the *LTIØ* dimensional basis with an alternative ordering of variables.

	τ	i	V	l	r	
	t	I	v	L	R	
${E_1}^{(0)}$	0	0	0	0	0	0
${E_2}^{(0)}$	1	0	0	1	0	0
${E_3}^{(0)}$	0	1	0	−1	−1	0
${E_4}^{(0)}$	0	0	1	1	1	0
π_3	−1	1	−1	1	0	
π_4	0	1	−1	0	1	

Now, the three basis variables t, L, and v are not assigned to consecutive columns, and though the matrix under them is, in fact, a unit matrix, it might not readily appear as such (due to lack of visual adjacency). In the lower part of Table 7, we interchange the columns for R and v so as to place all columns with pivots consecutively at the left to form an identity matrix. Both parts of Table 7 yield the two products: $\pi_5 = tR/L$ and $\pi_6 = IL/vt$, which constitute yet another complete set of dimensionless products, again related to the earlier sets, since π_5 and π_6 are equal to π_1 and π_3, respectively. The total number of complete sets of dimensionless products is at most (here strictly less than) the number of choosing two regime variables out of five variables (without order or repetition), which is ten [53].

The non-uniqueness of the complete set of dimensionless products is occasionally cited as a limitation of dimensional analysis [54]. However, we note that Eq. (14) is the desirable solution of the problem, and it can be reached in a variety of ways, such as directly from Table 4, or via Table 6 together with Eqs. (15b).

Results similar to those of this subsection are obtained by Middendorf [33] and Rushdi & Rushdi [57] for the dual problem in which a DC *voltage* source of value V is imposed for time $t \geq 0$ on a *series* combination of a *resistance* R and a *capacitance* C, and wherein the transient *current* $i(t)$ is required. For both problems, the dimension of length L is dispensable with, in the sense that (a) the dimensional basis $LTI\emptyset$ can be replaced by its $TI\emptyset$ subset, since each of the pertinent variables has a zero exponent for the dimension of length L, and (b) an all-0 row appears right from the outset in the initial stage of the Gauss-Jordan algorithm. Generally, for circuit problems, the $LTI\emptyset$

dimensional basis (or its $TI\emptyset$ subset) has a definite advantage.

A very famous problem in electromagnetics is the problem of Coulomb, in which one seeks the inverse square law for the dependence of the far-field intensity of the electric field E on the distance from the origin r, at which a point source is located. To demonstrate the elegance and power of DA solutions, we solve a generalization of this problem. Specifically, we give a DA solution of a problem that comprises six primitive problems, one of which is the aforementioned problem of Coulomb. We will consider a general electric source S, located at (or in the vicinity of) the origin (practically located at the origin under the far-field assumption). This source has a dimension of $[S] = I\ T\ L^j$, and it might be

6.2. Far-Field Observations due to an Electric Source at the Origin

1. A point electric charge (monopole) $S = Q$ ($j = 0$, $[S] = I\ T$), located at the origin (0,0,0).
2. An electric dipole of moment $S = Qa$ ($j = 1$, $[S] = I\ T\ L$), comprising two charges of equal magnitudes and opposite signs: a positive charge $(+Q)$ located at $(a/2,0,0)$, and a negative one $(-Q)$ located at $(-a/2,0,0)$, where $a \ll r$.
3. An electric quadrupole of moment $S = Qa^2$ ($j = 2$, $[S] = I\ T\ L^2$), comprising four charges of equal magnitudes and alternating signs: a positive charge $(+Q)$ located at $(a/2, a/2,0)$, a negative one $(-Q)$ at $(a/2, -a/2,0)$, a second positive charge $(+Q)$ situated at $(-a/2, -a/2,0)$, and finally another negative charge $(-Q)$ located at $(-a/2, a/2,0)$, where $a \ll r$.
4. We also consider an observed quantity O of dimension $[O] = \emptyset\ L^{-i} = M\ L^{2-i}\ T^{-3}\ I^{-1}$, where this quantity can be the electric potential $\emptyset$ ($i = 0$), or the electric field intensity E ($i = 1$). The variable O must be a regime variable, and it is placed last in a proposed dimensionless product
5. $\pi = k\ r^R\ \epsilon^p\ S^s\ O^o$, (16)
6. where k is a dimensionless constant. Table 8 demonstrates the Gauss-Jordan procedure for solving this problem in the $LTI\emptyset$ dimensional basis, while Table 9 demonstrates the same procedure for solving this problem in the $MLTI$ dimensional basis. The same final solution is obtained in both tables. However, the $LTI\emptyset$-based solutions is obviously more efficient, and hence less error prone, and it is, once more, quicker to detect an all-0 row in the dimensional matrix. The $LTI\emptyset$-based solution requires 2 stages beyond the initial stage involving $(f + 4s + 2a)$ operations. The $MLTI$-based solution requires also 2 stages beyond the initial stage involving $(4f + s + n + 2a)$ operations.
7. Each of the two versions of the matrix $\boldsymbol{K}$ at the bottom of Tables 8 and 9 indicates that there is a single dimensionless product $\pi_1 = k\ r^{1+i+j}\ \epsilon^1\ S^{-1}\ O^1$. According to Buckingham Pi Theorem, this product must be a constant, and hence the observed quantity is
8. $O = k_{ij}\ S\ /(\epsilon\ r^{1+i+j})$. (17)
9. The far field potentials $\emptyset$ due to a charge ($S = Q$), a dipole ($S = Qa$), and a quadrupole ($S = Qa^2$) are $k_{00}\ Q\ /\ \epsilon\ r$, $k_{01}\ Qa\ /\ \epsilon\ r^2$, and $k_{02}\ Qa^2/\ \epsilon\ r^3$, respectively, while the corresponding far electric field intensities E are $k_{10}\ Q\ /\ \epsilon\ r^2$, $k_{11}\ Qa\ /\ \epsilon\ r^3$, and $k_{12}\ Qa^2/\ \epsilon\ r^4$, respectively. These results are in agreement with those derived by analytic techniques of electromagnetics [71]. In particular, we recover the celebrated inverse square law ($E = k_{10}\ Q\ /\ \epsilon\ r^2$) of Coulomb.

6.3. The leakage current through the electrolyte on a wet contaminated insulator

Piah and Darus [41] employed Dimensional Analysis to model the leakage current (I) due to the electrolyte formed on a wet contaminated insulator. The other variables included in the analysis were: the electrolyte conductivity (σ), the electrolyte volumetric flow rate (Q), environmental pressure (P), humidity (H), and the applied electric field (E). The variable I must be a regime variable [53, 54, 70], and it is placed last in a proposed dimensionless product

$$\pi = k\ \sigma^s\ Q^q\ P^p\ H^h\ E^e\ I^i, \quad (18)$$

where k is a dimensionless constant. The most important variable among the remaining variables is E, and it is placed immediately before I. Table 10 demonstrates the Gauss-Jordan procedure for solving this problem in the $LTI\emptyset$ dimensional basis, while Table 11 demonstrates the same procedure for solving this problem in the $MLTI$ dimensional basis. The same final solution is obtained in both tables, and it is in agreement with the one obtained earlier in [41]. However, the $LTI\emptyset$-based solution is only slightly more efficient, and hence somewhat less error prone. The $LTI\emptyset$-based solution requires 4 stages beyond the initial stage involving $(7f + 4s + 2n + 3a)$ operations. The $MLTI$-based solution requires also 4 stages beyond the initial stage involving $(10f + 3s + 2n + 2a)$ operations. The computations for this problem are dramatically more complex than those in the earlier subsections, and in this case the dimensional matrix is of full rank. The superiority of the $LTI\emptyset$-based solution is less pronounced in the present case (compared with the cases in the earlier subsections), since the present problem is not dominantly an electromagnetic one. Anyhow, the superiority of the $LTI\emptyset$-based solutions for dominantly electromagnetic DA problems was extensively verified by considering such problems in many and diverse recent publications [72-80].

In passing, we observe that the dimensional bases associated with the international system of units (SI system) have been claimed (criticized!) to suffer from inherent redundancy [22, 81].

Table 7. The Gauss-Jordan procedure for solving the circuit problem of Sec. 6.1 in the $LTI\emptyset$ dimensional basis, repeated twice for two different orderings of variables.

	τ	l	r	V	i	
	t	L	R	v	I	
$E_1{}^{(0)}$	0	0	0	0	0	0
$E_2{}^{(0)}$	1	1	0	0	0	0
$E_3{}^{(0)}$	0	-1	-1	0	1	0
$E_4{}^{(0)}$	0	1	1	1	0	0
$E_2{}^{(1)} \leftarrow E_2{}^{(0)} + E_3{}^{(0)}$	1	0	$\mathbf{-1}$	0	**1**	0
$E_3{}^{(1)} \leftarrow -E_3{}^{(0)}$	0	1	**1**	0	$\mathbf{-1}$	0
$E_4{}^{(1)} \leftarrow E_4{}^{(0)} + E_3{}^{(0)}$	0	0	**0**	1	**1**	0
π_5	**1**	$\mathbf{-1}$	1	**0**	0	
π_6	$\mathbf{-1}$	**1**	0	$\mathbf{-1}$	1	

	τ	l	V	r	i	
	t	L	v	R	I	
	1	0	0	$\mathbf{-1}$	**1**	0
	0	1	0	**1**	$\mathbf{-1}$	0
	0	0	1	**0**	**1**	0
π_5	**1**	$\mathbf{-1}$	**0**	1	0	
π_6	$\mathbf{-1}$	**1**	$\mathbf{-1}$	0	1	

Table 8. The Gauss-Jordan procedure for solving the far-field problem of Sec. 6.2 in the *LTIØ* dimensional basis.

	R	p	s	o	
	r	ϵ	S	O	
${E_1}^{(0)}$	1	-1	j	$-i$	0
${E_2}^{(0)}$	0	1	1	0	0
${E_3}^{(0)}$	0	1	1	0	0
${E_4}^{(0)}$	0	-1	0	1	0
${E_1}^{(1)} \leftarrow {E_1}^{(0)} + {E_2}^{(0)}$	1	0	$1+j$	$-i$	0
${E_2}^{(1)} \leftarrow {E_2}^{(0)}$	0	1	1	0	0
${E_3}^{(1)} \leftarrow {E_3}^{(0)} - {E_2}^{(0)}$	0	0	0	0	0
${E_4}^{(1)} \leftarrow {E_4}^{(0)} + {E_2}^{(0)}$	0	0	1	1	0
${E_1}^{(2)} \leftarrow {E_1}^{(1)} - (j+1){E_4}^{(1)}$	1	0	0	$-i-1-j$	0
${E_2}^{(2)} \leftarrow {E_2}^{(1)} - {E_4}^{(1)}$	0	1	0	-1	0
${E_4}^{(2)} \leftarrow {E_4}^{(1)}$	0	0	1	1	0
π_1	$1+i+j$	1	-1	1	

Table 9. The Gauss-Jordan procedure for solving the far-field problem of Sec. 6.2 in the *MLTI* dimensional basis.

	p	R	s	o	
	ϵ	r	S	O	
${E_1}^{(0)}$	-1	0	0	1	0
${E_2}^{(0)}$	-3	1	j	$2-i$	0
${E_3}^{(0)}$	4	0	1	-3	0
${E_4}^{(0)}$	2	0	1	-1	0
${E_1}^{(1)} \leftarrow -{E_1}^{(0)}$	1	0	0	-1	0
${E_2}^{(1)} \leftarrow {E_2}^{(0)} - 3\,{E_1}^{(0)}$	0	1	j	$-1-i$	0
${E_3}^{(1)} \leftarrow {E_3}^{(0)} + 4\,{E_1}^{(0)}$	0	0	1	1	0
${E_4}^{(1)} \leftarrow {E_4}^{(0)} + 2\,{E_1}^{(0)}$	0	0	1	1	0
${E_1}^{(2)} \leftarrow {E_1}^{(1)}$	1	0	0	-1	0
${E_2}^{(2)} \leftarrow {E_2}^{(1)} - j\,{E_3}^{(1)}$	0	1	0	$-1-i-j$	0
${E_3}^{(2)} \leftarrow {E_3}^{(1)}$	0	0	1	1	0
${E_4}^{(2)} \leftarrow {E_4}^{(1)} - {E_3}^{(1)}$	0	0	0	0	0
π_1	1	$1+i+j$	-1	1	

Such redundancy is manifested in many problems with electromechanical/ electromagnetic problems, in which the dimensional matrix in the $MLTI$ or $LTI\emptyset$ is not of full rank (see, for example, the problems in subsections 6.1 and 6.2). However, no redundancy appears in the problem of our current subsection, with the dimensional matrix being of full rank. To mitigate the purported redundancy, several authors suggested the use of a dimensional basis of three fundamental quantities only [22, 81]. One such basis uses the three quantities of length, time, and energy as fundamental quantities, and assumes 'voltage' to be dimensionless [22]. This basis shows no redundancy in handling the problems of subsections 6.1 and 6.2, as it produces full-rank matrices. However, it fails to reproduce the solution obtained herein by either the $MLTI$ basis or the $LTI\emptyset$ basis.

We have demonstrated that the $LTI\emptyset$ basis is the basis of choice in the matrix solution of dimensional-analysis problems involving predominantly electromagnetic quantities. Interestingly, the basis of choice in the matrix solution of dimensional-analysis problems involving predominantly mechanical quantities is not the familiar $MLTI$ basis, but seems to be a mechanical basis that is analogous to the $LTI\emptyset$ basis. In 'direct' electromechanical analogy mechanical force F is represented by voltage or potential $\emptyset$ and mechanical velocity v by electric current I, and hence, mass M is represented by inductance $\mathcal{L}$ and length L by electric charge Q, while time T is left intact [82-84]. This means that the $QTvF$ basis can be proposed as an efficient one for predominantly mechanical systems [64]. However, in 'inverse' or 'indirect' electromechanical analogy, mechanical force F is represented by electric current I and mechanical velocity v by voltage or potential $\emptyset$, and hence mass M is represented by admittance $\mathcal{C}$ and length L by magnetic flux Φ, while time T is again left intact [82-84]. This means that the ΦTFv basis can be another efficient one for predominantly mechanical systems. Unfortunately, the use of mass as a fundamental quantity in the familiar $MLTI$ basis is analogous to using inductance or admittance as a fundamental quantity in an electromagnetic dimensional system.

7. Conclusions

This paper proposed a novel approach of Dimensional Analysis, which makes the most of the Gauss-Jordan algorithm through the use of an electromagnetically-oriented basis (the $LTI\emptyset$ basis) for handling EM problems. The paper starts by investigating the issue of selecting fundamental dimensions for electromagnetics. The problem of transformations between the $LTI\emptyset$ basis and the $MLTI$ basis is subsequently explored, first by scalar techniques, and later by a novel application of the Gauss-Jordan algorithm. We list the dimensional exponents for EM and non-EM quantities in both the $LTI\emptyset$ and $MLTI$ bases, and point out certain superior features possessed by the $LTI\emptyset$ basis. Several illustrative examples expose the details of the proposed method, and demonstrate its merits and effectiveness.

Table 10. The Gauss-Jordan procedure for expressing the leakage current of Sec. 6.3 in the $LTI\emptyset$ dimensional basis.

	s	q	p	h	e	i	
	σ	Q	P	H	E	I	
${E_1}^{(0)}$	-1	3	-3	-5	-1	0	0
${E_2}^{(0)}$	0	-1	1	3	0	0	0
${E_3}^{(0)}$	1	0	1	1	0	1	0
${E_4}^{(0)}$	-1	0	1	1	1	0	0
${E_1}^{(1)} \leftarrow -{E_1}^{(0)}$	1	-3	3	5	1	0	0
${E_2}^{(1)} \leftarrow {E_2}^{(0)}$	0	-1	1	3	0	0	0
${E_3}^{(1)} \leftarrow {E_3}^{(0)} + {E_1}^{(0)}$	0	3	-2	-4	-1	1	0
${E_4}^{(1)} \leftarrow {E_4}^{(0)} - {E_1}^{(0)}$	0	-3	4	6	2	0	0
${E_1}^{(2)} \leftarrow {E_1}^{(1)} - 3\,{E_2}^{(1)}$	1	0	0	-4	1	0	0
${E_2}^{(2)} \leftarrow -{E_2}^{(1)}$	0	1	-1	-3	0	0	0
${E_3}^{(2)} \leftarrow {E_3}^{(1)} + 3\,{E_2}^{(1)}$	0	0	1	5	-1	1	0
${E_4}^{(2)} \leftarrow {E_4}^{(1)} - 3\,{E_2}^{(1)}$	0	0	1	-3	2	0	0
${E_1}^{(3)} \leftarrow {E_1}^{(2)}$	1	0	0	-4	1	0	0
${E_2}^{(3)} \leftarrow {E_2}^{(2)} + {E_3}^{(2)}$	0	1	0	2	-1	1	0
${E_3}^{(3)} \leftarrow {E_3}^{(2)}$	0	0	1	5	-1	1	0
${E_4}^{(3)} \leftarrow {E_4}^{(2)} - {E_3}^{(2)}$	0	0	0	-8	3	-1	0
${E_1}^{(4)} \leftarrow {E_1}^{(3)} + 4\,{E_4}^{(4)}$	1	0	0	0	$-4/8$	$4/8$	0
${E_2}^{(4)} \leftarrow {E_2}^{(3)} - 2\,{E_4}^{(4)}$	0	1	0	0	$-2/8$	$6/8$	0
${E_3}^{(4)} \leftarrow {E_3}^{(3)} - 5\,{E_4}^{(4)}$	0	0	1	0	$7/8$	$3/8$	0
${E_4}^{(4)} \leftarrow {E_4}^{(3)}/(-8)$	0	0	0	1	$-3/8$	$1/8$	0
π_1	$4/8$	$2/8$	$-7/8$	$3/8$	1	0	
π_2	$-4/8$	$-6/8$	$-3/8$	$-1/8$	0	1	

Table 11. The Gauss-Jordan procedure for expressing the leakage current of Sec. 6.3 in the *MLTI* dimensional basis.

	s	q	p	h	e	i	
	σ	Q	P	H	E	I	
${E_1}^{(0)}$	-1	0	1	1	1	0	0
${E_2}^{(0)}$	-3	3	-1	-3	1	0	0
${E_3}^{(0)}$	3	-1	-2	0	-3	0	0
${E_4}^{(0)}$	2	0	0	0	-1	1	0
${E_1}^{(1)} \leftarrow -{E_1}^{(0)}$	1	0	-1	-1	-1	0	0
${E_2}^{(1)} \leftarrow {E_2}^{(0)} - 3\,{E_1}^{(0)}$	0	3	-4	-6	-2	0	0
${E_3}^{(1)} \leftarrow {E_3}^{(0)} + 3\,{E_1}^{(0)}$	0	-1	1	3	0	0	0
${E_4}^{(1)} \leftarrow {E_4}^{(0)} + 2\ {E_1}^{(0)}$	0	0	2	2	1	1	0
${E_1}^{(2)} \leftarrow {E_1}^{(1)} + {E_3}^{(1)}$	1	-1	0	2	-1	0	0
${E_2}^{(2)} \leftarrow {E_2}^{(1)} + 4\,{E_3}^{(1)}$	0	-1	0	6	-2	0	0
${E_3}^{(2)} \leftarrow {E_3}^{(1)}$	0	-1	1	3	0	0	0
${E_4}^{(2)} \leftarrow {E_4}^{(1)} - 2\,{E_3}^{(1)}$	0	2	0	-4	1	1	0
${E_1}^{(3)} \leftarrow {E_1}^{(2)} - {E_2}^{(2)}$	1	0	0	-4	1	0	0
${E_2}^{(3)} \leftarrow -{E_2}^{(2)}$	0	1	0	-6	2	0	0
${E_3}^{(3)} \leftarrow {E_3}^{(2)} - {E_2}^{(2)}$	0	0	1	-3	2	0	0
${E_4}^{(3)} \leftarrow {E_4}^{(2)} + 2\,{E_2}^{(2)}$	0	0	0	8	-3	1	0
${E_1}^{(4)} \leftarrow {E_1}^{(3)} + 4\,{E_4}^{(4)}$	1	0	0	0	$-4/8$	$4/8$	0
${E_2}^{(4)} \leftarrow {E_2}^{(3)} + 6\,{E_4}^{(4)}$	0	1	0	0	$-2/8$	$6/8$	0
${E_3}^{(4)} \leftarrow {E_3}^{(3)} + 3\,{E_4}^{(4)}$	0	0	1	0	$7/8$	$3/8$	0
${E_4}^{(4)} \leftarrow {E_4}^{(3)}/(8)$	0	0	0	1	$-3/8$	$1/8$	0
π_1	$4/8$	$2/8$	$-7/8$	$3/8$	1	0	
π_2	$-4/8$	$-6/8$	$-3/8$	$-1/8$	0	1	

Acknowledgements

The authors are greatly indebted to Dr. Ahmad Ali Rushdi for the technical help he generously and proficiently offered during the preparation of this manuscript. They are really appreciative of his perseverance and his expertise. The authors are also grateful to an anonymous reviewer, who generously provided an in-depth and in-detail constructive criticism on an earlier version of this paper. This reviewer is a rare, albeit urgently needed, counter-example for many wide-spread assertions that belittle the role of peer review.

References

[1] Buckingham, E., On physically similar systems; Illustrations of the use of dimensional equations, *Physical Review*, 4(4): 345-376, (1914).

[2] Buckingham, E., The Principle of Similitude, *Nature*, 96(2405): 396-397 (1915).

[3] D'Agostino, S., A Historical Role for Dimensional Analysis in Maxwell's Electromagnetic Theory of Light. In *A History of the Ideas of Theoretical Physics* (pp. 45-75), Springer Netherlands (2000).

[4] Manfredi, G. (2013) Non-relativistic limits of Maxwell's equations, *European Journal of Physics*, 34(4): 859-872.

[5] Botchev, M. A., Faragó, I., and Horváth, R. Application of operator splitting to the Maxwell equations including a source term, *Applied Numerical Mathematics*, 59(3-4): 522-541 (2009).

[6] Deschamps, G. A. Electromagnetics and differential forms, *Proceedings of the IEEE*, 69(6): 676-696 (1981).

[7] Warnick, K. F., Selfridge, R. H., and Arnold, D. V., Teaching electromagnetic field theory using differential forms, *IEEE Transactions on Education*, 40(1): 53-68 (1997).

[8] Teixeira, F. L., and Chew, W. C., Differential forms, metrics, and the reflectionless absorption of electromagnetic waves, *Journal of Electromagnetic Waves and Applications*, 13(5): 665-686 (1999).

[9] Warnick, K. F., and Russer, P. H., Differential forms and electromagnetic field theory, *Progress In Electromagnetics Research*, 148: 83-112 (2014).

[10] Holm, G. R., The dimensional structure of the electromagnetic field, *American Journal of Physics*, 18(8): 509-514 (1950).

[11] Young, L., Electrical units and dimensions, *Transactions of the American Institute of Electrical Engineers, Part I: Communication and Electronics*, 75(6): 767-771 (1957).

[12] Kinitsky, V. A., Kalantaroff dimension system, *American Journal of Physics*, 30(2): 89-93 (1962).

[13] Guissard, A., Electrical units and electromagnetic field vectors, *IEEE Transactions on Education*, 15(1): 41-48 (1972).

[14] Spies, B. R., The derivation of absolute units in electromagnetic scale modeling, *Geophysics*, 41(5): 1042-1047 (1976).

[15] Leroy, B., Conversion of electromagnetic quantities from MKSA to Gaussian units (and vice versa) using dimensional analysis, *American Journal of Physics*, 52(3): 230-233 (1984).

[16] Brown, W., Tutorial paper on dimensions and units, *IEEE Transactions on Magnetics*, 20(1): 112-117 (1984).

[17] Studentsov, N. V., Unit systems and the fundamental constants, *Measurement Techniques*, 40(3), 197-202 (1997).

[18] D'Agostino, S., Absolute systems of units and dimensions of physical quantities: A link between Weber's electrodynamics and Maxwell's electromagnetic theory of light, *Physis-Firenze*, 33(1): 5-52 (1996).

[19] Young, L., Electromagnetic units and equations, *IEEE Transactions on Microwave Theory and Techniques*, 50(3): 1021-1027 (2002).

[20] Hehl, F. W., and Obukhov, Y. N., Dimensions and units in electrodynamics, *General Relativity and Gravitation*, 37(4): 733-749 (2005).

[21] Trifonov, I. S., A system of units for physical quantities involved in electromagnetics: an alternative to the International System of Units, *Journal of Communications Technology and Electronics*, 54(7): 783-790, (2009).

[22] Abdelhady, S., An Approach to a Universal System of Units, *Journal of Electromagnetic Analysis and Applications*, 2(9): 549-556 (2010).

[23] Olness, F., and Scalise, R., Regularization, renormalization, and dimensional analysis: Dimensional regularization meets freshman E&M. *American Journal of Physics*, 79(3): 306-312 (2011).

[24] Cooper, G., and Humphry, S. M., The ontological distinction between units and entities, *Synthese*, 187(2): 393-401 (2012).

[25] Selvan, K. T., Fundamentals of electromagnetic units and constants, IEEE *Antennas and Propagation Magazine*, 54(3): 100-114 (2012), Addendum, *ibid.*, 54(5): 130.

[26] Jaén, X., Bohigas, X., and Pejuan, A., A conceptual discussion on electromagnetic units–Extending mechanical units towards a global system of units. Studies in History and Philosophy of Science Part B: Studies in History and Philosophy of Modern Physics, 46: 265-272, (2014).

[27] Carron, N., Babel of Units. The Evolution of Units Systems in Classical Electromagnetism, arXiv preprint arXiv:1506.01951 (2015).

[28] Wikipedia, the free encyclopedia, List of physical quantities, (2022). Available at

https://en.wikipedia.org/wiki/List_of_physical_quantities. Accessed on 2 April, 2022.

[29] Gupta, S. V., *Units of Measurement: History, Fundamentals and Redefining the SI Base Units*, 81-96, Springer, Berlin, Heidelberg (2020).

[30] Gibbings, J. C., and Hignett, E. T., Dimensional analysis of electrostatic streaming current, *Electrochimica Acta*, 11(7): 815-826 (1966).

[31] Rizk, F. A., Application of dimensional analysis to flashover characteristics of polluted insulators, *Proceedings of the Institution of Electrical Engineers*, 117(12): 2257-2260 (1970).

[32] Stevenson, P. M., Dimensional analysis in field theory. *Annals of Physics*, 132(2): 383-403, (1981).

[33] Middendorf, W. H., The use of dimensional analysis in present day design environment, *IEEE Transactions on Education*, E-29(4): 190-195, (1986).

[34] Strasberg, M., Dimensional analysis of windscreen noise, *The Journal of the Acoustical Society of America*, 83(2): 544-548 (1988).

[35] Zhendong, S., Chunsheng, D., and Jiayu, C., Dimensional analysis and physical similarity of lossy electromagnetic systems, *Chinese Physics Letters*, 10(6): 347-350 (1993).

[36] Zhendong, S., and Hongwei, L., Physical similarity of lossy scatterers. *Chinese Physics Letters*, 11(10): 611-613 (1994).

[37] Mah, M. Y., Liou, L. L., Ewing, R. L., and Ferendeci, A. M., Design methodology of microstrip lines using dimensional analysis, *IEEE microwave and guided wave letters*, 8(7): 248-250 (1998).

[38] Leung, K. W., Dimensional analysis of two-layer spherical dielectric resonator; *IEEE microwave and guided wave letters*, 10(4): 139-141 (2000).

[39] Bartley, P. G., Nelson, S. O., and McClendon, R. W., Dimensional analysis of a permittivity measurement probe, *IEEE Transactions on Instrumentation and Measurement*, 51(6): 1312-1315 (2002).

[40] Salam, M. A., Ahmad, H., and Tamsir, T., Calculation of time to flashover of contaminated insulator by Dimensional Analysis technique. Computers & Electrical Engineering, 27(6): 419-427 (2001).

[41] Piah, M. A. M., and Darus, A., Modeling leakage current and electric field behavior of wet contaminated insulators, *IEEE Transactions on Power Delivery*, 19(1): 432-433 (2004).

[42] Takhistov, P., Dimensionless analysis of the electric field-based food processes for scale-up and validation, *Journal of Food Engineering*, 78(3): 746-754 (2007).

[43] Szirtes, T., *Applied Dimensional Analysis and Modeling*, Second Edition, Butterworth Heinemann, Burlington, MA, USA (2007).

[44] Van Elsen, M., Al-Bender, F., and Kruth, J. P., Application of dimensional analysis to selective laser melting, *Rapid Prototyping Journal*, 14(1): 15-22 (2008).

[45] Ortiz, F. G., Navarrete, B., and Cañadas, L., Dimensional analysis for assessing the performance of electrostatic precipitators, *Fuel Processing Technology*, 91(12): 1783-1793 (2010).

[46] Bo, Z., Lu, G., Wang, P., and Chen, J., Dimensional analysis of detrimental ozone generation by negative wire-to-plate corona discharge in both dry and humid air, *Ozone: Science & Engineering*, 35(1): 31-37 (2013).

[47] Du, W., Xue, N., Sastry, A. M., Martins, J. R., and Shyy, W., Energy density comparison of Li-ion cathode materials using dimensional analysis, *Journal of the Electrochemical society*, 160(8): A1187-A1193 (2013).

[48] Gao, L., Shi, Z., Li, D., Yang, Y., Zhang, G., McLean, A., and Chattopadhyay, K., Dimensionless analysis and mathematical modeling of electromagnetic levitation (EML) of

metals, *Metallurgical and Materials Transactions B*, 47(1): 67-75 (2016).

[49] Oladigbolu, J. O., and Rushdi, A. M. A. Investigation of the corona discharge problem based on different computational approaches of dimensional analysis, *Journal of Engineering Research and Reports*, 15(3): 17-36 (2020).

[50] Hutter, K., and Jöhnk, K., Theoretical Foundation of Dimensional Analysis, In Hutter K., (Editors), *Continuum Methods of Physical Modeling*, pp. 339-392, Springer Berlin Heidelberg (2004).

[51] Palanthandalam-Madapusi, H. J., Bernstein, D. S., and Venugopal, R., Dimensional analysis of matrices state-space models and dimensionless units, *IEEE Control Systems*, 27(6): 100-109 (2007).

[52] Taylor, M., Diaz, A. I., Sánchez, L. A. J., and Micó, R. J. V. A matrix generalisation of dimensional analysis: new similarity transforms to address the problem of uniqueness, *Theoretical Physics*, 2(20): 979-995 (2008).

[53] Rushdi, M. A., and Rushdi, A. M., On the fundamental masses derivable by dimensional analysis, *Journal of King Abdulaziz University: Engineering Sciences*, 27(1): 35-42 (2016).

[54] Rushdi, M. A., and Rushdi, A. M., Modeling virus spread rate via modern techniques of dimensional analysis. *Journal of King Abdulaziz University: Computing and Information Technology Sciences*, 9(2): 47-66 (2020).

[55] Rushdi, M. A., and Rushdi, A. M., Modeling coronavirus spread rate utilizing dimensional analysis via an irredundant set of fundamental quantities, *International Journal of Pathogen Research*, 5(3): 8-21 (2020).

[56] Muktiadji, R. F., and Rushdi, A. M. A., Utilization of dimensional analysis in the study of corona discharge, *Journal of Qassim University: Engineering and Computer Sciences*, 13(2): 61-92 (2020).

[57] Rushdi, M. A., and Rushdi, A. M., Matrix dimensional analysis for electromagnetic quantities, *International Journal of Mathematical, Engineering and Management Sciences (IJMEMS)*, 6(2): 636-644 (2021).

[58] Budiman, F. N., and Rushdi, A. M., Dimensional analysis of partial discharge initiated by a metallic particle adhering to the spacer surface in a gas-insulated system, *Communications in Science and Technology (CST)*, 6(2): 91-100 (2021).

[59] Hidayat, T., and Rushdi, A. M., Dimensional analysis of the effect of wind speed on corona discharge current, *International Journal of Innovative Research in Sciences and Engineering Studies (IJIRSES)*, 2(1): 20-32 (2022).

[60] Burden, R. L., and Douglas Faires, J., *Numerical Analysis*, Ninth Edition, Brooks/Cole, Boston, MA, USA, (2011).

[61] Bridgman, P.W., *Dimensional Analysis*, Yale University Press, New Haven, CT, USA, (1922).

[62] Chen, W. K., Algebraic theory of dimensional analysis, *Journal of the Franklin Institute*, 292(6): 403-422 (1971).

[63] Winzemer, A. M., Dimensional analysis of electromagnetic equations. *Proceedings of the IRE*, 35 (11): 1383-1384 (1947).

[64] Thomas, G. Dimensional analysis applied to electricity and mechanics, *Physics Education*, 14(2): 116-119 (1979).

[65] Mie, G. *Lehrbuch der Elektrizität und des Magnetismus: Eine Experimentalphysik des Weltäthers für Physiker, Chemiker, und Electrotekniker (*Textbook of Electricity and Magnetism: An Experimental Physics of the World Ether for Physicists, Chemists, and Electro-Technicians*)*, Stuttgart, Verlag von Ferdinand Enke (1910), In German.

[66] Harrington, R. F. *Time-Harmonic Electromagnetic Fields*, New York, McGraw-Hill (1961).

[67] Kommer, C., Tugendhat, T., and Wahl, N. *Elektromagnetische Wellen (Electromagnetic Waves)*, In Tutorium Physik fürs Nebenfach (pp. 458-472). Springer Spektrum, Berlin, Heidelberg (2015), In German.

[68] Lakhtakia, A., Varadan, V. K., and Varadan, V. V. *Time-Harmonic Electromagnetic Fields in Chiral Media*, Berlin, Springer (1989).

[69] Rushdi, A. M., Development of modified nodal analysis into a pedagogical tool, *IEEE Transactions on Education*, E-28(1): 17-25, (1985).

[70] Bhaskar, R., and Nigam, A., Qualitative physics using dimensional analysis, *Artificial Intelligence*, 45(1): 73-111, (1990).

[71] Ulaby, F. T., and Ravaioli, U. *Fundamentals of Applied Electromagnetics*, Seventh Edition, Pearson Education (2014).

[72] Vasyliunas, V. M., Kan, J. R., Siscoe, G. L., and Akasofu, S. I. Scaling relations governing magnetospheric energy transfer, *Planetary and Space Science*, 30(4): 359-365 (1982).

[73] Zhendong, S., Chunsheng, D., and Jiayu, C. Dimensional analysis and physical similarity of lossy electromagnetic systems, *Chinese Physics Letters*, 10(6): 347-350 (1993).

[74] Bartley, P. G., Nelson, S. O., and McClendon, R. W. Dimensional analysis of a permittivity measurement probe, *IEEE Transactions on Instrumentation and Measurement*, 51(6): 1312-1315 (2002).

[75] Pelesko, J. A., Cesky, M., and Huertas, S. Lenz's law and dimensional analysis, *American Journal of Physics*, 73(1): 37-39 (2005).

[76] Gratton, J., and Perazzo, C. A. Applying dimensional analysis to wave dispersion, *American Journal of Physics*, 75(2): 158-160 (2007).

[77] Garner, A. L., and Lewis, K. Buckingham Pi analysis of railgun Multiphysics, *IEEE Transactions on Plasma Science*, 42(8): 2104-2112 (2014).

[78] Carlstedt, M., née Porzig, K. W., Ziolkowski, M., Schmidt, R., and Brauer, H. Estimation of Lorentz force from dimensional analysis: similarity solutions and scaling laws, *IEEE Transactions on Magnetics*, 52(8): 1-13 (2016).

[79] Gao, L., Shi, Z., Li, D., Yang, Y., Zhang, G., McLean, A., and Chattopadhyay, K. Dimensionless analysis and mathematical modeling of electromagnetic levitation (EML) of metals, *Metallurgical and Materials Transactions B*, 47(1): 67-75 (2016).

[80] Singh, R. K., Gangwar, S., and Singh, D. K. Experimental investigation on temperature-affected magnetic abrasive finishing of aluminum 6060, *Materials and Manufacturing Processes*, 34(11): 1274-1285 (2019).

[81] Abubakr M. On dimensional analysis, redundancy in set of fundamental

[82] quantities and proposal of a new set. arXiv preprint arXiv:0710.3483; (2007).

[83] Firestone, F. A. A new analogy between mechanical and electrical systems, *The Journal of the Acoustical Society of America*, 4(3): 249-267 (1933).

[84] Mason, W. P. Electrical and mechanical analogies, *The Bell System Technical Journal*, 20(4): 405-414 (1941).

[85] Bloch, A. Electromechanical analogies and their use for the analysis of mechanical and electromechanical systems, *Journal of the Institution of Electrical Engineers-Part I: General*, 92(52), 157-169 (1945).

تحليل الأبعاد بواسطة مجموعة للأبعاد الأساسية معنية بالكهرومغناطيسيات

مصطفى علي رشدي[١] و علي محمد رشدي[٢]

[١]كلية الهندسة والتقانة، جامعة المستقبل في مصر، القاهرة الجديدة، جمهورية مصر العربية،

(حاليا معهد أبحاث الميكانيكا التطبيقية، جامعة كيوشو، فوكوكا ، اليابان)

[٢]قسم الهندسة الكهربائية وهندسة الحاسبات، كلية الهندسة، جامعة الملك عبد العزيز،

جدة، ٢١٥٨٩، المملكة العربية السعودية،

rushdimostafa@riam.kyushu-u.ac.jp; Mostafa.Roshdi@fue.edu.eg; arushdi@kau.edu.sa}

المستخلص. تصف ورقة البحث هذه قاعدة الأبعاد *ط زت ج* المعنية بالكهرومغناطيسيات والتي تستخدم الأبعاد الإسنادية للطول (*ط*)، والزمن (*ز*)، والتيار الكهربائي (*ت*)، والجهد الكهربائي (*ج*). ننتفع بهذه القاعدة في الحل المصفوفي لمسائل تحليل الأبعاد (ح ب) التي يغلب عليها استعمال كميات كهرومغناطيسية . إن تمثيلات الكميات الكهرومغناطيسية في قاعدة الأبعاد الجديدة *ط زت ج* (مقارنة مع قاعدة الأبعاد المعيارية *ك ط زت* (التي تستخدم الكتلة (*ك*) بدلا من الجهد (*ج*)) تكسبنا معلومات أوفر وتتسم بسهولة أوضح ولها خصائص مزاوجة بارزة. وفضلا عن ذلك، فإن حسابات تحليل الأبعاد لمسائل الكهرومغناطيسيات باستخدام خوارزمية غاوس-جوردان في قاعدة الأبعاد *ط زت ج* تعد أكثر كفاية وأقل عرضة للأخطاء وأسرع في اكتشاف الاعتماد الخطي بين معادلات الأبعاد. يتم استكشاف كلا من تفصيلات ومزايا الطريقة المقترحة من خلال أمثلة توضيحية، كلها تتمتع بأهمية واضحة في تعلم وتعليم الكهرومغناطيسيات.

الكلمات الدالة : تحليل الأبعاد، المضروبات عديمة الأبعاد، متغيرات الدخل والخرج، حذف غاوس-جوردان، قاعدة أبعاد معنية بالكهرومغناطيسيات، تعلم وتعليم الكهرومغناطيسيات.

Radiation Safety While Providing Bedside Care During Portable Radiography Procedures: Knowledge and Awareness of Respiratory Therapists and ICU Nurses

Khalid Alshamrani [1,4], Rawiah Humaiyan [1], Aisha Alghamdi [1], Ghadi Alwthinane [1], Dalal Tammar[1], Abdulsalam Alzahrani [3,4], Essam Banoqitah[5§] , Ahmed Subahi [2,4], Shrooq Aldahery [6], Abdulaziz Qurashi [7]

[1] College of Applied Medical Sciences, King Saud bin Abdulaziz University for Health Sciences, Jeddah, Saudi Arabia
[2] College of Science and Health Professions, King Saud Bin Abdulaziz University for Health Sciences, National Guard, Jeddah, Saudi Arabia
[3] Respiratory Services Department, Ministry of the National Guard - Health Affairs, Jeddah, Saudi Arabia
[4] King Abdullah International Medical Research Center, Jeddah, Saudi Arabia
[5] Nuclear Engineering Department, Faculty of Engineering, King Abdulaziz University
[6] Applied Radiologic Technology, College of Applied Medical Sciences, University of Jeddah, Jeddah, Saudi 16 Arabia
[7] Diagnostic Radiology Technology, College of Applied Medical Sciences, Taibah University, Madinah, Kingdom of Saudi Arabia

Abstract Respiratory Therapists (RTs) and Intensive Care Unit (ICU) nurses are at a potential risk of undesirable exposure to ionizing radiation when providing bedside care to patients requiring portable radiography. This study aimed to investigate RTs' and ICU nurses' knowledge of radiation safety and their attitude towards portable X-ray examinations. A total of 71 RTs and 29 ICU nurses were recruited in this cross-sectional descriptive study using non-probability convenience sampling during September and November 2020. The study setting was at King Abdulaziz Medical City, Jeddah, Kingdom of Saudi Arabia. Eight-item questionnaire were used. An expert panel confirmed the content validity of the questionnaire. The outcome of the study shows that; the level of awareness to the ionizing radiations potential risk amongst the RTs and ICU nurses was in a good comparable level. Due to the fact that 79.3% of ICU nurses and 87.3% of RTs did not take previous radiation safety educational course. 55.2% of ICU nurses and 78.9% of RTs never read an article pertaining to radiation safety. The radiation protection knowledge was limited as 51.7 % of the participating ICU nurses and 77.5 % RTs were not aware of the minimum safe distance to maintain during exposure without an intervening barrier. Hence, this study highlights the need for in-service educational programs and radiation protection training for both RTs and ICU nurses.

Keyword Radiation safety, Knowledge and Awareness, Respiratory Therapists, Nurses, Portable X-ray

§ Corresponding Author :

1. Introduction

Ionizing radiation has continuously been used for a variety of diagnostic and therapeutic purposes [1]. For healthcare personnel, being aware of the potential hazard associated with exposure to ionizing radiation as well as the proper radiation protection practice is of high importance [2-3]. In September 2019 and out of all diagnostic radiological examinations performed in England, radiography (i.e., X-rays) were the commonest accounting for 1.86 million X-rays performed [4]. The bedside (i.e., portable or mobile) chest X-ray is still one of the most frequently sought tests for the diagnosis and monitoring for Intensive Care Unit (ICU) patients [5]. ICU nurses and Reparatory Therapists (RTs) most often work with radiation sources from either mobile radiographic or C-arm fluoroscopy units. Although ICU nurses and RTs are considered non-occupationally exposed as they do not routinely and regularly work near radiation sources; however, they should have an appreciation and better understanding of concepts related to radiation safety precautions and how to implement the "As Low As Reasonably Achievable" (ALARA) principle. Some of these precautions include recognizing radiation sources (i.e., recognizing the international ionizing radiation hazard symbol), reducing exposure time through proper planning so that the procedure is completed as quickly as possible, increasing distance from radiation source as the farther away you place yourself, the less exposure to radiation according to the inverse square law, and using lead shields when available (i.e., wearing lead apron and lead gloves) [6]. Inadequate radiation safety awareness, limited knowledge of radiation protection practice, and negative attitude towards radiation safety policies and procedures have been reported previously among nurses, operation theaters' healthcare workers, physicians, fellows, residents, interns, medical students, medical technicians, and support staff [1, 3, 7-13]. Reports regarding evaluating radiation safety awareness towards portable X-ray examinations in particular within King Abdulaziz Medical City, Jeddah (KAMC-J), Kingdom of Saudi Arabia (KSA), and for exclusively ICU nurses and RTs do not exist. Thus, this study aimed to investigate RTs' and ICU nurses' knowledge of radiation safety precautions and their attitude towards portable X-ray examinations.

2. Material and Methods

This is a cross-sectional, and prospective questionnaire study conducted at KAMC, Jeddah, KSA. Of the all 140 RTs and ICU nurses working at KAMC-J, a total of 71 RTs and 29 ICU nurses were recruited using non-probability convenience sampling during September and November 2020.

Eight structured close-ended multiple-choice questions (MCQs) were developed. The questionnaire encompassed two sections: (a) Demographic section included three questions pertaining to gender, profession (i.e., RT or ICU nurse), and experience (b) Knowledge and attitude section consisted of five questions pertaining to participants knowledge of ionizing radiation associated risks, knowledge of the minimum safe distance to maintain during exposure without an intervening barrier, frequency of portable X-rays encounter, and whether or not participants previously took any course or read any article related to radiation safety precautions. The developed questionnaire was piloted by expert panel consisting of three radiology technologists, two medical physicists, one nurse and one RT to ensure the validity and reliability of its contents, and to ensure that the questionnaire is concise and has clear focus and purpose. The questionnaire was then translated into an electronic format via a survey administration application (Google Forms) and distributed directly to the participant's emails, and responses were exported into Microsoft Excel sheet for further analysis.

Institutional Review Board (IRB) approval form the local authority was obtained prior to

collecting data. Confidentiality and anonymity were maintained throughout.

Data were analyzed using statistical package IBM SPSS (version 24). Initial descriptive analysis (i.e., frequency and percentages) was generated. Chi-squared test was used to examine the differences in the level of awareness between categorical variables (i.e., RTs and ICU nurses). P-value of less than 0.05 was considered significant.

3. Results

Out of the total 29 ICU nurses included, 3 (10.3 %) were male, and 26 (89.7 %) were female; while for the 71 RTs included 39 (54.9 %) were male, and 32 (45.1 %) were female as shown in (Fig. 1).

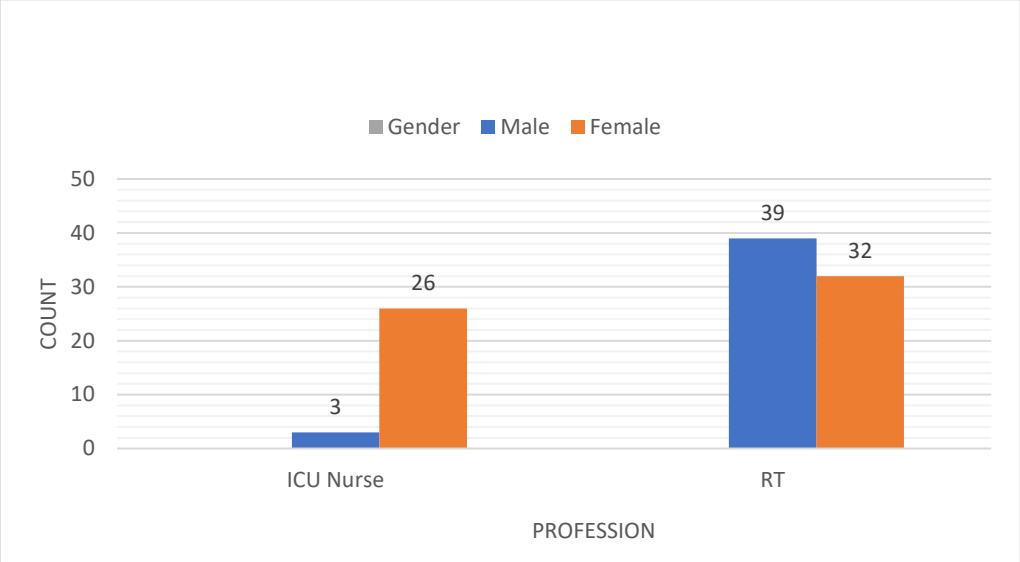

Fig. 1. Gender distribution among population

The analyzed data showed that 19 (65.5 %) of ICU nurses had less than 1 year of experience, 4 (13.8 %) had between 1 to 3 years of experience, and 6 (20.7 %) had more than 3 years of experience. On the other hand, 55 (77.5 %) of RTs had less than 1 year of experience, 9 (12.7 %) had between 1 to 3 years of experience, and 7 (9.8 %) had more than 3 years of experience as shown in (Fig. 2).

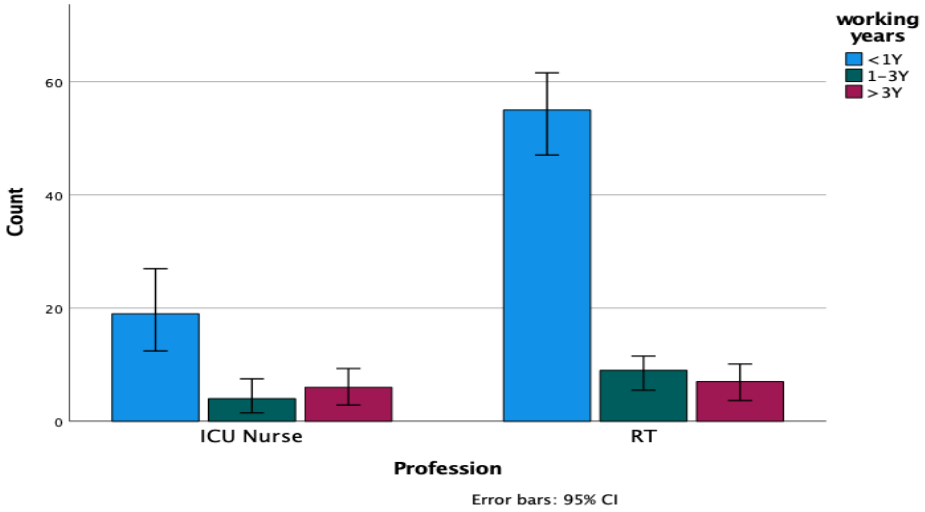

Fig.2. Years of experience among population

There was no significant difference in the level of awareness for ionizing radiation potential risks between ICU nurses and RTs (p = 0.258), as 26 (89.7 %) of ICU nurses and 57 (80.3 %) of RTs were aware of the ionizing radiation associated risks. This indicates that both ICU nurses and RTs have comparable knowledge of ionizing radiation associated risks.

Overall, RTs had more bedside portable X-rays encounters, compared to ICU nurses as illustrated in (Fig. 3).

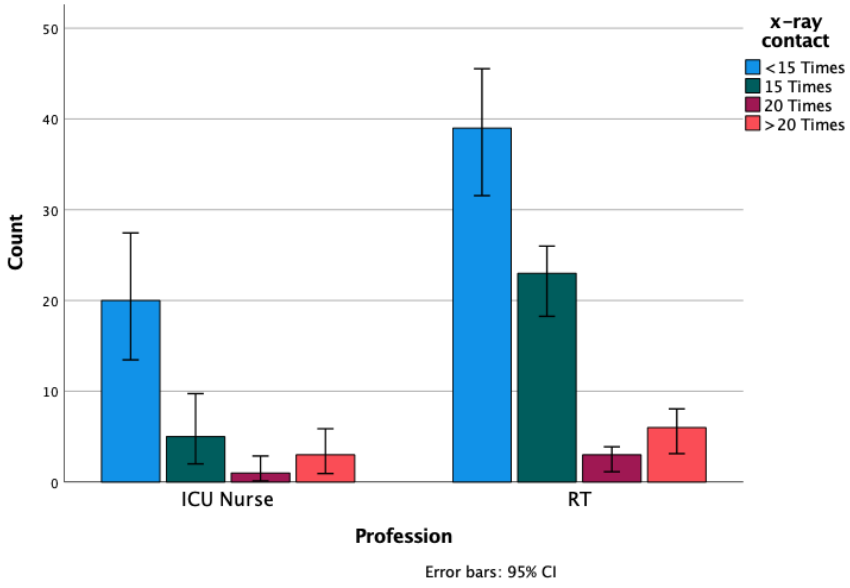

Fig.3. Number of Portable X-rays encounters among population

As reported in table 1, 23 (79.3 %) of ICU nurses and 62 (87.3 %) of RTs did not take previous radiation safety educational course.

Moreover, 16 (55.2 %) of ICU nurses and 56 (78.9 %) of RTs never read an article pertaining to radiation safety.

Table 1. Population response to questions pertaining to taking previous course or reading articles about radiation safety precautions

	ICU Nurses (n = 29)		**Respiratory Therapists** (n = 71)	
	Yes n (%)	No n (%)	Yes n (%)	No N (%)
- Taking previous course related to radiation safety precautions.	6 (20.7 %)	23 (79.3 %)	9 (12.7%)	62 (87.3 %)
- Read any article related to radiation safety precautions.	13 (44.8 %)	16 (55.2 %)	15 (21.1 %)	56 (78.9 %)

As reported in Table 2 and considering the recommended minimum safe distance of 2 meters to be maintained during exposure without an intervening barrier, about a half of the ICU nurses (51.7 %) either did not know the answer or chose the wrong answer. On the other hand, roughly three quarters of the RTs (77.5 %) either did not know the answer or chose the wrong answer.

Table 2. Population response to question pertaining to the minimum safe distance to maintain during exposure without an intervening barrier

	Distance from X-ray source (Meters)			
	5	2	1	I do not know
ICU Nurses (n = 29)	7 (24.1 %)	14 (48.3 %)	2 (6.9 %)	6 (20.7 %)
Respiratory Therapists (n = 71)	36 (50.7 %)	16 (22.5 %)	4 (5.7 %)	15 (21.1 %)

4. Discussion and Conclusion

In this study, we investigated and compared the level of knowledge and awareness regarding radiation safety among RTs and ICU nurses at KAMC- J. The main finding is that the level of awareness to ionizing radiation potential risks was in a good level of comparability among RTs and ICU nurses. Although still considered deficient, ICU nurses may have more radiation protection knowledge compared to RTs as 48.3 % of ICU nurses were aware of the minimum safe distance to maintain during exposure without an intervening barrier compared to 22.5 % for RTs, as a distance of roughly 2 meters is recommended [3, 14].

The deficiency in radiation protection knowledge may be attributed to the lack of experience as 65.5 % of ICU nurses and 77.5 % of RTs had less than 1 year of experience. Another potential reason is the low enrollment in courses and low interest in reading articles pertaining to radiation safety precautions among both ICU nurses and RTs.

The findings of this study are in agreement with previous work reporting limited knowledge of radiation protection practice among nurses, operation theaters' healthcare workers, physicians, fellows, residents, interns, medical students, medical technicians, and support staff [1, 3, 7-13].

To our knowledge, this is the first study reporting radiation safety awareness and knowledge of radiation protection practice for exclusively respiratory therapists' cohort in Saudi Arabia.

The limitations of this study may stem from the low sample size, which may have affected statistical significance. This highlights the need for future multicenter work within Saudi Arabia to include more ICU nurses and RTs sample.

In conclusion, awareness of ionizing radiation risks as well as knowledge of radiation protection practice are essential for all healthcare professionals. This study highlights the need for in-service educational programs and radiation protection training for both RTs and ICU nurses.

References:

[1] Dianati M, Zaheri A, Talari HR, Deris F, Rezaei S. Intensive Care Nurses' Knowledge of Radiation Safety and Their Behaviors Towards Portable Radiological Examinations. Nurs Midwifery Stud. 2014;3(4).

[2] Zervides C, Sassis L, Kefala-Karli P, Christou V, Derlagen A, Papapetrou P, Assessing radiation protection knowledge in diagnostic radiography in the Republic of Cyprus. A questionnaire survey. Radiography. 2020;26(2): 88–93.

[3] Abuzaid MM, Elshami W, Hasan H. Knowledge and Adherence to Radiation Protection among Healthcare Workers at Operation Theater. Asian J Sci Res. 2018;12(1):54–9.

[4] Dixon S. Diagnostic Imaging Dataset Statistical Release. NHS England and NHS Improvement [Internet]. 2019 Jul 18;(1.0):1–18. Available from: https://www.england.nhs.uk/statistics/wp-content/uploads/sites/2/2019/07/Provisional-Monthly-Diagnostic-Imaging-Dataset-Statistics-2019-07-18.pdf

[5] Eisenhuber E, Schaefer-Prokop CM, Prosch H, Schima W. Bedside Chest Radiography. Respir Care. 2012;57(3):427–43.

[6] Johnston P. SP-0009: IAEA Safety Guide on Radiation Protection and Safety in Medical Uses of Ionizing Radiation. Radiother Oncol. 2020;152:S2.

[7] Dehghani A, Ranjbarian M, Mohammadi A,Zade M. S, and Ahangar A. D. Radiation Safety Awareness amongst Staff and Patients in the Hospitals. Int J Occup Hyg. 2015 Oct 11;6(3):114–119.

[8] Szarmach A, Piskunowicz M, Świętoń D, Muc A, Mockałło G, Dzierżanowski J, Radiation Safety Awareness Among Medical Staff. Pol J Radiology. 2015;80:57–61.

[9] Abdellah RF, Attia SA, Fouad AM, Abdel-Halim AW. Assessment of Physicians' Knowledge, Attitude and Practices of Radiation Safety at Suez Canal University Hospital, Egypt. Open J Radiology. 2015;05(04):250–8.

[10] Faggioni L, Paolicchi F, Bastiani L, Guido D, Caramella D. Awareness of radiation protection and dose levels of imaging procedures among medical students, radiography students, and radiology residents at an academic hospital: Results of a comprehensive survey. Eur J Radiol. 2017;86:135–42.

[11] Erkan I, Yarenoglu A, Yukseloglu EH, Ulutin HC. The investigation of radiation safety awareness among healthcare workers in an education and research hospital. Int J Radiat Res. [Internet] 2019;17(3):455–61. Available from: http://ijrr.com/article-1-2602-en.html

[12] Partap A, Raghunanan R, White K, Seepaul T. Knowledge and practice of radiation safety among health professionals in Trinidad. Sage Open Medicine. 2019;7:2050312119848240.

[13] Shafiee M, Rashidfar R, Abdolmohammadi J, Borzoueisileh S, Salehi Z, Dashtian K. A study to assess the knowledge and practice of medical professionals on radiation protection in interventional radiology. Indian J Radiology Imaging. 2020;30(1):64.

[14] Bohan M. HPS Specialists in Radiation Protection: Ask the Experts [Internet]. null. 2010 [cited 2021 Mar 12]. Available from: https://hps.org/publicinformation/ate/q9456.html

السلامة من الإشعاع أثناء تقديم الرعاية بجانب السرير عند إجراءات التصوير الإشعاعي المتنقل: معرفة وموقف أخصائيين العلاج التنفسي وممرضات وحدة العناية المركزة

خالد الشمراني [١،٤]، وعائشة الغامدي [١]، وغدي الوذيناني [١]، وراوية حميان[١]، ودلال تمار[١]، وعبد السلام الزهراني [٣،٤]، وعصام بانقيطة [٥]، وأحمد سبحي [٢،٤]، وشروق الظاهري [٦]، وعبد العزيز القرشي[٧]

١- كلية العلوم الطبية التطبيقية، جامعة الملك سعود بن عبد العزيز للعلوم الصحية، جدة، المملكة العربية السعودية

٢- كلية العلوم والمهن الصحية، جامعة الملك سعود بن عبد العزيز للعلوم الصحية، جدة، المملكة العربية السعودية

٣- إدارة خدمات الجهاز التنفسي، وزارة الحرس الوطني - الشؤون الصحية، جدة، المملكة العربية السعودية

٤- مركز الملك عبد الله العالمي للأبحاث الطبية، جدة، المملكة العربية السعودية

٥- قسم الهندسة النووية، كلية الهندسة، جامعة الملك عبد العزيز، ص.ب. ٨٠٢٠٤، جدة ٢١٥٨٩

٦- تكنولوجيا الأشعة التطبيقية، كلية العلوم الطبية التطبيقية، جامعة جدة، جدة، المملكة العربية السعودية

٧- تكنولوجيا الأشعة التشخيصية، كلية العلوم الطبية التطبيقية، جامعة طيبة، المدينة المنورة، المملكة العربية السعودية

المستلخص:

يتعرض أخصائيو العلاج التنفسي (RTs) وممرضي وحدة العناية المركزة (ICU) لخطر محتمل للتعرض غير المرغوب فيه للإشعاع المؤين عند تقديم الرعاية بجانب السرير للمرضى الذين يحتاجون إلى تصوير إشعاعي محمول. هدفت هذه الدراسة إلى التحقيق في مدى معرفة ممرضات العناية المركزة وأخصائيو العلاج التنفسي بالسلامة الإشعاعية وموقفهم تجاه فحوصات الأشعة السينية المحمولة. تم تعيين مجموعه ٧١ أخصائي/ة علاج التنفسي و٢٩ ممرضًا/ة في وحدة العناية المركزة في هذه الدراسة الوصفية المقطعية باستخدام أخذ عينات ملائمة غير احتمالية خلال شهري سبتمبر ونوفمبر ٢٠٢٠. كان إعداد الدراسة في مدينة الملك عبد العزيز الطبية، جدة، المملكة العربية السعودية. تم استخدام استبيان مكون من ثمانية بنود. وأكدت لجنة خبراء صحة محتوى الاستبيان. كان مستوى الوعي بالسلامة الإشعاعية قابلاً للمقارنة بين الممرضين في وحدة العناية المركزة وأخصائيو العلاج التنفسي. ٧٩.٣٪ من ممرضي وحدة العناية المركزة و٨٧.٣٪ من أخصائيي العلاج التنفسي لم يأخذوا دورة تعليمية سابقة عن السلامة الإشعاعية. ٥٥.٢٪ من ممرضي وحدة العناية المركزة و٧٨.٩٪ من أخصائيي العلاج التنفسي لم يقرؤوا أبدًا مقالة تتعلق بالسلامة الإشعاعية. كانت معرفة الحماية من الإشعاع محدودة حيث لم يكن ٥١.٧٪ من ممرضي وحدة العناية المركزة المشاركين و٧٧.٥٪ من أخصائيي العلاج التنفسي على دراية بالحد الأدنى للمسافة الآمنة للحفاظ عليها أثناء التعرض للأشعة دون حاجز. ومن ثم، تسلط هذه الدراسة الضوء على الحاجة إلى برامج تعليمية أثناء الخدمة وتدريب على الحماية من الإشعاع لكل من أخصائيي العلاج التنفسي والممرضات في وحدة العناية المركزة.

كلمات مفتاحية:

السلامة من الإشعاع / الحماية من الإشعاع / أخصائيين العلاج التنفسي / ممرضين وحدة العناية المركزة / الأشعة السينية المحمولة.

Dose Measurements of Relatives, together with Dose Mapping of Common Areas in the Nuclear Medicine Department at KAMC-Jeddah

Lulwah Alsalem [1], Rawah Nasser [1], Dania Karsou [1], Essam Banoqitah[2], Yasir Al-barakati[3], Mohammed Maslmani[4], Ahmad Subahi[5]

1 Radiological Sciences Department, College of Applied Medical Science, King Saud Bin Abdulaziz University for Health Sciences, National Guard Health Affairs, Jeddah, Saudi Arabia

2 Nuclear Engineering Department, Faculty of Engineering, King Abdulaziz University, Jeddah 21589, Saudi Arabia

3 Radiation Therapy Department, King Abdulaziz Medical City, Ministry of the National Guard Health Affairs, Jeddah, Saudi Arabia

4 Nuclear Medicine Department, King Abdulaziz Medical City, Ministry of National Guard Health Affairs, Jeddah, Saudi Arabia

5 Basic Science Department, College of Science and Health Professions, King Saud Bin Abdulaziz University for Health Sciences, National Guard Health Affairs, Jeddah, Saudi Arabia

Abstract. The enormous hazard that radiation has on public in The Nuclear Medicine Department (NM) has necessitated the Nuclear Regulatory Commission (US-NRC) to set limits for the public doses. Regardless of the consequences of radiation, a small quantity of hospitals such as the Princess Noura Center at King Abdulaziz Medical City in Jeddah in Saudi Arabia does not have an estimated dose measurement for the NM department's areas nor public (patients' relatives). Therefore, the purpose of this study is to measure the doses for patient relatives and dose map the areas in the NM department. The data were measured in the form of Equivalent doses using OSL dosimeters. The methodology of collecting the data for relatives is based on three common procedures which are cardiac, bone, and renal scans. While collecting the data for the areas was fixed in seven positions which are two corridors, two waiting areas, two toilets and an injection room. A comparison between the data and US-NRC regulations were mainly based on the duration and the category. The date for the patient relative's category resulted in 74 samples size while the dose mapping measurements resulted in 7 readings. The public regulation for the US-NRC is 0.002 mSv per hour, while for the area is 1.6 mSv per month. This study showed that the areas and public do not receive dose that exceeds the limits which is recommended by the regulations of US-NRC. Furthermore, several recommendations have been suggested in order to lower the dose for patient relatives and in the common area of the NM department.

Keywords. Nuclear Medicine, Radiation Protection, OSL, Radiology, Dose, EqD.

1. INTRODUCTION

Nuclear Medicine (NM) is a branch of medical physics that utilizes radioactive materials in order to diagnose treat certain diseases [1]. The radioactive materials are active substances that can be injected, inhaled or ingested to evaluate the body's biological functions [2]. Moreover, these radioactive materials emit electromagnetic waves that can be detected by the gamma camera in order to build the images [1,4]. There are many procedures that are performed in the NM department such as bone, cardiac, and renal scan. NM functions by using radioactive materials that emit high ionizing radiation, which can be harmful to the population like patient relatives in the NM department [1]. Therefore, the Nuclear Regulatory Commission (US-NRC) publicized a restricted regulation for which is 20 mSv per year to ensure establishing the principle of ALARA that stands for (as low as reasonably achievable) that is defined as a safety principle designed to maintain the equivalent dose (EqD) and keep it low as possible [5,6]. However, estimating the amount of ionizing radiation that the relatives of the patient, and areas in the NM receive from patients with radioactive sources is unspecified. Since, they are not provided with dosimeter devices such as OSL (optical stimulation luminescence), which is used to calculate the equivalent dose [7]. The equivalent dose (EqD) is known as a measure of the absorbed dose that a person or an area receives, and the unit for the EqD is milli-sievert [8]. It is important to monitor the dose measurements for relatives and dose mapping for areas that are unsheltered from radioactive patients to facilitate the process of lowering the dose rate. Therefore, many studies have been conducted for the purpose of maintaining the dose rate within the range limit in the NM department. For example, in May 2018, Kinsey Smith performed a research study in Indiana University Purdue University Indianapolis in the United States of America, on calculating the radiation exposure to visitors to NM department waiting areas. The study has been performed in three different hospitals with different NM departments waiting areas. The calculation methodology was obtained by placing two OSL on the walls of each waiting areas' room for three months, at the end of each month the areas' monitors will be sent to be read, and to document the radiation exposure dose rates. Next, the total visitors dose rates for all the three hospitals were compared to the 20 microsievert US-NRC limit regulation dose rate, the study's results calculations were less than the US-NRC limit regulation [1]. Nevertheless, since the result of the study depends on the hospital waiting rooms designs, the population and the methodology used for calculating the radiation exposure it is crucial to be aware of the doses. Hence, the purpose of our research is to calculate the dose measurements of relatives together with dose mapping areas in the NM department at KAMC-Jeddah, by using the OSL dosimeters and compare the readings to the US-NRC regulation limit to confirm that the equivalent doses are within the dose limitation.

The use of radioactive tracers in patients undergoing procedures in NM present a concern on the safety of the patients and their relatives [10]. Therefore, it is crucial to conduct further research in KAMC-Jeddah to measure and estimations of the relatives of the patients, and to reduce their doses with time spent in the NM department. In brief, using radiopharmaceutical source for patients undergoing procedures in NM, might also affect people who are in the same area, such as relatives and workers.

2. METHODOLOGY

The study area is located in Jeddah, Saudi Arabia, King Abdulaziz Medical City (KAMC). The study was conducted in the Nuclear Medicine (NM) department. The research was performed within four months (16 weeks).

A total of 336 adult patients' relatives who were subject to NM procedures were included in this study. [11] This study was conducted in the Nuclear Medicine Department at KAMC-Jeddah, Saudi Arabia. The OSL dosimeters were used to measure the patients' relatives' equivalent doses along with the areas in the NM department. Furthermore, the OSL provides a wide range of sensitivity for detecting the lowest levels of radiation, hence it provides accurate readings. For that reason, it is used internationally by the Radiology Departments' workers as a safety regulation.

A Wilcoxon test is a non-parametric test that is used to show the difference between two statistical data's as shown here between the female and male category as shown in Table 1. The Wilcoxon was used specifically since our data weren't normally disturbed.

The data is analytic cross-sectional. The data was obtained from the OSL in the form of Absorbed dose(D), furthermore these absorbed doses were converted into EqDs which is calculated by Absorbed dose(D)x weighting factor(wR) the unit is millie-sievert. After that the mean of all equivalent doses was analyzed and calculated using the JMP analysis software [12].

3. RESULTS

A group of 74 relatives of patients who were injected with radioactive materials were given the OSL dosimeter device, along with dose mapping 7 areas which are two corridors, female waiting area, female restroom, male waiting area, male restroom, and the injection room at the NM department at KAMC-J.

Table 1 shows that the males were 46 participants who represent 62.2% of the whole 74 sample, while the females were 28 participants who represent 37.8% of the whole 74 sample.

The cardiac represented 39 procedures which is 52.8% from the whole procedures performed, and the number of the bone scan procedures is 29 and it represents 39.1% from the whole percentage of the procedures. Moreover, the number of the renal scan procedures are 6 which is 8.1% from the sum of performed procedures.

Table.1 Frequency distributions obtained from Wilcoxon test that represent the number of the EqDs for each gender.

Characteristic of the Participant and their Percentage (N=74)		
Gender	**Number**	**Percentage**
Male	46	62.2%
Female	28	37.8%

Table.2 Frequency distributions obtained from Wilcoxon test that represent the number of EqDs per hour for public in each type of procedures.

Characteristic of Procedure and their Percentage (N=74)		
Procedure	**Number**	**Percentage**
Cardiac	39	52.8%
Bone Scan	29	39.1%
Renal	6	8.1%

Table 3 shows that the mean for equivalent doses for each participant is 0.116, the standard deviation is 0.046. The standard error resulted in 0.003, and the median was 0.11 while the interquartile range is 0.04. The maximum was 0.4 and the minimum is 0.04.

Figure 1 shows a schematic diagram of the NM department layout and the OSL dosimeters position assigned to the 7 locations to evaluate the dose map. In Figure 2, the EqD for corridor 1 was 0.18 mSv while in the injection room the EqD was 0.24 mSv. Moreover, the male toilet EqD was 0.26 mSv followed by corridor 2 which was 0.4 mSv. The female toilet was 0.41 mSv and the male waiting area was 0.53 mSv, in addition to the female waiting area which was 0.82 mSv.

In Figure 3, the cardiac scan procedure had the highest mean, center, variation, and it is the only category with outliers. Additionally, the bone scan is the second. The comparison between the average of the EqDs per hour of the relatives is 0.04 mSv and the public EqD per one hour for NRC is 0.002 mSv (0.002 > 0.04), showed that the EqDs for the public is 4% of 0.002 mSv NRC limitation per hour. The

second comparison was between the NRC regulation for restricted areas per month which is 1.6 mSv and the average of the EqDs of the areas is 0.405 mSv. As a result, (1.600 > 0.405), which shows that areas average EqDs is 40.5% of 1.6 mSv NRC limitation per month.

Table.3 Descriptive statistics of the equivalent dose for each participant.

Characteristics of the Equivalent Dose per Participant (N=74)					
Mean	**Std Dev**	**Median**	**Interquartile Range**	**Max**	**Min**
0.116	0.046	0.11	0.04	0.4	0.04

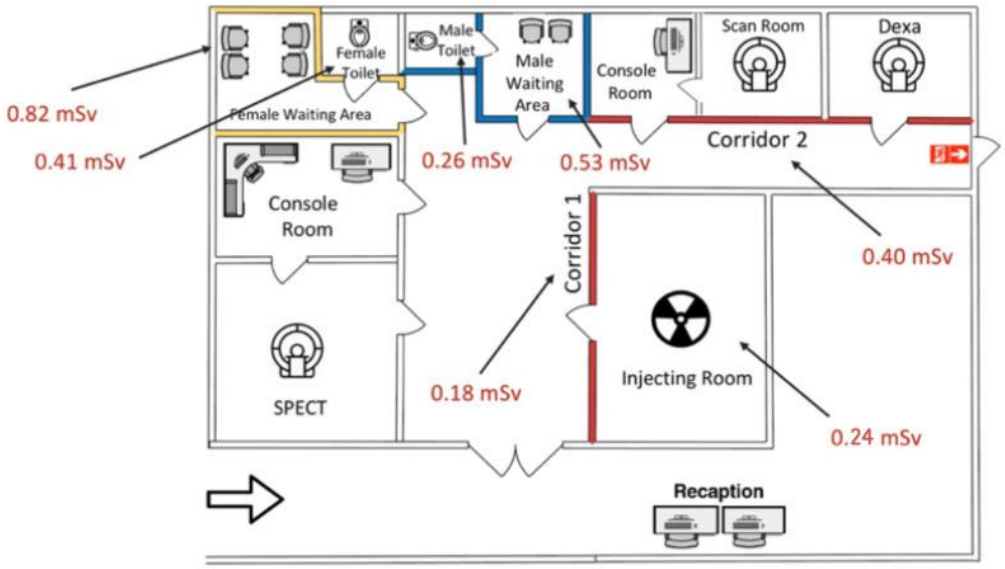

Figure 1 Map of the NM department at KAMC-J

4. DISCUSSION

The radiation exposure at the NM department can be a risk hazard to the relatives of the patients, since they spend 2-4 hours near patients injected with radioactive materials in the waiting areas [13]. Therefore, US-NRC has set regulations for public dose which is 0.002 mSv per hour while for the areas' EqDs 1.6 mSv per month.

This study aims to measure the EqDs for the relatives along with dose mapping seven areas in the NM department at KAMC-J. The null hypothesis (H_o) states that the average public doses per hour is exactly 0.002 mSv per hour. Whereas the alternative hypothesis (H_I) states that the mean of the public EqDs per hour is different from 0.002 mSv per hour. Therefore, based on the t test results, the P-value is less than (P > 0.05). Thus, there is a significant difference suggesting the rejection of the null hypothesis. The results also show that the average of the EqDs for the patient relatives represent 4% from 0.002 mSv per hour as recommended by the US-NRC.

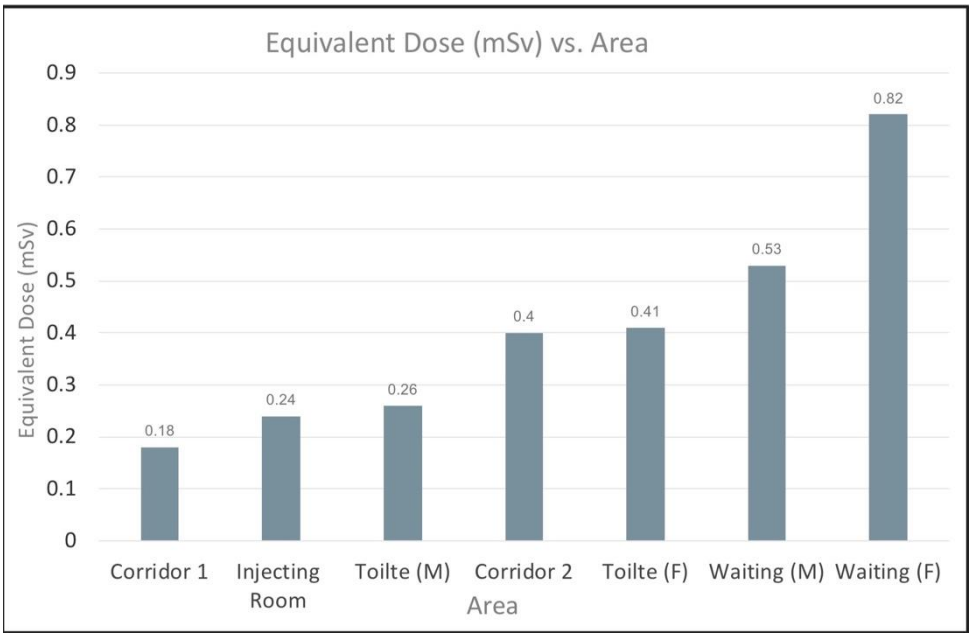

Figure 2 Bar Chart that demonstrates the relation between the EqDs for each area

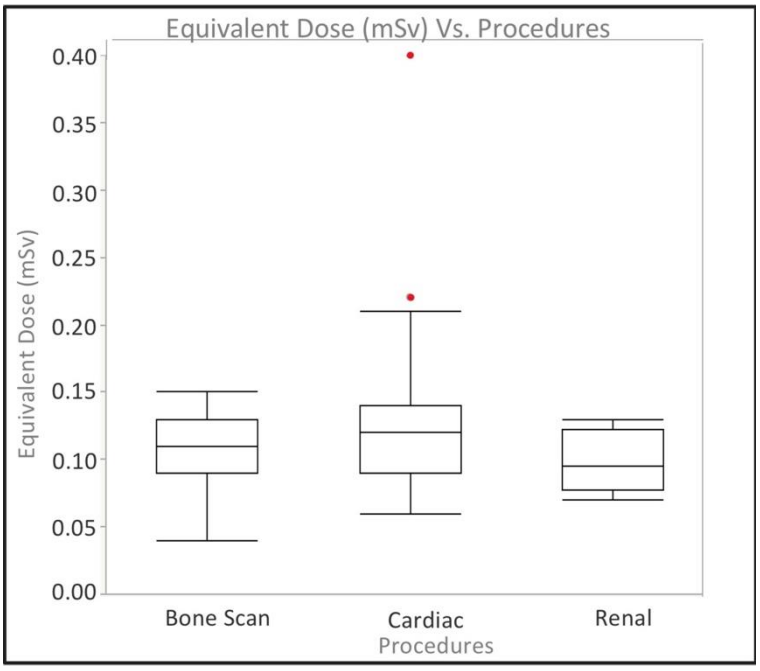

Figure 3 Comparison by the Box Plot graph based on center, variation and outliers of the EqDs in each procedure

Regarding the areas' average radiation exposure, the H_o states that average of the areas' EqDs per month is precisely 1.6 mSv per month. On the other hand, the H_I states that the average of the areas' EqDs per month is different from 1.6 mSv per month. Hence, based on the t test results, the P-value is less than 0.05 ($P > 0.05$). Which shows significant difference indicating the rejection of the H_o. In addition, the result shows that the average of the EqDs for the areas is 40.5% from the US-NRC regulation, which is 1.6 mSv per month.

There has been a similar study conducted in the NM departments of three different hospitals in order to compare the measured doses to the US-NRC regulations. In the Kinsey Smith study on Radiation Exposure to Visitors in the NM Department' Waiting Areas, the study sample was conducted by dose mapping the waiting areas only in the NM department. However, this study is mainly focused on the waiting area, which does not show accuracy in estimating the EqDs that the public receive, since relatives are constantly present in different areas in the NM department to accompany patients. Therefore, in our study we dose mapped seven different areas in the NM department. The Kinsey Smith study resulted in an average for the waiting area that is less than the US-NRC regulations limits which shows correspondence with our results for the waiting areas [5]. However, our study's result for the areas is less than Kinsey Smith study's result when compared to the NRC restricted areas limitation.

The limitations in this study were majorly due to shortage of time, the specificity of the data and the poor relative education. The duration of the data collection period was insufficient, since the majority of the patients present to the NM department without relatives. Also, the data were acquired from three specific procedures; however, that were not performed daily. As a result, two months of data collection were not enough to reach the preferred sample size. Also, the unfamiliarity with the insignificant size of the OSL caused the relatives' patients to dismember passing back the dosimeter which resulted in affecting the readings of the data.

A high restriction of radiation protection procedure in the NM department is an essential element. Therefore, it is recommended to separate the patients and relative's waiting areas. In the case of disabled patients, it is recommended that the relatives should leave the NM every few minutes to minimize the continuous exposure to radiation. Finally, it is also recommended to put fixed sign boards on the toilets in the NM department to demonstrate the restrictiveness of this area and that it is only permitted to patients along with guide maps that guide the relatives to the nearest safe restroom.

5. CONCLUSION

The results of this research states, the public and the areas in the Nuclear Medicine Department in Princess Noura Center at King Abdulaziz Medical City do not receive doses that exceeds the regulations of the US-NRC. Thus, the dose measurements show compliance to US-NRC regulations which confirm that the NM department at KAMC-J lies under excellent criteria for high quality protection.

Furthermore, and according to the latest technology of radiation online dose monitoring, which can measure dose and location. It is advisable to make it available in the NM department to monitor radiation dose to the patient relatives of pediatric and elderly patients, and unmonitored workers to improve the quality of radiation protection in NM at KAMC- Jeddah.

Acknowledgment

Several people played an important role in accomplishing this paper. We thank Ms. Maeen Ramadan for her help through the data collection process. We thank Eng. Mohammed Hamdan for his assistance in providing and reading the OSL devices. Finally, we thank Dr. Majid Althaqafi for teaching us the basics of Research Methodolgy. This work was supported by King Saud Bin Abdulaziz University for Health Sciences and King Abdulaziz Medical City in Jeddah (National Guard Hospital).

REFERENCES:

[1] S. Cherry, J. Sorenson, and M. Phelps, *Physics in Nuclear Medicine*. Elsevier Inc., 2012.

[2] F. M. Jr and M. Guiberteau, *Essentials of Nuclear Medicine Imaging: Expert Consult-Online and Print*. 2012.

[3] H. A. Ziessman, J. P. O'Malley, J. H. Thrall, and F. H. Fahey, *Nuclear Medicine: Fourth Edition*. Elsevier Inc., 2013.

[4] K. Smith, "Radiation Exposure to

Visitors to Nuclear Medicine Department Waiting Areas," *Soc Nucl. Med*, 2018.

[5] E. S. Amis, P. F. Butler, K. E. Applgate, S.B. Birnbaum, L. F. Brateman, J. M. Hevezi, R. K. Zeman, "American College of Radiology White Paper on Radiation Dose in Medicine," *J. Am. Coll. Radiol.*, vol. 4, no. 5, pp. 272–284, 2007, doi: 10.1016/j.jacr.2007.03.002.

[6] V. Schembri and B. J. M. Heijmen, "Optically stimulated luminescence (OSL) of carbon-doped aluminum oxide (Al2O3:C) for film dosimetry in radiotherapy," *Med. Phys.*, vol. 34, no. 6Part1, pp. 2113–2118, May 2007, doi: 10.1118/1.2737160.

[7] C. Park, L. Papiez, S. Zhang, M. Story, and R. D. Timmerman, "Universal Survival Curve and Single Fraction Equivalent Dose: Useful Tools in Understanding Potency of Ablative Radiotherapy," *Int. J. Radiat. Oncol. Biol. Phys.*, vol. 70, no. 3, pp. 847–852, Mar. 2008, doi: 10.1016/j.ijrobp.2007.10.059.

[8] L. K. Harding, A. B. Mostafa, and W. H. Thomson, "Staff radiation doses associated with nuclear medicine procedures - a review of some recent measurements," *Nucl. Med. Commun.*, vol. 11, no. 4, pp. 271–277, 1990, doi: 10.1097/00006231-199004000-00003.

[9] M. Kamen, *Radioactive Tracers in Biology*. Elsevier, 1951.

[10] "Sample Size Calculator by Raosoft, Inc." [Online]. Available: http://www.raosoft.com/samplesize.html. [Accessed: 16-Dec-2020].

[11] "Statistical Software | JMP Software from SAS." [Online]. Available: https://www.jmp.com/en_us/home.html. [Accessed: 16-Dec-2020].

[12] S. Mattsson, "Introduction: The importance of radiation protection in nuclear medicine," in *Radiation Protection in Nuclear Medicine*, Springer Berlin Heidelberg, 2013, pp. 1–3.

قياسات الجرعة الإشعاعية للأقارب مع رسم خرائط التعرض في المناطق المشتركة في قسم الطب النووي بمدينة الملك عبدالعزيز الطبية بجدة

لولوة السالم [١] ، روعه ناصر [١] ، دانية كرسوع [١] ، عصام بانقيطة[٢] ، ياسر البركاتي [٣] ، محمد المسلماني [٤] ، أحمد سبحي [٥]

١ قسم العلوم الإشعاعية، كلية العلوم الطبية التطبيقية، جامعة الملك سعود بن عبد العزيز للعلوم الصحية، الشؤون الصحية بالحرس الوطني، جدة، المملكة العربية السعودية.

٢ قسم الهندسة النووية، كلية الهندسة، جامعة الملك عبد العزيز، جدة ٢١٥٨٩، المملكة العربية السعودية

٣ إدارة العلاج الإشعاعي، مدينة الملك عبد العزيز الطبية، الشؤون الصحية بوزارة الحرس الوطني، جدة، المملكة العربية السعودية

٤ إدارة الطب النووي، مدينة الملك عبد العزيز الطبية، الشؤون الصحية بوزارة الحرس الوطني، جدة، المملكة العربية السعودية

٥ ـ كلية العلوم والمهن الصحية، جامعة الملك سعود بن عبد العزيز للعلوم الصحية، جدة، الشؤون الصحية بالحرس الوطني، المملكة العربية السعودية

الملخص:

تم وضع حدود للجرعات الطاقة الإشعاعية من قبل لجنة التنظيم النووي (US-NRC) في قسم الطب النووي ومع ذلك فإن الجرعة الإشعاعية لمرافقين المرضى، ومناطق الانتظار، و الممرات، وغرفة الحقن، والمرحاض في قسم الطب النووي في مركز الأميرة نورة في مدينة الملك عبد العزيز الطبية في جدة في المملكة العربية السعودية قد تكون تخطت الحد الذي تم السماح به. لذلك، الغرض من هذه الدراسة هو قياس الجرعات لمرفقين المرضى والمناطق داخل قسم الطب النووي.

تم العمل على هذه الورقة البحثية عن طريق معرفة الجرعات باستخدام جهاز قياس يسمى ب الOSL . تعتمد منهجية جمع البيانات الخاصة بالمرافقين على ثلاثة إجراءات وهي فحوصات القلب والعظام والكلى. أثناء جمع البيانات الخاصة بالمناطق تم تثبيت أجهزة ال OSL في سبعة مواضع وهي عبارة عن ممران ، منطقتان انتظار ، مرحاضان وغرفة حقن. استندت المقارنة بين البيانات ولوائح لجنة التنظيم النووي بشكل أساسي على المدة والفئة.

أوضحت البيانات الخاصة بفئة مرافقين المرضي وهي عبارة عن ٧٤ عينة بينما تم قياس جرعات المناطق لمدة ٧ قراءات نظرًا لأنها ثابتة ومتنوعة فقط في المدة.

حددت اللائحة العامة للجنة التنظيم النووي جرعة 0.002 ملي سيفرت في الساعة بالنسبة لمرافقين المرضي ، بينما بالنسبة للمنطقة ١,٦ ملي سيفرت في الشهر. أظهرت هذه الدراسة أن المناطق والعامة لم يتعرضوا لجرعة تتجاوز الحدود التي أوصت بها لوائح لجنة التنظيم النووي. علاوة على ذلك ، تم اقتراح العديد من التوصيات من أجل خفض الجرعة لأقارب المرضى وفي المنطقة المشتركة لقسم الطب النووي.

King Abdulaziz Journal: Engineering Sciences, 2022 Volume 32 No 1 pp.:41-57, O DOI:xx.xxx/

Impressions of the Community of Makkah on the Hajj in the Light of Covid-19 Pandemic: Quantitative and AI-based Sentiment Analyses

Hani A. Aldhubaib

Department of Electrical Engineering, College of Engineering and Islamic Architecture, Umm Al-Qura University, Makkah, Saudi Arabia
Email: hadhubaib@uqu.edu.sa

Abstract. Throughout history, the community of Makkah has been known to make every effort to serve the Muslims who come to perform the Hajj ritual (Pilgrimage), the fifth pillar of Islam. However, the Hajj of 1441 H (2020) was different due to the outbreak of the new Coronavirus (Covid-19). This effect caused numerous changes in many aspects of human life in various societies, including the community of Makkah. While the people of Makkah were preparing to provide what they used to do every year to support and facilitate services for pilgrims, they had to follow the instructions of the Ministry of Health to implement many precautionary and preventive measures to avoid infection of Covid-19; most important of which is staying home. This study mainly aims to observe and analyze social-related changes that may be present or absent for the first time in the community of Makkah during the Hajj of 1441 H. Two main methods were used: AI-based sentiment analysis for a sample of tweets as well as a questionnaire for a random sample of Makkah residents.

Keywords: Covid-19, Hajj, sentiment analysis, Twitter

1. Introduction

Since late 2019, the outbreak of Covid-19 has had adverse effects on almost all sectors, including economic, health, educational and social [1], which significantly impacted many aspects of life, including the Hajj. In the Hajj of 1441 H, a limited number of pilgrims were allowed to perform the Hajj rituals, adhering to the instructions issued by the Ministry of Health following specific preventive and precautionary protocols to prevent the spread of the Covid-19. This incident had a significant effect on the feelings of individuals who found social media platforms, particularly Twitter, as free spaces to express their emotions, impressions, and opinions. Several techniques have been used in the literature to investigate the impression and feelings of individuals in social media, one important of which is sentiment analysis.

Recently, there has been a growing interest in sentiment tracking and analysis of news and commentary on various social media platforms, which has targeted several subjects of human life, including, for instance, health [2]–[4], disasters [5], [6], tourism [7], [8], political [9], [10]. Analysis of this data helps understand the behavior and thoughts of individuals and society about specific events and issues and predict future trends. Many studies in the literature have discussed numerous topics related to tracking and sentiment analytics; nevertheless, research studies addressing this subject in Arabic have been relatively modest compared to the English language [11]–[13].

This paper studies the feelings and impressions of the Makkah residents towards the Hajj of 1441 H (2020), considering the changes associated with the Covid-19 pandemic. The data was collected using two primary methods: Twitter and questionnaires. More than 14 thousand Arabic tweets were collected and classified according to positive, neutral, and negative classes using the sentiment analysis (SA) method described in section 3. Finally, the impressions of the Makkah community were obtained and discussed according to several issues closely related to the Hajj and Eid days. These Islamic festival days begin on the tenth day of Dhu Al-Hijjah month (the twelfth and last month of the Islamic Calendar).

The remainder of the paper is as follows: Section 2 provides a brief review of the related studies. Section 3 describes the methodology used in this paper, and a discussion of the results is given in section 4. Finally, Section 5 concludes this paper.

2. Related literature

Social media has become very popular and fast-growing globally, such as Twitter, Facebook, and Instagram. Due to the technological-related evolution that changed how information is exchanged globally, the public uses social media platforms to express their opinions. Although many challenges are associated with social media data, social media has become the primary source of obtaining and the most influential in forming public opinion. Several reports and studies discussed this issue in the literature, including [14]–[17]. In the fourth quarter of 2021, the average monetizable daily active users (mDAU) reached 217 million worldwide [18]. In Saudi Arabia, about 9.9 million people use Twitter regularly, ranking the fourth-highest usage percentage in the world [19]. Twitter has become one of the most popular social networking sites that allow users to express their feelings, opinions, and ideas. Many other uses have enabled users to benefit from Twitter in different aspects, for example, education [20], managing business [21], socialization [19], and others [22]–[24]. Given the great importance of Twitter in societies, many researchers and scientists have used the Twitter platform to conduct many studies and research in various sciences. Many research attempts dealt with Hajj and Umrah system applications from other disciplines and research areas [25]–[28]. The literature survey of this paper addresses studies that focused on the use of social media in general and Twitter in particular to support and develop the Hajj and Umrah system.

Al-Sadiq and Ahmed [29] studied the attitudes and motives of pilgrims for using the social media websites of the General Presidency of Haramain (GPH). The authors used a questionnaire distributed among a sample of 400 pilgrims who use GPH's social media, including Facebook, YouTube, Twitter, Instagram, and Google Plus accounts. The study indicated that 84.75% of the 400-pilgrim sample found that GPH's social media helped them know the services provided by GPH, which shows the significance of social media platforms to facilitate the performance of pilgrims' rituals.

Many techniques can perform sentiment analysis (SA) for Twitter tweets [30]. Twitter tweets were tracked, and the sentiments of the tweeters were analyzed in various fields. For example, [31], [32] explored sports fans' feelings on Twitter during football matches and how their feelings were affected by the different events during the game. Bati [33] discussed the most prominent big data tools and techniques used in the SA field to collect, analyze, and represent data related to Twitter users' feelings and impressions and use these impressions as feedback to develop and improve the services provided. In another research, Zahrani et al. [34] collected and analyzed nearly five million Arabic and English tweets to monitor Twitter users' impressions of the Hajj of 1437 H (2016). According to specific keywords related to Hajj, the analyzed tweets were classified into two main categories, spatial and temporal. The analysis results showed a significant discrepancy in the impressions of the tweeters between positive, negative, and neutral due to many events that occurred during the pilgrimage, including spiritual and faith values that represent positive impressions. In contrast, the stampede in Mina, which caused some deaths, represents negative impressions.

The above-discussed studies show the importance of using social media to observe individuals and communities' opinions, perceptions, and feelings, which can support recommendations to decision-makers and officials. Due to the changes caused by the Covid-19 that had a significant impact on the whole world, the Hajj season is not immune to these changes. Therefore, this paper mainly aims to investigate the social-related changes that occurred during the Hajj season of 1441 H within the community of Makkah.

3. Methodology

The research methodology used in this paper mainly consists of four steps summarized in Figure 1. The first step begins with reviewing the literature and previous studies related to tracking and analyzing the impressions and feelings of individuals in societies. Data collection is the second step that uses two methods to collect data from the Makkah community. The first was conducted through a questionnaire, and the other by collecting tweets from the Twitter platform. Data analysis is the third step

in which appropriate analysis procedures are applied. Finally, the last step includes the presentation of the results and discussion. An additional explanation for each step is given as follows:

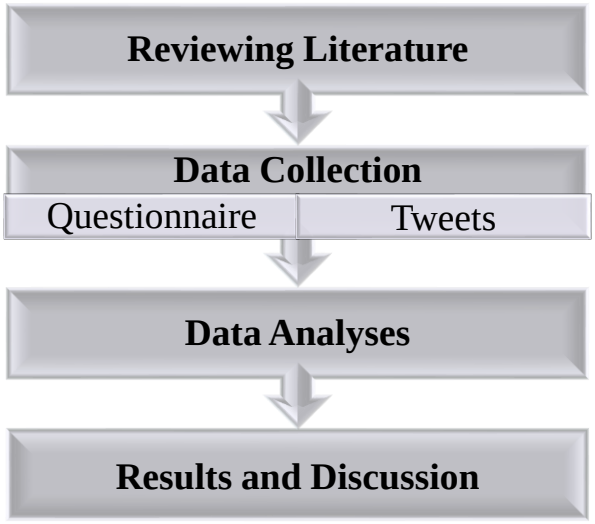

Figure 1. Methodology

3.1. Reviewing the literature

Reviewing previous research studies is an essential part of starting any research. It allows the researcher to investigate the last steps to handle similar problems and determine the research gaps. The previous section of this paper discussed some of the studies related to this paper's topic.

3.2. Data collection

The data collection process consists of two main methods:

The first method is based on a 12-item questionnaire in which a random sample of 155 people from the Makkah community voluntarily participated. The questionnaire covers some information about the aspects of Hajj 1441 H, given in Table 1.

Table 3. Questionnaire items

	Item
Demographics	Nationality
	Gender
	Educational level
	Age
Social aspect	The similarity in the attendance of Eid prayers for the Hajj season of 1441 H compared to previous years
	The similarity of family gathering for breakfast on Eid for the Hajj season of 1441 H compared to previous years
	The continuation of the Eid celebration activities during the days of 11-13 Dhu al-Hijjah for the year of 1441 H
	The similarity of Eid celebration in the Hajj season of 1441 H compared to previous years
	The degree of traffic congestion in Makkah during the Hajj season of the year 1441 H compared to previous years
	The presence of volunteers in Makkah to serve pilgrims in the year 1441 H compared to previous years
	The extent to which Makkah residents are interested in purchasing Eid-related goods in the Hajj season of 1441 H compared to previous years
	The presence of street vendors during the Hajj season of 1441 H compared to previous years

The second method is based on collecting tweets from Twitter users within the holy city of Makkah using the Twitter application programming interface. The number of tweets used in this paper was about 45,000 tweets collected during the first 20 days of Dhul Al-Hijjah month, using a set of keywords including المساجد ، النحر ، عرفة ، الحجاج، زحام، الإفطار، منى، الحرم، الحج، أضحية، شوارع، وصلاة العيد.

3.3. Data analysis

Data analysis is the third step of the methodology used, in which appropriate analysis methods were applied to analyze the data, and extract and visually present the results. Firstly, the questionnaire data were analyzed using essential statistical tools from which results and information were obtained and then visually represented using statistical charts.

Secondly, the collected tweets were analyzed using three main stages: preprocessing stage, text representation stage, and model architecture stage, as shown in Figure 2 [12], [13].

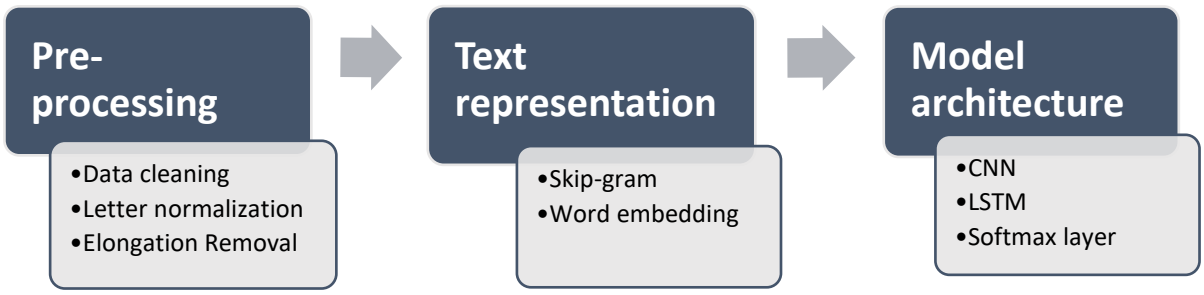

Figure 2. Components of the applied system

Stage 1. Data preprocessing:

The data preprocessing stage (also referred to as data normalization) is the primary stage in all SA methods. It includes a set of operations to process the source data in another format that allows it to be processed effectively. The procedures applied in this stage are identified according to the nature of the data and the application [18]. However, the preprocessing steps involved in this work are as follows [13]:

- Data cleaning: meaningless words and symbols are removed, including URLs, punctuation marks, special characters, and diacritics.
- Letter normalization: In this step, the different forms of letters are recognized and unified, such as the letters {أ, إ,آ } are mapped to {ا}, {ة } is mapped to {ه } and {ى} is mapped to {ي}, as discussed in [23].
- Elongation Removal: Repetitive characters and letters are removed, such as {لا لالا, اكيدددددد، ياااااااا}.

Stage 2. Text representation:

The skip-gram model is used to construct a new word embedding. The texts are represented as a 2D matrix $m \times n$, where m is the number of words and n is the embedding dimension, set to 300.

Stage 3. Model architecture

This stage presents two consecutive phases, Convolutional Neural Networks (CNN) and Long Short-Term Memory (LSTM) models. CNN model is used to extract features that are not expressed by the embeddings, whereas LSTM model detects the correlation between extracted

features. The output of LSTM is entered into softmax layer to generate the probability distribution of sentiment classes (i.e., positive, neutral, and negative). More details of the applied system components can be found in [12], [13].

3.4. Results and discussion

The result and discussion section is the last step of the research methodology used in this paper, where the obtained results are presented and discussed.

4. Results and discussion

This section provides the impressions of the Makkah community for the changes associated with the Hajj of 1441 H.

4.1 Questionnaire analysis results

The questionnaire data was collected for 155 participants during the Eid days in ten different locations in the holy city of Makkah. The results of the questionnaire were analyzed using essential statistical functions.

4.1.1 Demographic data

Figure 3 and Figure 4 show the nationality and gender of individuals who participated in the study questionnaire, respectively. Saudis represented 83.9% of the participants, whereas 16.1% were non-Saudis. The participation of females was more extensive with 62.6%, compared to males, whose participation did not exceed 37.4%.

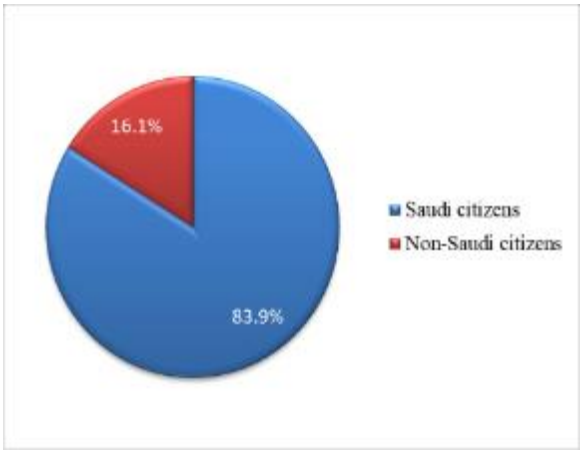

Figure 3. Percentage of participants according to nationality

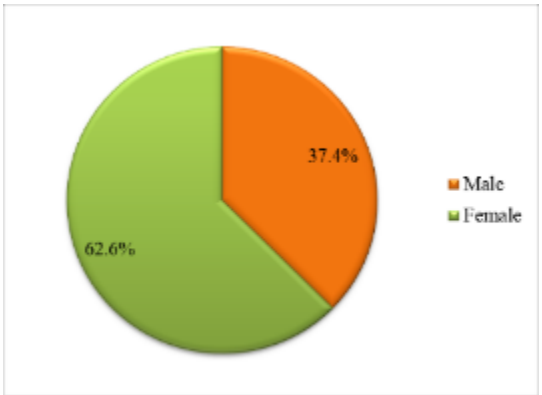

Figure 4. Percentage of participants according to gender

The results show that the most significant proportion of the participants were university graduates with 60%, followed by post-university with 28.4%, as shown in Figure 5.

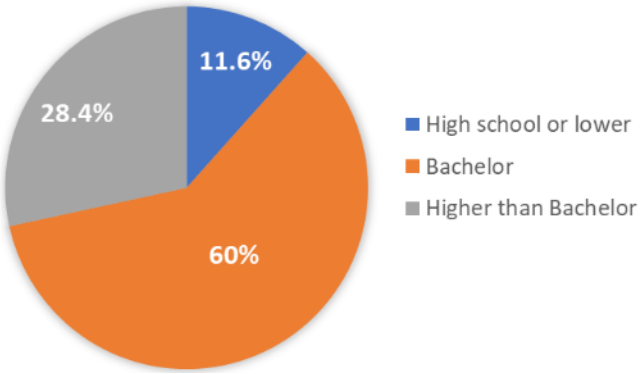

Figure 5. Percentage of participants according to educational level

Figure 6 shows that 79.5% of the participants were between 20-and 50 years old, while only 1.3% were under 20-year-old.

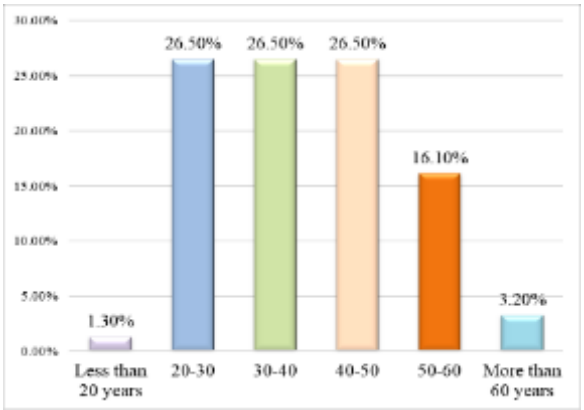

Figure 6. Percentage of participants according to age

4.1.2A comparison between the attendance for the Eid prayer of Hajj 1441 H and previous years

Figure 7 illustrates the participants' perception of the similarity in the attendance for Eid prayers in Hajj of 1441 H compared to previous years. Results show that 2.6% strongly agree that the attendance of the Eid prayer of Hajj 1441 H is like previous years, whereas 25.8% strongly disagree. The results indicate an increase in the attendance to Eid prayers for the Hajj of the year 1441 H compared to the previous years. This increase is because most of Makkah's people were not busy serving the pilgrims that year due to adherence to Covid-19 precautionary measures.

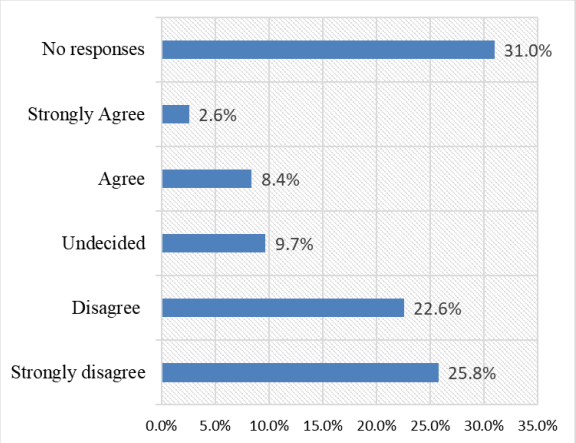

Figure 7. Participants' perception of the similarity in the attendance of Eid prayers in 1441 H compared to previous years

4.1.3A comparison between the gathering of families for breakfast on Eid for the Hajj season of 1441 H and previous years

Figure 8 shows that most of the participants believe that the gathering of families for breakfast on Eid for the Hajj of 1441 H is different than previous years, with a total of 54.9%. These results denote a significant social-related change in the society of Makkah for the first time. Because of allowing a limited number of pilgrims to perform Hajj in 1441 H, families of Makkah society had the opportunity to have their Edi's breakfast together this year, which rarely happened in the previous years.

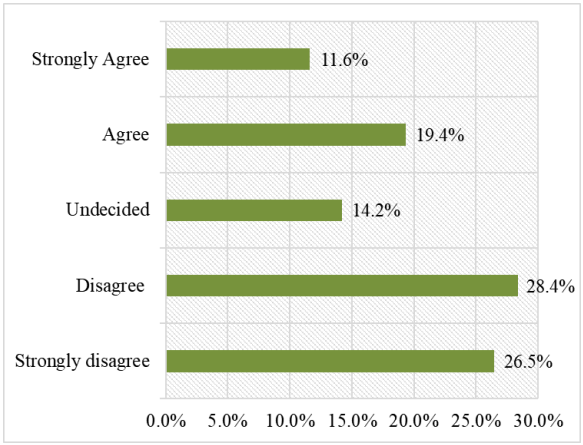

Figure 8. Participants' perception of the similarity of family gathering for breakfast on Eid days in 1441 H compared to previous years

4.1.4A comparison between the continuation of the Eid celebration in Hajj 1441

Figure 9 shows that the most significant percentage of participants (72.3%) did not extend the celebration of Eid in 1441 H to several days after the day of Eid. The limitation of the Eid celebration to only one day could be due to the continued spread of the COVID-19 pandemic.

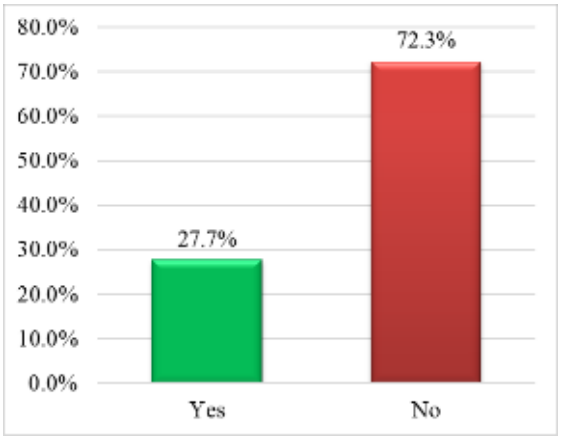

Figure 9. Participants' perception of the continuation of the Eid celebration in 1441 H compared to previous years

4.1.5A comparison between the Eid celebration of Hajj 1441 H and previous years

Figure 10 shows the percentage of those who noticed the presence of celebration manifestations in Makkah during the Hajj of 1441 H. A total of 17.4% (for both: "yes definitely" and "yes, to some extent") believe that the celebration manifestations during Eid days of Hajj 1441 H are similar to previous years, while the most significant percentage of participants, 53.5% believe that there were no celebration manifestations. This result is consistent with the analysis of the previous question that the celebrations did not extend to the rest of Eid days.

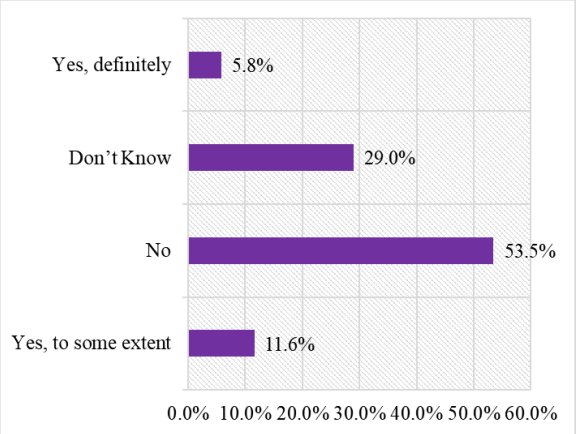

Figure 10. Participants' perception of the presence of celebration manifestations of Eid of Hajj 1441 H compared to previous years

4.1.6 A comparison between the degree of traffic congestion in Makkah during the Hajj season of 1441 H and previous years

The results indicate that 83.2% of the participants found that the traffic congestion was lower than in previous years, as shown in Figure 11. In contrast, about 3.2% of the participants believed that the degree of traffic congestion was the same or greater than the previous years.

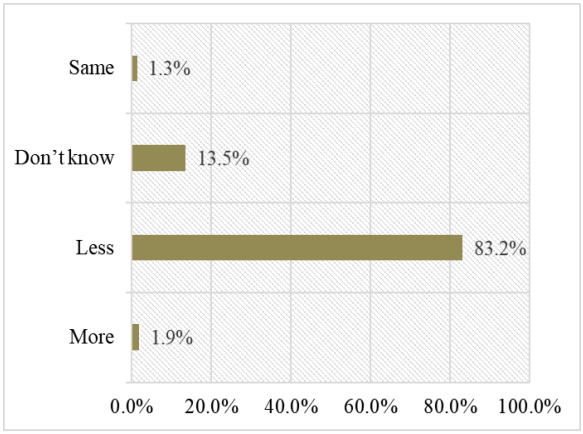

Figure 11. Participants' perception of the traffic congestion degree in Makkah during the Hajj season of 1441 H compared to previous years

4.1.7 A comparison between the presence of volunteers in Makkah to serve pilgrims during the Hajj of 1441 H and previous years

The results illustrate that 47.1% of the participants believed that the presence of volunteers is less in Hajj 1441 H compared to previous years, as shown in Figure 12. The results show that 49% of the participants are unaware of the presence of volunteers who serve pilgrims, which is due to the adherence to the instructions of the Ministry of Health to stay at home.

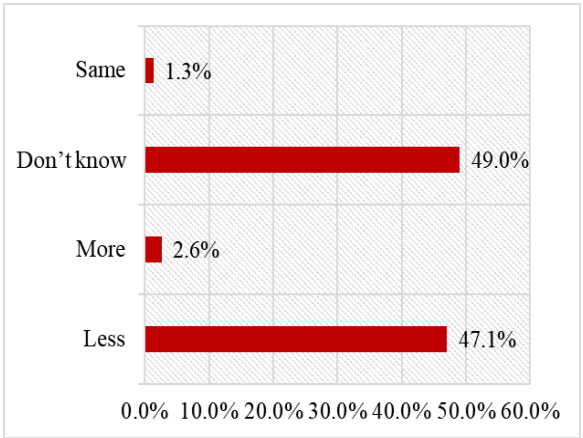

Figure 12. Participants' perception of the presence of volunteers in Makkah to serve pilgrims during the Hajj of 1441 H compared to previous years

4.1.8 A comparison between the interest of Makkah residents to purchase Eid-

related goods in the Hajj season of 1441 H and previous years

Figure 13 shows that 45% of participants believed that the interest in purchasing Eid-related goods in the Hajj season of 1441 H is less compared to previous years. This observation results from the fear of many people from being in public places due to the outbreak of Covid-19. The results also show that 47% were unaware of the difference.

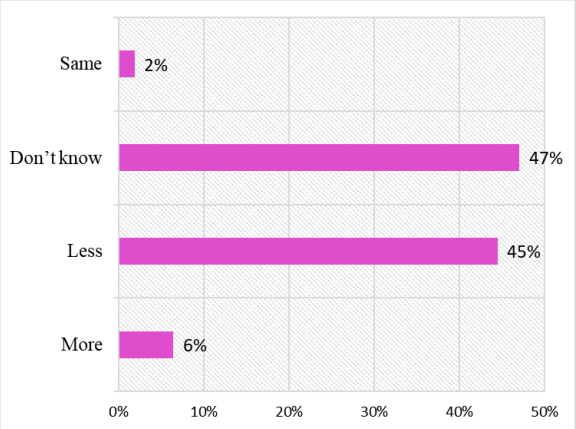

Figure 13. Participants' perception of the interest to purchase Eid-related goods in the Hajj season of 1441 H compared to previous years

4.1.9 A comparison between the presence of street vendors during the Hajj season of 1441 H and previous years

The results in Figure 14 demonstrate that the most significant percentage of the participants, 49%, are unaware of whether there are street vendors. However, 46.5% of the participants indicated that the presence of street vendors was lower than in previous years.

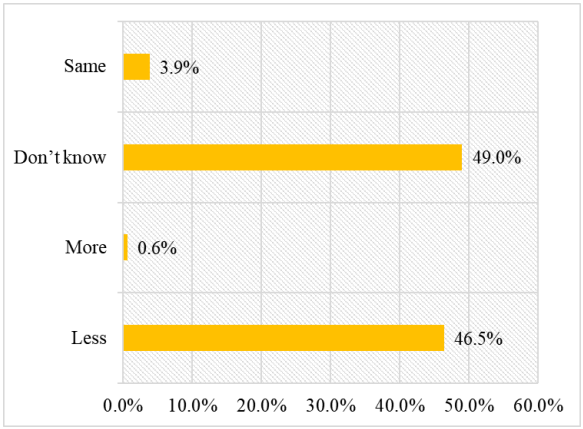

Figure 14. Participants' perception of the presence of street vendors during the Hajj season of 1441 H compared to previous years

4.2 Tweet's analysis results

Several keywords were used to collect tweets from the Twitter platform. The collected tweets are then analyzed, and SA values are extracted according to the method used in [12], [13]. It should be noted that the average SA score for all tweets is between 1 and 5, where 1 represents the minimum sentiment value of "not quite satisfied" and 5 represents the maximum sentiment value of "extremely satisfied."

4.2.1 Analyzing tweets using specific keywords related to Hajj

4.2.1.1 Analysis of the tweets of Makkah people for the keyword "عرفة" ("Arafa").

During the Hajj days of 8-13 Dhu Al-Hijjah 1441 H, the number of tweets collected that include the keyword "عرفة" within the city of Makkah was 977, 59% of which were recorded on the 9th of Dhul Al-Hijjah, as shown in Figure 15. Results show that the SA rate ranged between 4.02 to 4.75, and the overall average was 4.38 for all days, reflecting the happiness of the tweeters, especially on day 9.

Figure 16 shows the sentiment classes rate of tweets for the keyword "عرفة," which were categorized into three classes: positive, neutral, and negative. The results show that positive tweets recorded the highest rate in all Hajj days, while negative tweets were the lowest.

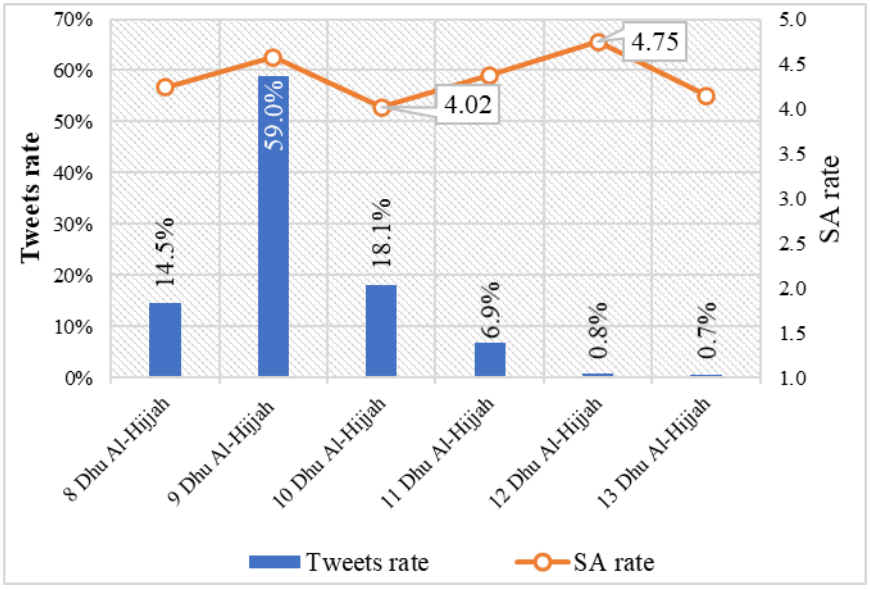

Figure 15. SA rate for tweets that include the keyword"عرفة" ("Arafa ")

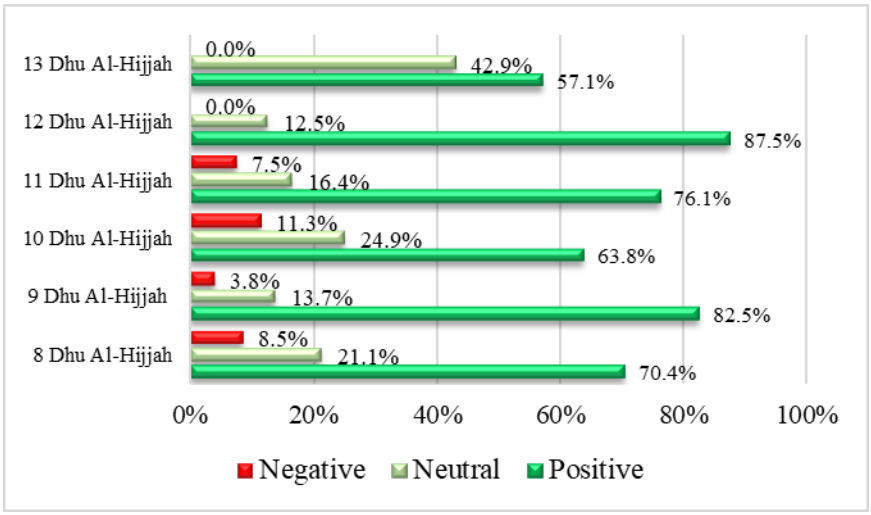

Figure 16. Sentiment classes for tweets that include the keyword "عرفة" ("Arafa")

4.2.1.2 Analysis of the tweets of Makkah people for the keyword "الحجاج" ("Al-Hujaj")

For the keyword "الحجاج," 169 tweets were collected during the Hajj days (8-13 Dhu Al-Hijjah), 55.6% of which were recorded on the 8th of Dhul Al-Hijjah, as shown in Figure 17. The results show that the SA rate ranged between 3.4 and 4.8, with a total average of 4.15, indicating the happiness rate and satisfaction of the tweeters on most Hajj days.

Figure 18 shows that the rate of positive tweets was the highest on all Hajj days except for the tenth day, where the neutral tweets were the largest due to the emergence of some news related to the movement and transportation of pilgrims.

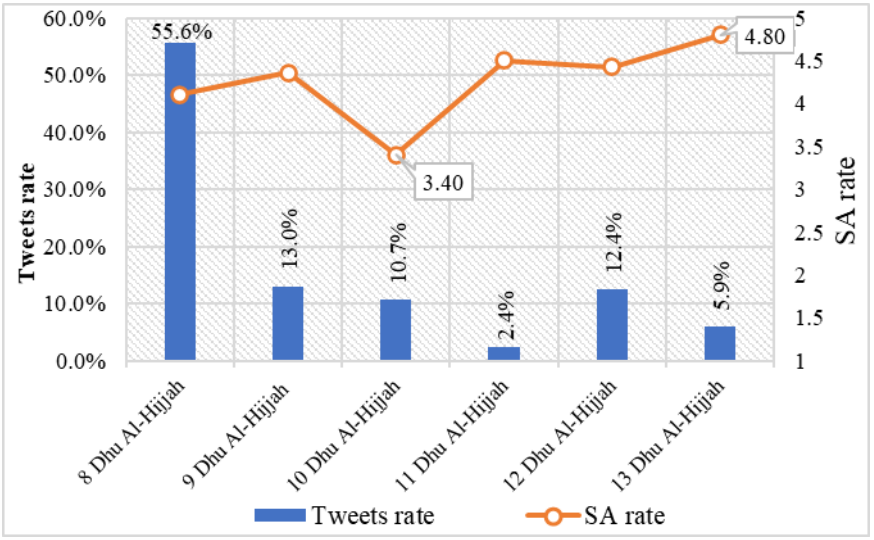

Figure 17. SA rate for tweets that include the keyword "الحجاج" ("Al-Hujaj")

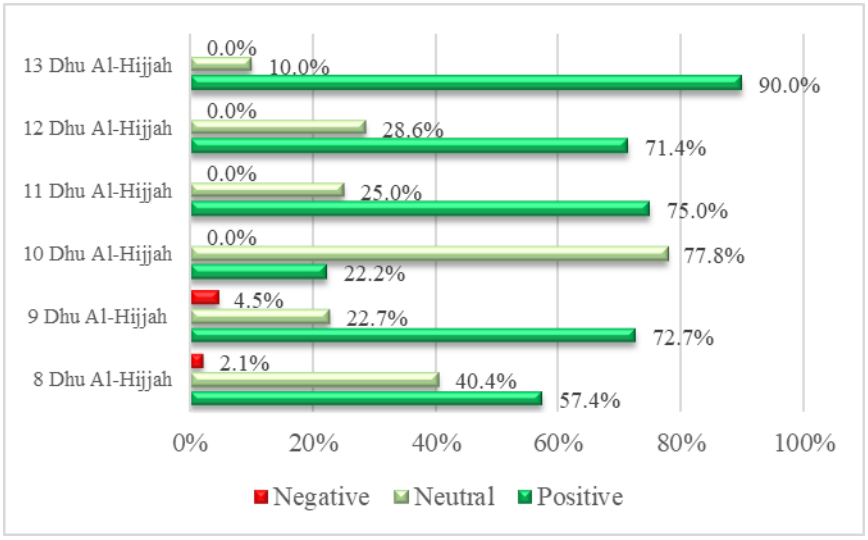

Figure 18. Sentiment classes for tweets that include the keyword "الحجاج" ("Al-Hujaj")

3.2.1.3 . Analysis of the tweets of Makkah people for the keyword "العيد" ("Eid")

Regarding the keyword "العيد," the number of tweets collected was 12,165 recorded during the days of 9-14 Dhu al-Hijjah. The largest percentage of tweets was recorded on day 9 of Dhul Al-Hijjah with 42%, as shown in Figure 19. The results show the SA rate was between 3.69 and 4.33, with a total average of 3.97 for all Hajj days, indicating high satisfaction and happiness of the tweeters in the celebration of Eid.

Figure 20 shows the rate of tweets categorized as positive, neutral, and negative tweets for the keyword "Eid". The figure shows that positive tweets were the most common on all days of Hajj except for days 12 and 13, where neutral tweets were the most.

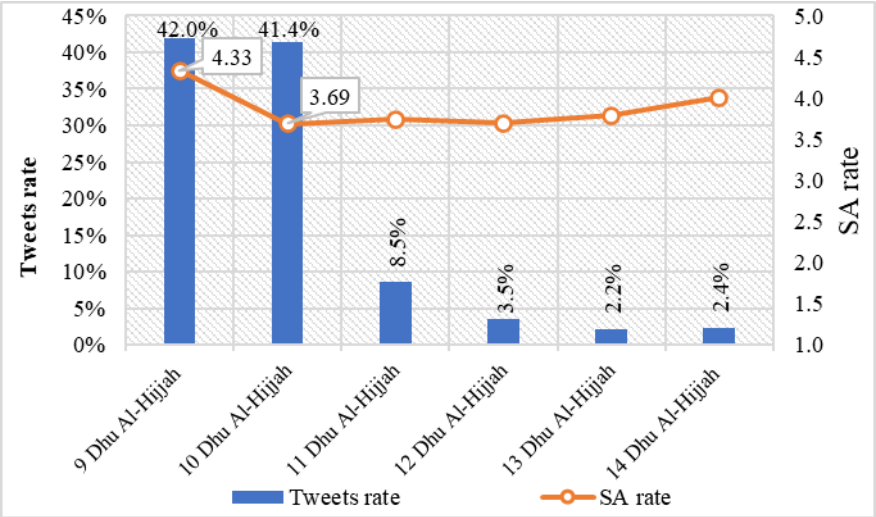

Figure 19. SA rate for tweets that include the keyword "العيد" ("Eid")

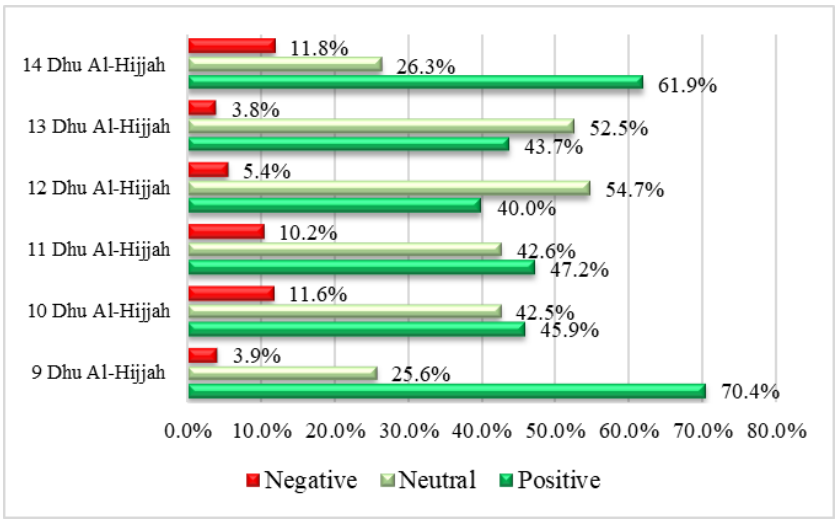

Figure 20. Sentiment classes for tweets that include the keyword "العيد" ("Eid")

3.2.1.4. Analysis of the tweets of Makkah people for the keyword "الحج" ("Hajj")

Figure 21 shows the percentage rates of 1,442 tweets collected for the days of 1-13 Dhul Al-Hijjah, including the keyword "الحج". The recorded results show that days 8 and 9 Dhul Al-Hijjah were the largest, with 31.5% and 23.2%, respectively. The results show that the SA rate before day 8 (i.e., before starting Hajj rituals) was between neutrality and satisfaction degrees. In contrast, the SA rate changed on day 8 from less than satisfaction degree (3.59) to higher than satisfaction degree (4.28). In other words, the start of the Hajj rituals shows a positive impact on the emotions and feelings of the tweeters, which reflects their happiness.

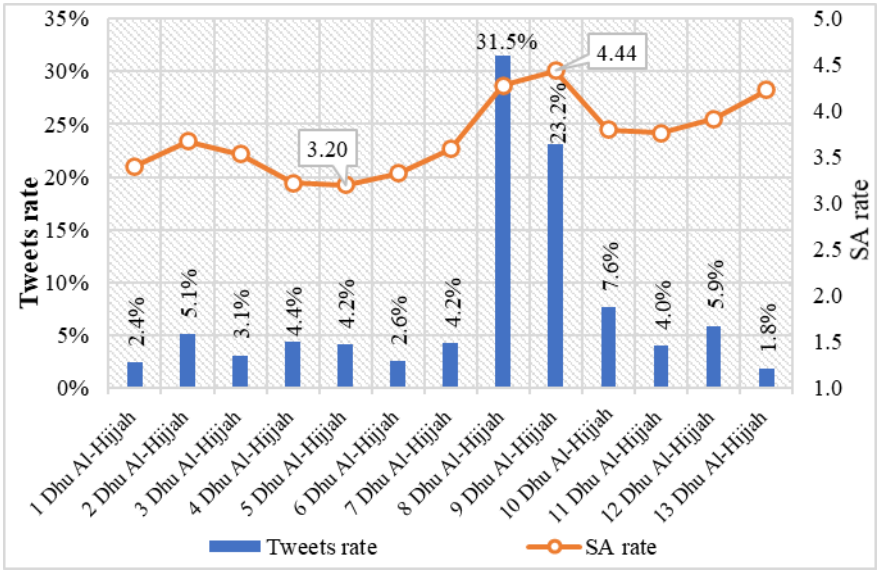

Figure 21. SA rate for tweets that include the keyword "الحج" ("Hajj")

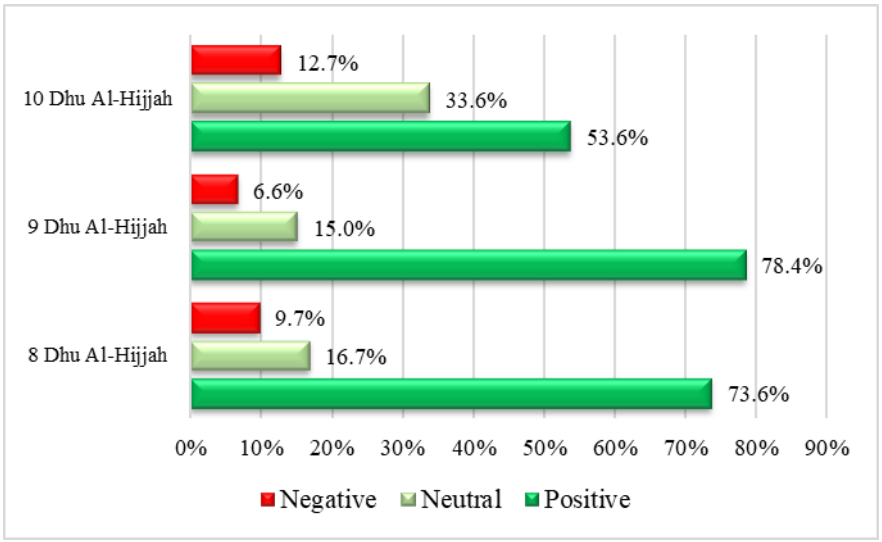

Figure 22. Sentiment classes for tweets that include the keyword "الحج" ("Hajj")

Figure 22 presents the sentiment classes rate of tweets that include the keyword "الحج" ("Hajj") for the days 8,9 and 10 Dhul Al-Hijjah. The results show that the positive tweets achieve the highest rates on all days, which indicates the happiness and positive impression of the Makkah people for the coming hajj days, especially on the days 8 and 9 Dhu Al-Hijjah.

Moreover, most tweets under the neutral sentiment category include news related to Hajj events, instructions, and regulations. Most of the negative impressions of the tweets include feeling sad about not being able to see roads, shops, hotels, restaurants, and other places as crowded with pilgrims as they were in the previous years.

3.2.2. Analysis of tweet types

Figure 23 shows the type of tweets in the original tweet, retweet, or replied tweet. The most significant proportion was the response to tweets among users, with 43% of the total tweets, which indicates the large volume of participation and interaction by replying to original tweets. The percentage of original tweets and retweets was 36.2% and 20.5%, respectively.

3.2.3. Analysis of tweet source

Figure 24 presents the primary sources through which the tweets were posted. Most tweets were posted through iPhone devices with 77.3%, followed by devices running on Android systems with 19.3%, and then Web Apps with 2.2%.

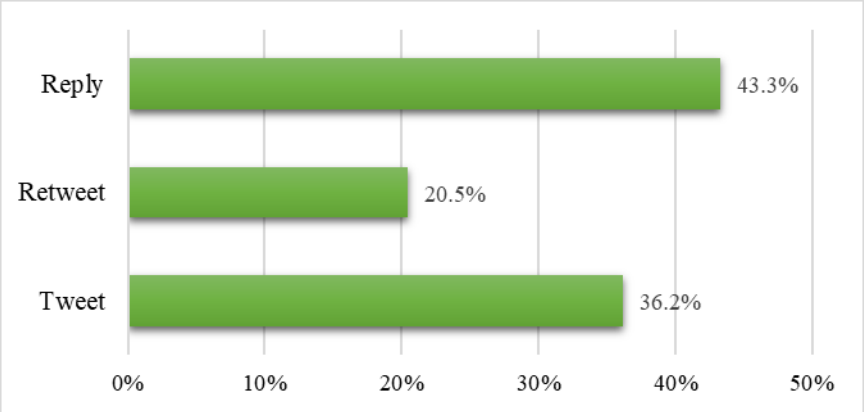

Figure 23. Tweet types

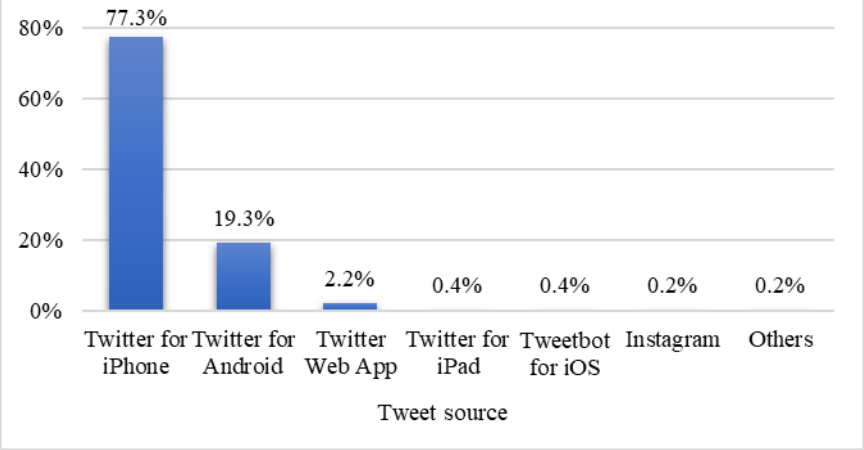

Figure 24. Tweet sources

5 Conclusion and future work

In this paper, the most prominent social aspects of the Makkah community during the Hajj season of 1441 H were studied and analyzed, focusing on the social-related changes in the lifestyle of the Makkah community under the circumstances of the COVID-19 pandemic compared to previous Hajj seasons. Two methods were used to collect data from the Makkah community using a questionnaire and the Twitter platform. The results show an increase in the Eid prayer of Hajj 1441 H attendance compared to previous years, which is one of the new social manifestations that does not usually occur. The results also reveal that families are more interested in tacking Eid of Hajj breakfast together in 1441 H compared to previous years. In addition, this paper noticed some other observations that emerged in Hajj of 1441 H due to COVID-19, including Eid celebration manifestations, traffic congestion, presence of volunteers, interest in shopping, and the presence of street vendors.

The analysis results for 14,753 tweets showed positive results for sentiment analysis, where the overall rate of sentiment analysis ranged between satisfaction and more than satisfied. Furthermore, happiness was noticeable in the

tweets during all the days of Hajj, especially after the start of the Hajj rituals. On the other hand, some tweets contained feelings of longing and sadness for not seeing the places of Makkah crowded with pilgrims, compared to previous years, which were classified as negative tweets.

Future work may include using data mining tools to study the impact of COVID-19 on human lifestyle in the cities of Makkah and Medina. In addition, the study will continue to collect and analyze tweets from the Makkah and Medina communities and conduct comparative studies before and after the end of COVID-19.

References

[1] M. Douglas, S. V. Katikireddi, M. Taulbut, M. McKee, and G. McCartney, "Mitigating the wider health effects of covid-19 pandemic response," *BMJ*, vol. 369, Apr. 2020, doi: 10.1136/BMJ.M1557.

[2] G. Saranya, G. Geetha, K. Chakrapani, K. Meenakshi, and S. Karpagaselvi, "Sentiment analysis of healthcare Tweets using SVM Classifier," Dec. 2020. doi: 10.1109/ICPECTS49113.2020.9336981.

[3] Q. B. Baker, F. Shatnawi, S. Rawashdeh, M. Al-Smadi, and Y. Jararweh, "Detecting Epidemic Diseases Using Sentiment Analysis of Arabic Tweets," *Journal of Universal Computer Science*, vol. 26, no. 1, pp. 50–70, 2020, Accessed: Mar. 17, 2022. [Online]. Available: https://www.jucs.org/jucs_26_1/detecting_epidemic_diseases_using.html

[4] M. Ilyas and J. Alowibdi, "Disease Tracking in GCC Region Using Arabic Language Tweets," in *Proceedings of The Web Conference 2018*, 2018, pp. 417–421. doi: 10.1145/3184558.3186357.

[5] U. H. H. Zaki, R. Ibrahim, S. A. Halim, K. A. M. Khaidzir, and T. Yokoi, "Sentiflood: Process model for flood disaster sentiment analysis," in *2017 IEEE Conference on Big Data and Analytics, ICBDA 2017*, Feb. 2018, vol. 2018-Janua, pp. 37–42. doi: 10.1109/ICBDAA.2017.8284104.

[6] Z. S. Dong, L. Meng, L. Christenson, and L. Fulton, "Social media information sharing for natural disaster response," *Natural Hazards*, vol. 107, no. 3, pp. 2077–2104, Jul. 2021, doi: 10.1007/S11069-021-04528-9.

[7] K. Starosta, S. Budz, and M. Krutwig, "The impact of German-speaking online media on tourist arrivals in popular tourist destinations for Europeans," *Applied Economics*, vol. 51, no. 14, pp. 1558–1573, Mar. 2019, doi: 10.1080/00036846.2018.1527463.

[8] Y. Chaabani, R. Toujani, and J. Akaichi, "Sentiment analysis method for tracking touristics reviews in social media network," in *International Conference on Intelligent Interactive Multimedia Systems and Services*, 2018, vol. 76, pp. 299–310. doi: 10.1007/978-3-319-59480-4_30.

[9] I. Al-Agha and O. Abu-Dahrooj, "Multilevel analysis of political sentiments using twitter data: A case study of the Palestinian-Israeli conflict," *Jordanian Journal of Computers and Information Technology*, vol. 5, no. 3, pp. 195–215, Dec. 2019, doi: 10.5455/JJCIT.71-1562700251.

[10] R. Liu, X. Yao, C. Guo, and X. Wei, "Can We Forecast Presidential Election Using Twitter Data? An Integrative Modelling Approach," *Ann GIS*, vol. 27, no. 1, pp. 43–56, 2020, doi: 10.1080/19475683.2020.1829704.

[11] L. Yue, W. Chen, X. Li, W. Zuo, and M. Yin, "A survey of sentiment analysis in social media," *Knowledge and Information Systems*, vol. 60, no. 2, pp.

617–663, Aug. 2019, doi: 10.1007/S10115-018-1236-4/TABLES/7.

[12] I. A. Farha and W. Magdy, "Mazajak: An online arabic sentiment analyser," in *The 4th Arabic Natural Language Processing Workshop*, 2019, pp. 192–198. doi: 10.18653/V1/W19-4621.

[13] I. Farha and W. Magdy, "A comparative study of effective approaches for Arabic sentiment analysis," *Information Processing & Management*, vol. 58, no. 2, p. 102438, Mar. 2021, doi: 10.1016/J.IPM.2020.102438.

[14] X. Dong and Y. Lian, "A review of social media-based public opinion analyses: Challenges and recommendations," *Technology in Society*, vol. 67, p. 101724, Nov. 2021, doi: 10.1016/J.TECHSOC.2021.101724.

[15] "The impact of social media on public opinion - CC Plus," Aug. 23, 2021. https://cc-plus.com/articles/2021/08/23/the-impact-of-social-media-on-public-opinion/ (accessed Mar. 30, 2022).

[16] J. A. Kwak and S. K. Cho, "Analyzing public opinion with social media data during election periods: A selective literature review," *Asian Journal for Public Opinion Research*, vol. 5, no. 4, pp. 285–301, 2018, doi: 10.15206/AJPOR.2018.5.4.285.

[17] M. M. Skoric, J. Liu, and K. Jaidka, "Electoral and public opinion forecasts with social media data: A meta-analysis," *Information (Switzerland)*, vol. 11, no. 4, pp. 1–16, 2020, doi: 10.3390/info11040187.

[18] "Twitter, Inc. - Financial information - Quarterly results." https://investor.twitterinc.com/financial-information/quarterly-results/default.aspx (accessed Jul. 09, 2021).

[19] H. G. Dailah and M. Naeem, "A social media organizational productivity model: Insights from public health professionals," *Journal of Medical Internet Research*, vol. 23, no. 5, May 2021, doi: 10.2196/23792.

[20] R. Junco, G. Heiberger, and E. Loken, "The effect of Twitter on college student engagement and grades," *Journal of Computer Assisted Learning*, vol. 27, no. 2, pp. 119–132, Apr. 2011, doi: 10.1111/J.1365-2729.2010.00387.X.

[21] "Benefits of Twitter for business | Business Queensland," 2016. https://www.business.qld.gov.au/running-business/marketing-sales/marketing-promotion/online-marketing/twitter/benefits (accessed Jul. 05, 2021).

[22] S. R. El-Beltagy, M. el kalamawy, and A. B. Soliman, "NileTMRG at SemEval-2017 Task 4: Arabic Sentiment Analysis," in *International Workshop on Semantic Evaluation 2017 (SemEval-2017)*, Jan. 2017, pp. 790–795. doi: 10.18653/V1/S17-2133.

[23] K. Darwish and W. Magdy, *Arabic Information Retrieval*, 1st ed. Hanover, United States: Now Publishers Inc, 2014. Accessed: Mar. 23, 2022. [Online]. Available: https://www.bookdepository.com/Arabic-Information-Retrieval-Kareem-Darwish/9781601987761

[24] A. Al-Laith and M. Shahbaz, "Tracking sentiment towards news entities from Arabic news on social media," *Future Generation Computer Systems*, vol. 118, no. 1, pp. 467–484, May 2021, doi: 10.1016/J.FUTURE.2021.01.015.

[25] E. Felemban, A. A. Sheikh, and A. Naseer, "Improving response time for crowd management in hajj," *Computers*, vol. 10, no. 4, Apr. 2021, doi: 10.3390/COMPUTERS10040046.

[26] M. K. Shambour and E. Khan, "A Heuristic Approach for Distributing Pilgrims over Mina Tents," *journal of King Abdulaziz University Engineering Science*, vol. 30, no. 2, pp. 11–23, Jun. 2019, doi: 10.4197/ENG.30-2.2.

[27] M. K. Y. Shambour, "Assessing the Usability of Hajj and Umrah Websites," in *2021 International Conference on Information Technology, ICIT 2021 - Proceedings*, Jul. 2021, pp. 876–881. doi: 10.1109/ICIT52682.2021.9491780.

[28] M. K. Shambour and E. Khan, "A Heuristic Approach for Distributing Pilgrims over Mina Tents," *journal of King Abdulaziz University Engineering Science*, vol. 30, no. 2, pp. 11–23, 2019, doi: 10.4197/eng.30-2.2.

[29] D. Al-Sadiq and M. Ahmed, "The use of pilgrims to the social media sites of the General Presidency for the affairs of the two Holy Mosques and their attitudes towards it," in *19th Scientific Forum for the Research of Hajj, Umrah and Madinah Visit*, 2019, pp. 318–327. [Online]. Available: https://drive.uqu.edu.sa/_/hajj/files/multaqa/144019.pdf

[30] G. Kaur and K. Malik, "A comprehensive overview of sentiment analysis and fake review detection," in *Mobile Radio Communications and 5G Networks*, 2020, vol. 140, pp. 293–304. doi: 10.1007/978-981-15-7130-5_22.

[31] S. Aloufi, F. Alzamzami, M. Hoda, and A. el Saddik, "Soccer Fans Sentiment through the Eye of Big Data: The UEFA Champions League as a Case Study," in *2018 IEEE Conference on Multimedia Information Processing and Retrieval (MIPR)*, Jun. 2018, pp. 244–250. doi: 10.1109/MIPR.2018.00058.

[32] S. Aloufi and A. el Saddik, "Sentiment Identification in Football-Specific Tweets," *IEEE Access*, vol. 6, pp. 78609–78621, 2018, doi: 10.1109/ACCESS.2018.2885117.

[33] G. Bati, "Using big data tools to analyze tweets related to Hajj sentimentally," 2015. Accessed: Jul. 05, 2021. [Online]. Available: https://drive.uqu.edu.sa/_/hajj/files/multaqa/15_English.pdf

[34] R. Zahrani, I. Khaldi, and K. Qahtani, "The impact of understanding social media content on improving performance during the Hajj season, a Twitter case study for the Hajj season 1436 AH," in *17th Scientific Forum for the Research of Hajj, Umrah and Madinah Visit*, 2017, pp. 742–784. [Online]. Available: https://drive.uqu.edu.sa/_/hajj/files/multaqa/143817.pdf

انطباعات مجتمع مكة عن الحج في ظل جائحة كوفيد -١٩: تحليل كمي وتحليل مشاعر معتمد على الذكاء الاصطناعي

هاني عبدالله الضبيب

قسم الهندسة الكهربائية، كلية الهندسة والعمارة الإسلامية، جامعة أم القرى، مكة المكرمة ، المملكة العربية السعودية

hadhubaib@uqu.edu.sa

الملخص

على مر التاريخ ، اشتهر مجتمع مكة ببذل قصارى جهده لخدمة المسلمين الذين يأتون لأداء مناسك الحج (العمرة) ، الركن الخامس من أركان الإسلام. إلا أن حج عام ١٤٤١ هـ (٢٠٢٠ م) كان مختلفًا بسبب تفشي فيروس كورونا الجديد (كوفيد -١٩). وقد أحدث هذا الأثر تغييرات عديدة في العديد من جوانب الحياة البشرية في مختلف المجتمعات ، بما في ذلك مجتمع مكة المكرمة. بينما كان أهل مكة يستعدون لتقديم ما اعتادوا القيام به كل عام لدعم وتسهيل الخدمات للحجاج ، كان عليهم اتباع تعليمات وزارة الصحة لتنفيذ العديد من الإجراءات الاحترازية والوقائية لتجنب الإصابة بفيروس Covid-19 ؛ وأهمها البقاء في المنزل. تهدف هذه الدراسة بشكل أساسي إلى مراقبة وتحليل التغيرات الاجتماعية التي قد تكون حاضرة أو غائبة لأول مرة في مجتمع مكة المكرمة أثناء حج ١٤٤١ هـ. تم استخدام طريقتين رئيسيتين: تحليل المشاعر المعتمد على الذكاء الاصطناعي لعينة من التغريدات. وكذلك استبانة لعينة عشوائية من سكان مكة المكرمة.

King Abdulaziz Journal: Engineering Sciences, 2022 Volume 32 No 1 pp.:58-68, O DOI:xx.xxx/

Enhancing the Safety of Epoxy Flooring Materials in Wet Working Condition

Khamaj A.[1], AMM Ibrahim [2‡], Samy A. M.[2], Ameer A. K.[2]

[1]Dept. of Industrial Engineering, College of Engineering, Jazan University, jazan, Saudi Arabia

[2]Dept. of Production Engineering & Mechanical Design, Faculty of Engineering, Mini University, Egypt

Abstract. When a person walks across a floor, static electricity is generated purely by the contact and separation of the soles of the individual's shoes from the floor. In many industrial processes, electrostatic charges are fully common. They can cause breakdowns, damage, fires, and explosions. On the other side, without enough friction between shoes and flooring materials during walking, a slip is most probable to occur. There is an increasing demand to increase the coefficient of friction between shoes and flooring materials to eliminate slipping and prevent accidents. The present work aims to improve the frictional and electrostatic properties of epoxy as flooring materials for different applications. We proposed the iron machining chip wastes to use as filling materials for epoxy flooring to increase friction coefficient and decrease the electrostatic charge generated from the friction of shoes against flooring materials. The experimental results revealed that a remarkable reduction in static charge was noticed in wet sliding conditions. This behavior is referred to that the water helps for disposal static charge away from the contact surfaces. In presence of shoes "A" with hardness 65 shore A, the maximum values of friction coefficient values observed at epoxy floor containing 1% and 2% iron powder in wet condition. Meanwhile, 4 % iron powder was the optimum condition for reducing electrostatic charge. For shoes "B" with hardness 63 shore A, the maximum values of friction coefficient values were observed at 2% iron powder content. -In presence of shoes "C" with hardness 67 shore A, the maximum values of friction coefficient values were observed at 2% iron powder content.

Keywords: Epoxy, friction coefficient, electrostatic charge, water, iron powder.

1. INTRODUCTION

The static charge includes potentially dangerous electrical shocks that can cause fires and explosions. It can also reason intense damage to susceptible electronic components. Triboelectric charging is the conveyance of electrons which occurs when two materials are in contact and are then separated. One material gains an overflowing of negative ions and the other an overflowing of positive ions. The charge produced can be more than 25,000 volts. It is well familiar that when two various materials contact each other, they may bring charged. This tribocharging phenomenon is also famous as triboelectrification when materials rubbing against each other, [1-3]. The mechanism of charge transfer in tribocharging can be explained by three mechanisms: ion transfer, electron transfer, and material convey [4 – 6]. The metal-to-metal contact electrification is successfully explained by the electron conveys mechanism. When two distinct materials come to contact, electrons convey happens until their Fermi level equals. Diversity in work functions between those is the main leading force, [7]. As for insulators, the electron conveys only occur on the surfaces of insulators, where electrons get about from the loaded surface of one insulator to the vacuous surface of the other insulator, [8–10]. Few investigators have dragged up triboelectric series to foresee the polarity of the charge that is conveyed from one surface to the latest, [11]. When two kinds of materials contact each other, the upper one in the triboelectric series will bring positively charged

‡ Corresponding author: Abdelhalim196@hotmail.com

and the other one will be negatively charged. It is attractive increasingly obvious that more than one of these mechanisms may occur together, [12].

Safe walking on the floor was estimated by the static coefficient of friction. Few investigators paying attention to the electric static charge produced during walking on the surface of the floor. It is well familiar that walking and crawling on flooring can produce an electric static charge of consistency depend on the material of flooring. The materials of the floors as well as footwear can influence the produced charge. The electric static charge and coefficient of friction of unclothed foot and foot onerous socks sliding against various types of flooring materials were scrupulous under dry sliding conditions, [13]. The tested flooring materials were marble, ceramic, moquette, rubber, and parquet. It was found that rubber flooring materials showed the highest produced voltage between the tested floorings. The highest voltage values were displayed by polyester hosiery, while cotton hosiery showed the lowest one. This monitoring can assure the emergency of carefully chosen flooring materials. Parquet flooring materials showed the lowest voltage between all tested flooring. Charge produced from rubbing amidst shoes and carpet were discussed, [14-15]. The impact of humidity was explained on the basis that water jot on the surfaces transfers charges in the form of ions to promote charge repose, [16-18]. The effect of the static charge generation on the ambiance is affected by the electrical accessibility of the sliding surfaces.

The influence of the type of flooring materials on the obstetrics of electric static charge and coefficient of friction was examined, [19]. It was spotted that voltage produced from sliding against ceramic flooring lightly. The metrical voltage values showed considerable squander as well known for the produced electric static charge, wherever the minimum and maximum values reached 360 and 850 volts. It is prospective that an electrical field will be created due to the electric charge created on the floor surfaces and footwear. Marble flooring displayed higher values than that spotted for ceramic flooring. As the load increased, the voltage increased. Based on the previous discussion, it can be suggested to choose flooring materials according to their impedance to produce electric static charge. The voltage produced from sliding of footwear against parquet ceramic flooring surface was lower than marble and higher than that produced from smooth ceramic. It seems that the surface topography of the parquet ceramic was accountable for that behavior. Voltage approaching a considerable increase when footwear sliding against porcelain flooring, where the maximum value reached 5995 volts. This behavior can be a hurdle in using porcelain as a flooring material, while flag flooring showed the lowest produced voltage, essentially at low loads.

Experimental results show that, rubber particles remarkably increased the coefficient of friction. This attitude concerning to the deformation of rubber through scratching. The minimum value of the coefficient of friction spotted for 100% epoxy was 1.5 at 4 N of applied loads, while the maximum value was 2.5 showed by epoxy filling by 10 wt. % rubber of 0.5 - 1.0 mm particle size, [20]. The examined material is polyester filled with various contents of recycled rubber 5, 10, 15, 20, and 25 % with various particle sizes. Experimental results show that, raise rubber content shows a considerable increase in the coefficient of friction for polyester composite. The maximum value of the coefficient of friction was (1.75) for polyester composite recorded for specimens filled by 25 % rubber. While the minimum friction value (0.18) was spotted at 100% polyester specimens. Increasing particle size of rubber shows a remarkable increase in wear of polyester composite, [21].

The present work discusses the friction coefficient displayed by footwear soles sliding against epoxy flooring materials. The electro static charge performance was investigated for avoiding the several problems caused by static charge. Measurement of friction coefficient is, therefore, of critical importance in assessing the proper friction properties of flooring materials and their suitability to be used in application to enhance the safety of the persons. The friction coefficient and static charge displayed by rubber footwear soles sliding against epoxy flooring materials filled by the powder of iron chip in water-lubricated conditions is discussed.

2. EXPERIMENTAL WORK

The (Ultra Stable Surface Voltmeter) was used to measure the electric static charge (electric static field) after contact and separation of the

specimens against rubber to measure the generated charge under applied loads, as shown in Fig. 1. It measures down to 1/10 volt on a surface, and up to 20 000 volts (20 kV). Readings (Volts) are normally done with the sensor 25 mm from the surface being tested.

Fig. 1 Electric static charge (voltage) measuring device.

Friction tests were carried out using a test rig designed and manufactured to measure the friction coefficient between the rubber test specimens and the tested flooring tiles by measuring the friction and normal forces. The tested flooring tiles are placed in a base supported by two load cells, the first measures the horizontal force (friction force), and the second measures the vertical force (normal load). The friction coefficient is determined by the ratio between the friction and the normal forces. The arrangement of the test rig is shown in Fig. 2 . Test specimens in a form of a layer of 150 × 150 mm^2 molded on a wooden block. The tested materials were epoxy filled by different contents of iron powder with 5-micron particle size, was added to epoxy with different content 1, 2, 3, 4 and 5 %. The Friction test was carried out at different values of normal load. The sliding behavior measure by use the rubber shoes with 63, 65 and 67 shore" A" hardness. The friction force measure from load cell and the normal load measure by variable weight. The rubber shoes used in experimental was shown in Fig. 3.

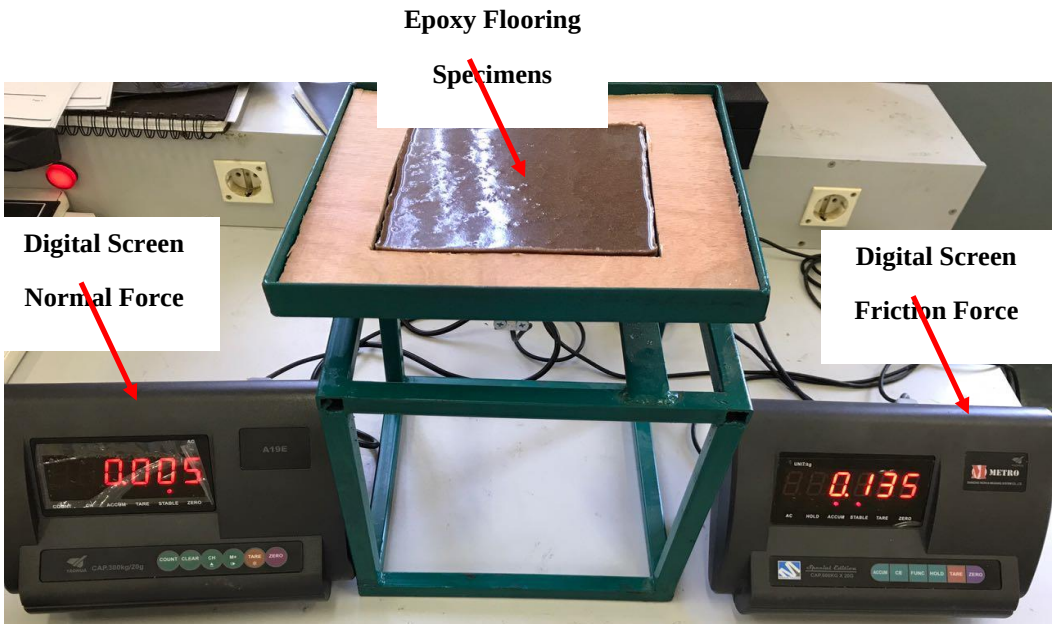

Fig. 2 Friction tester

Fig. 3. Tested Rubber shoes.

3. RESULTS AND DISCUSSION

The friction coefficient of water epoxy flooring material filled by the powder of iron chip is shown in Fig. 4 A. The friction coefficient decreases with increasing the normal load. Increase iron powder content show a significant effect in increasing friction coefficient. However, the increase in the hardness of rubber shoes shows decreasing in friction value. The minimum values of friction coefficient were observed for 100% epoxy specimens. Meanwhile, increasing iron powder content up to 3% show more influence in increasing friction coefficient. Figure 4, B. shows the relation between friction coefficient and normal load, for water epoxy test specimens filled by the powder of iron powder. It can be noticed that the friction coefficient decrease with increasing normal load. Increase the hardness of shoes in the presence of water can lessen the friction coefficient values. This behavior is referred to intrepid the water in the contact area. The minimum values of friction coefficient are displayed by pure epoxy test specimens

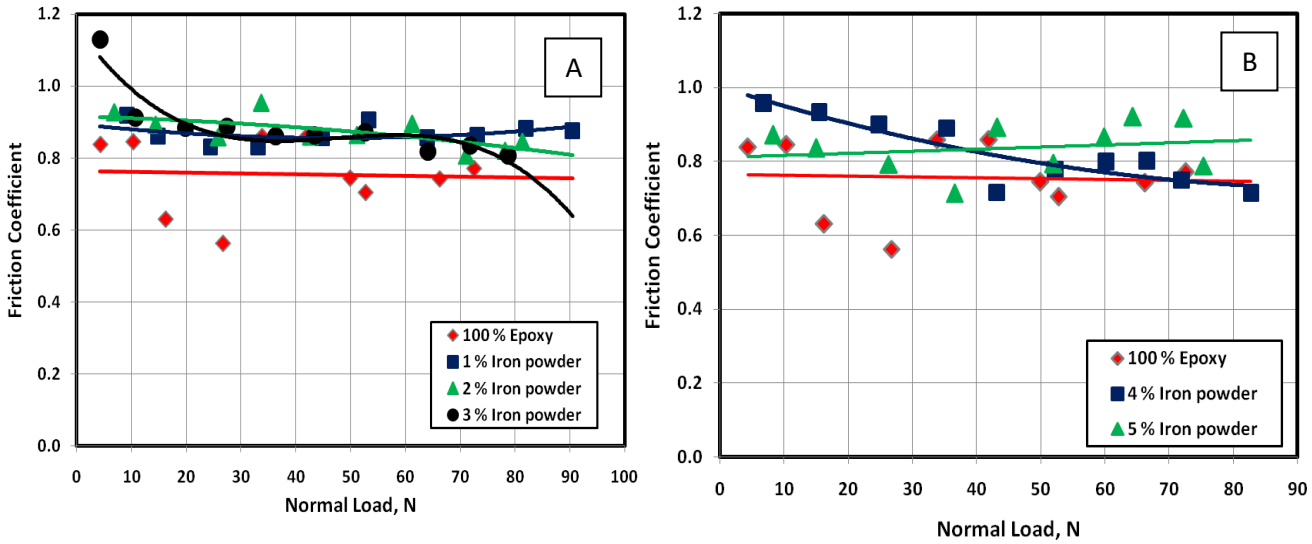

Fig. 4 Friction coefficient of rubber shoes with Hardness 63 shore A sliding against wet epoxy floor filled by iron powder.

Figure 5, A shows the relation between friction coefficient and normal load, for rubber shoes sliding against water epoxy floor filled by the powder of iron chip powder. It can be noticed that the friction coefficient increase with increasing iron powder content. This behavior may be related to increasing the ability of the floor to prevent sliding. Friction coefficient decrease with increasing normal load, this behavior is associated with the shoes type where the

rubber shoes and all polymeric material friction coefficient decreases with increasing normal load. The minimum friction coefficient was observed at 100 % epoxy flooring. The maximum friction coefficient was observed at 2 % iron powder. Increase powder of iron powder content in epoxy flooring is shown in Fig. 5, B. The friction coefficient shows an increase with increasing iron powder content. On the other hand, the Friction coefficient decreases with increasing normal load. This behavior is related to the presence of water in the contact area between shoes and the floor. Nonetheless, iron powder plays important role in increase friction coefficient, in which the iron particles permit the water to pass over iron powder and leakage out off contact area. Minimum values of friction coefficient were observed for 100% epoxy flooring.

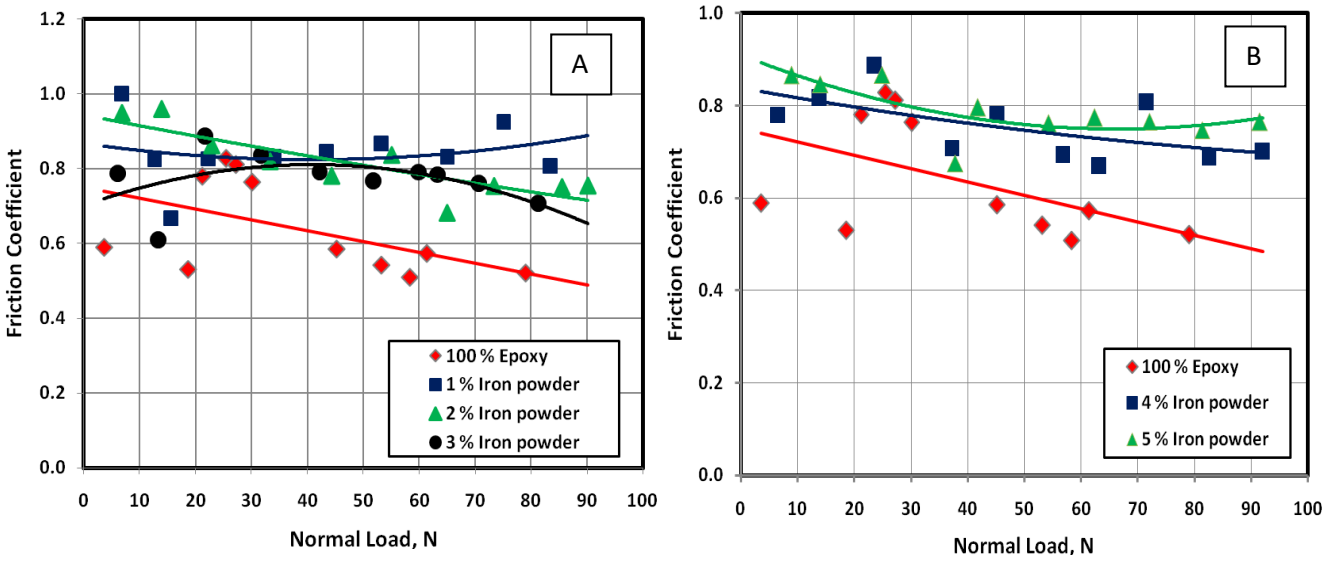

Fig. 5 Friction coefficient of rubber shoes with Hardness 65 shore A sliding against wet epoxy floor filled by iron powder**.**

The friction coefficient of rubber shoes sliding against water epoxy test specimens filled by the powder of iron chip is shown in Fig. 6, A. Friction coefficient increases with increasing powder of iron chip content. This behavior may be related to the easy escape of water from the contact area. The maximum value of friction coefficient was observed at specimens of epoxy filled by 2 % iron powder. Nevertheless, the minimum value of friction coefficient was observed at 100% epoxy flooring material. Figure 6, B. show the relation between friction coefficient and normal load, for epoxy test specimens at 4% and 5% iron powder. It can be noticed that the friction coefficient increase with increasing iron powder content. This behavior related to the escape of water from contact area and increase bonding between shoes and floor.

The electrostatic charge of wet epoxy flooring material filled by the powder of iron chip is shown in Fig. 7, A. Interestingly, the electrostatic charge decreases with increasing iron powder content. Increase hardness of shoes exhibited slight increase in electrostatic charge. This behavior is related to the decrease deformation of shoes and the gap between floor and shoes this gap allows electrostatic charge generated. The minimum values of electrostatic charge were observed at 3% iron powder. Figure 7, B. show the relation between electrostatic charge and friction coefficient, for wet epoxy test specimens filled by powder of iron chip. It can be noticed that the electrostatic charge decreases with increasing iron powder. Increasing iron powder to 4% show significant effect on reduction of electrostatic charge. In presence of water on sliding surface electrostatic charge increased for 100% epoxy floor. This behavior related to the epoxy is non-conduct and save this charge on surface of specimens, the iron help for disposal electrostatic charge to ground.

.

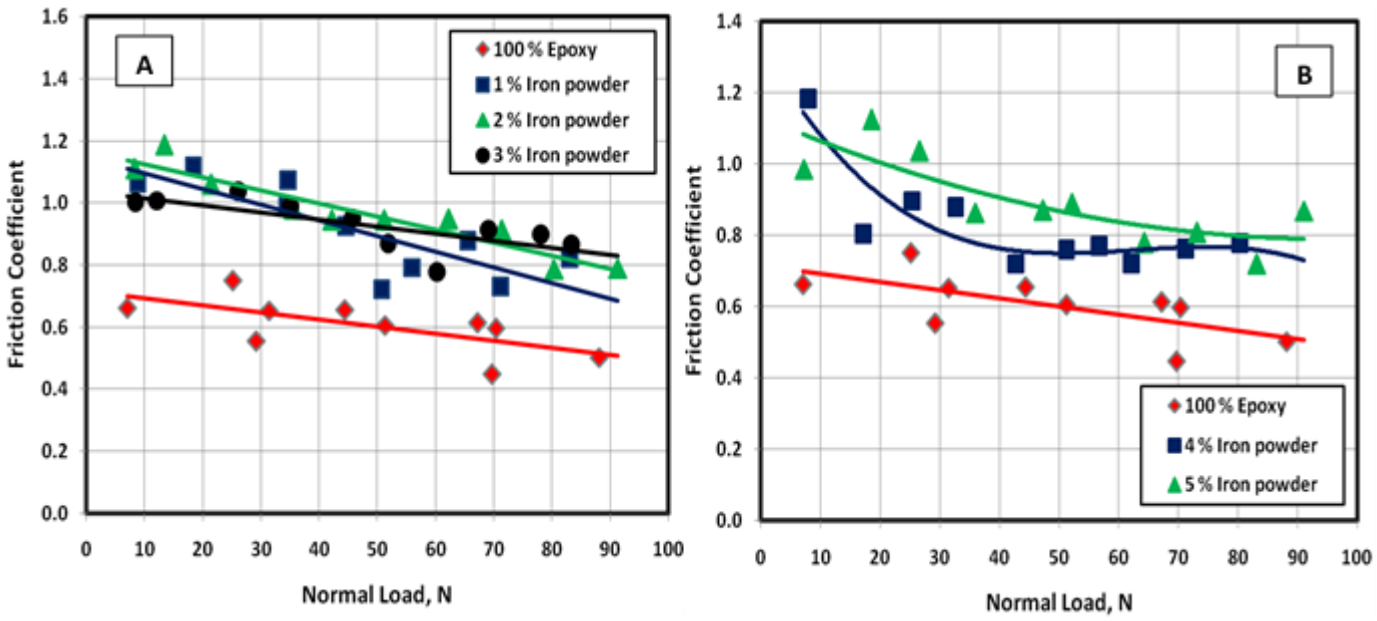

Fig. 6 Friction coefficient of rubber shoes with Hardness 67 shore A sliding against wet epoxy floor filled by iron powder.

.

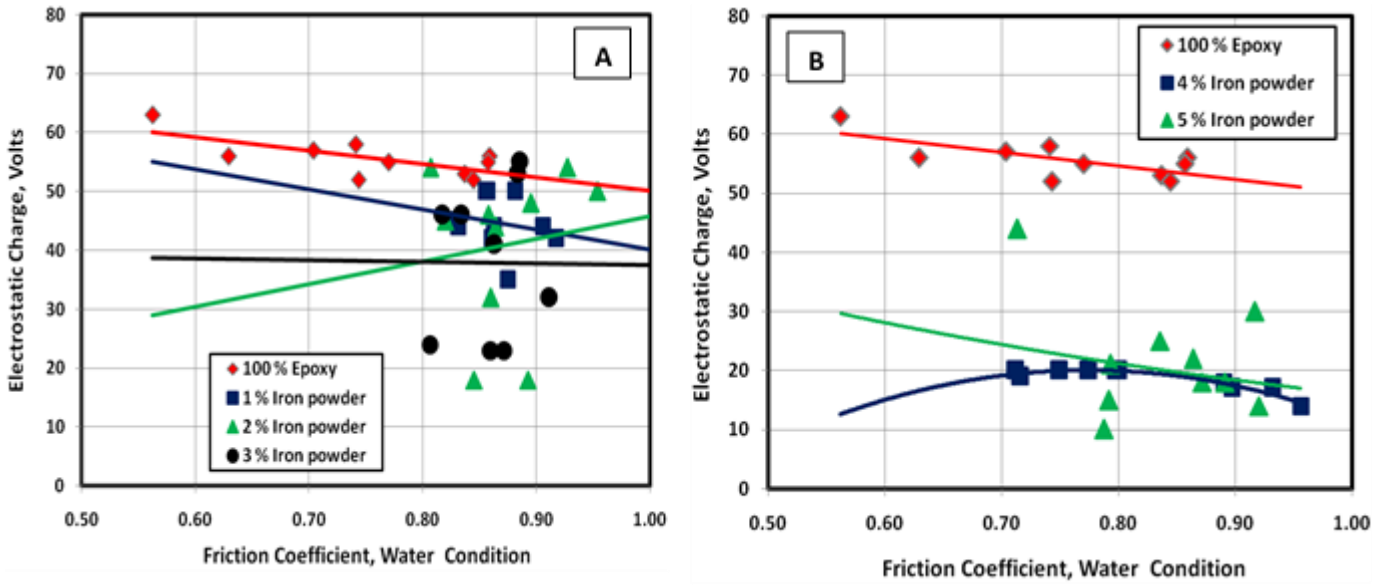

Fig. 7 Friction coefficient of rubber shoes with Hardness 63 shore A sliding against wet epoxy floor filled by iron powder.

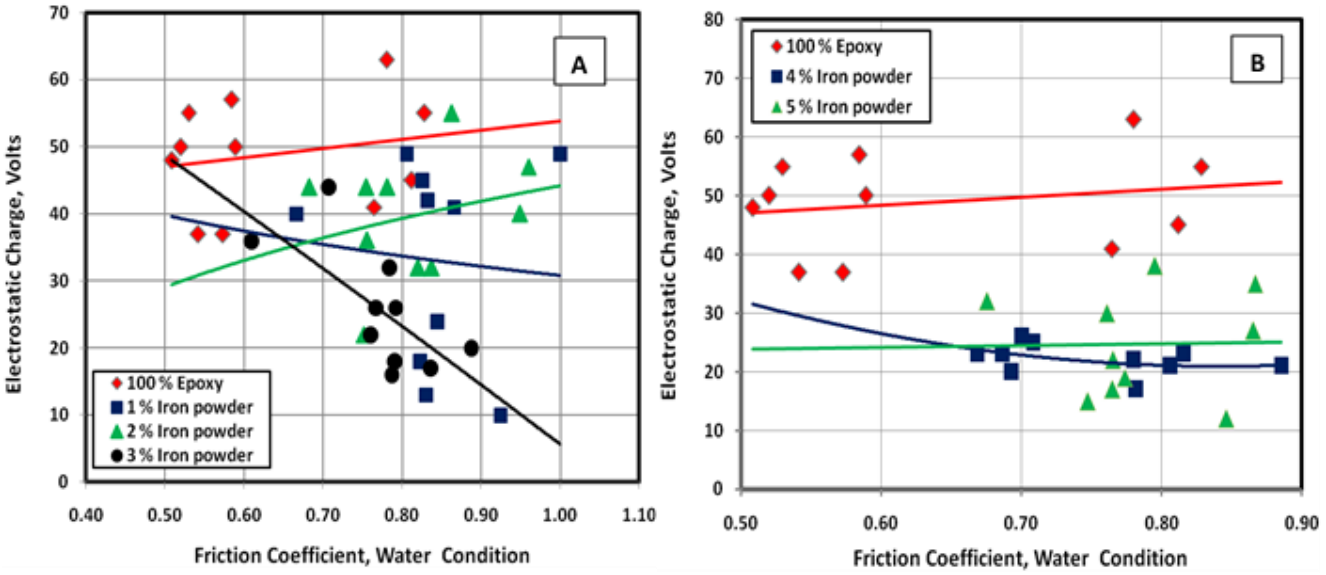

Fig. 8 Electrostatic charge of rubber shoes with Hardness 65 shore A sliding against wet epoxy floor filled by iron powder.

Figure 8, A. shows the relation between electrostatic charge and friction coefficient, for epoxy filled by the powder of iron chip, under water as a sliding condition. It can be noticed that the electrostatic charge decrease with increasing iron powder content. In presence of water, the electrostatic charge decreases to the minimum values at 3% iron powder content. This behavior can be explained as; the water distributes the charge on surface of floor and iron powder disposal from this charge to ground. Meanwhile, the minimum electrostatic charge was observed at 3 % iron powder. The maximum charge was observed at 100 % epoxy flooring. Increase powder of iron chip content in epoxy flooring was shown in Fig. 8, B. Electrostatic charge shows decreasing with increasing iron powder content. The values of electrostatic charge decrease to the minimum value at 4 % iron powder content. This behavior is related to the more effect of iron powder on the disposal of this charge. Maximum values of electrostatic charge were observed at 100 % epoxy floor. The best content for reducing charge was 4% iron powder.

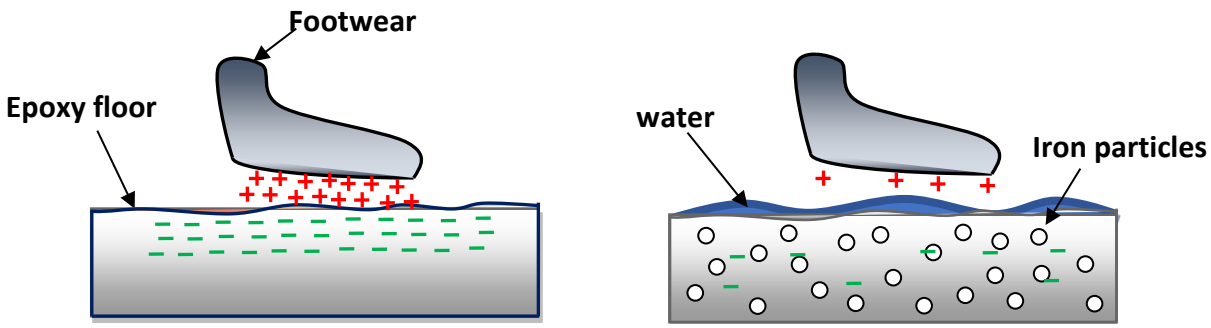

Fig. 9 The effect of water on reduction the electrostatic charge

The effect of iron powder on the reduction of the electrostatic charge generated from friction between shoes and epoxy flooring materials, shown in Fig 9. The iron is good conducting material and helps for the good distribution of the static charge on the contact surface. The water on the contact surface helps for disposal of the static charge from the contact surface.

The electrostatic charge of rubber shoes sliding against water epoxy test specimens filled by the powder of iron chip is shown in Fig. 10, A. Electrostatic charge decrease with increasing friction coefficient. This behavior may be related to increasing deformation of rubber shoes and decreasing the gap between shoes and the floor. Increasing iron powder content shows a significant decrease in electrostatic charge generated from friction. The maximum value of electrostatic charge was observed at 100% epoxy flooring material. Figure 10, B. shows the relation between electrostatic charge and friction coefficient, for epoxy test specimens at 4% and 5% iron powder content. It can be noticed that the electrostatic charge decrease with increasing iron powder content. Increase iron powder content to 5 % show a reduction in charge value. This behavior is related to the more effect of iron powder on the disposal of electrostatic charge to ground. Where found the iron powder in sliding surface help for good distribution this charge and not collect in any zone. This behavior helps the water to disposal of the electrostatic charge. The minimum value of electrostatic charge was observed at 5% epoxy specimens filled by 5% iron powder.

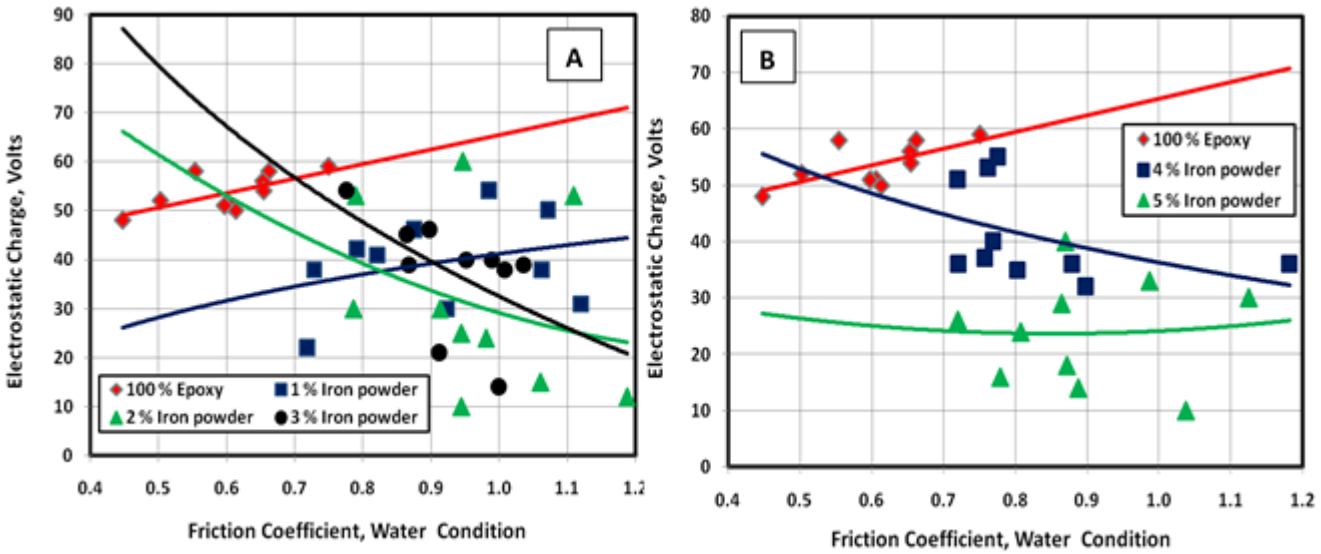

Fig. 10 Electrostatic charges of rubber shoes with Hardness 67 shore A sliding against wet epoxy floor filled by iron powder

4. CONCLUSIONS

1. As water sliding conditions the remarkable reduction in static charge was shown, this behavior related to the water helps for disposal of static charge away contact surfaces.

2. In presence of shoes “A” with hardness 65 shore A, the maximum values of friction coefficient values observed at epoxy floor contain 1% and 2% iron powder in water conditions. And 4 % iron powder for reducing electrostatic charge.

3. For shoes “B” with hardness 63 shore A, the maximum values of friction coefficient values were observed at 2% iron powder content. And 4 % iron powder for reducing electrostatic charge.

4. In presence of shoes “C” with hardness 67 shore A, the maximum values of friction coefficient values were observed at 2% iron powder content. And 4 % and 5% iron powder for reducing electro-static charge.

REFERENCES

[1] Wu G., Li J., Xu Z., "Triboelectrostatic separation for granular plastic waste recycling: A review", Waste Management 33, pp. 585 – 597, (2013).

[2] Lowell, J., Rose-Inne, A. C., "Contact electrification", Adv. Phys. 29, pp. 947 – 1023, (1980).

[3] Matsusaka, S., Maruyama, H., Matsuyama, T., Ghadiri, M., "Triboelectriccharging of powders: a review", Chem. Eng. Sci. 65, pp. 5781 – 5807, (2010).

[4] Lee, L. H., "Dual mechanism for metal–polymer contact electrification", J. Electrostat. 32, 1 - 29,(2003).

[5] Matsusaka, S., Masuda, H., "Electrostatics of particles" Adv. Powder Technol. 14, pp. 143 – 166, (1994).

[6] Saurenbach, F., Wollmann, D., Terris, B., Diaz, A., "Force microscopy of ioncontaining polymer surfaces: morphology and charge structure" Langmuir 8, pp. 1199 – 1203, (1992).

[7] Harper, W., "The Volta effect as a cause of static electrification", Proc. Roy. Soc. Lond. Ser. A. Math. Phys. Sci. 205, pp. 83 – 103, (1951).

[8] Anderson, J., "A comparison of experimental data and model predictions for tribocharging of two-component electrophotographic developers", J. Imag. Sci. Technol. 38, pp. 378 – 382, (1994).

[9] Gutman, E., Hartmann, G., "Triboelectric properties of two-component developers for xerography" J. Imaging Sci. Technol. 36, pp. 335 – 349, (1992).

[10] Yoshida, M., Ii, N., Shimosaka, A., Shirakawa, Y., Hidaka, J.,"Experimental and theoretical approaches to charging behavior of polymer particles", Chem. Eng. Sci. 61, pp. 2239 – 2248, (2006).

[11] Park, C. H., Park, J. K., Jeon, H. S., Chu, B. C., "Triboelectric series and charging properties of plastics using the designed vertical-reciprocation charger", J.Electrostat, 66, pp. 578 – 583, (2008).

[12] Meurig, W. Williams, L."Triboelectric charging in metal-polymer contacts - How to distinguish between electron and material transfer mechanisms", Journal of Electrostatics 71, pp. 53 – 54, (2013).

[13] El-Sherbiny Y. M., Samy A. M. and Ali W. Y., "Electric static charge generated from bare foot and foot wear sliding against flooring materials", Journal of the Egyptian Society of Tribology, Vol. 11, No. 1, January 2014, pp. 1 – 11, (2014).

[14] Greason W. D., "Investigation of a test methodology for triboelectrification", Journal of Electric statics, 49, pp. 245 - 56, (2000).

[15] Nomura T., Satoh T., Masuda H., "The environment humidity effect on the tribocharge of powder", Powder Technology (135 - 136), pp. 43 - 49, (2003).

[16] Diaz AF, Felix-Navarro RM., "A semi-quantitative triboelectric series for polymeric materials", Journal of Electric statics, 62, pp. 277 - 290, (2004).

[17] Nemeth E, Albrecht V, Schubert G, Simon F, "Polymer triboelectric charging: dependence on thermodynamic surface properties and relative humidity", Journal of Electric statics, 58, pp. 3 - 16, (2003).

[18] Al-Qaham Y., Mohamed M. K. and Ali W. Y., "Electric Static Charge Generated From the Friction of Textiles", Journal of the Egyptian Society of Tribology Vol. 10, No. 2, April 2013, pp. 45 – 56, (2013).

[19] El-Sherbiny Y. M., Abdel-Jaber G. T. and Ali W. Y., "Friction Coefficient and Electric static Charge Generated From Rubber Footwear Sliding Against Flooring Materials", Journal of the Egyptian Society of Tribology, Vol. 11, No. 4, October 2014, pp. 13 - 24, (2014).

[20] Samy A. M.," Tribological Behaviour of Epoxy Filled by Rubber Particles", Friction and Wear Research, Volume 3, December 2015, P.P 15: 21, (2015).

[21] Samy A. M.," Tribological Performance for Polyester filled by recycled Rubber", KGK-kautschuk gummi kunststoffe, Germany, April, 36-40, (2017).

تعزيز الأمان للإيبوكسي المستخدم كمواد أرضيات في ظروف العمل الرطبة

عبدالرحمن خمج[١]، احمد محمد محمود[٢]، عبدالحليم محمود سامي[٢]، أمير علي كامل[٢]
[١] قسم الهندسة الصناعية – كلية الهندسة – جامعة جازان- المملكة العربية السعودية

[٢] قسم هندسة الانتاج والتصميم الميكانيكي، كلية الهندسة، جامعة المنيا، جمهورية مصر العربية

عندما يمشي شخص ما علي الارضيات ، تتولد الكهرباء الساكنة عن طريق تلامس وفصل نعل الحذاء عن الأرض. في العديد من العمليات الصناعية تكون الشحنات الكهروستاتيكية شائعة التواجد وبالتالي يمكن أن تسبب الأعطال والأضرار والحرائق والانفجارات. بالاضافة الي ذلك بدون احتكاك كافٍ بين الأحذية ومواد الأرضيات أثناء المشي فمن المرجح أن يحدث الانزلاق والسقوط. لذلك هناك طلب متزايد على زيادة معامل الاحتكاك بين الأحذية ومواد الأرضيات لمنع الانزلاق ومنع وقوع الحوادث.

يهدف العمل الحالي إلى تحسين الخواص الاحتكاكية والكهربائية للإيبوكسي كمواد أرضيات لاستخدامها في العديد من التطبيقات. لقد اقترحنا استخدام الرائش الناتج من عملية تصنيع الحديد كمواد تعبئة للأرضيات الإيبوكسي بهدف زيادة معامل الاحتكاك وتقليل الشحنة الكهروستاتيكية الناتجة عن احتكاك الأحذية بمواد الأرضيات. أظهرت النتائج التجريبية انخفاضًا ملحوظًا في الشحنة الساكنة في ظروف الانزلاق الرطب. يرجع هذا الانخفاض الي أن الماء يساعد في التخلص من الشحنات الساكنة بعيدًا عن أسطح التلامس. في حالة الإحذية ذات صلادة ٦٥ مقاسة علي جهاز شورA ، لوحظت القيم القصوى لمعامل الاحتكاك عند أرضية الإيبوكسي التي تحتوي على ١٪ و ٢٪ مسحوق حديد في حالة وجود الماء. وفي الوقت نفسه ، كانت ارضيات الايبوكسي التي تحتوي علي ٤٪ مسحوق الحديد هي النسبة الأمثل لتقليل الشحنة الكهروستاتيكية. بالنسبة للأحذية ذات صلادة ٦٣ مقاسة علي جهاز شور Aو الأحذية ذات صلادة ٦٧ مقاسة علي جهاز شورA ، لوحظت القيم القصوى لمعامل الاحتكاك عند نسبة ٢٪ مسحوق الحديد.

الكلمات الرئيسية: الايبوكسي ، معامل الاحتكاك ، الشحنة الكهروستاتيكية ، الماء ، مسحوق الحديد.

مجلة جامعة الملك عبد العزيز
العلوم الهندسية

المجلد ٣٢ العدد ١ ٢٠٢٢ ردمك ١٠٤٧ـ ١٣١٩